Electronic Supporting Information for

Film thickness dependence of nanoscale arrangement of a chiral electron donor in its blends with an achiral electron acceptor

by

Giulia Pancotti,[a°] C. Elizabeth Killalea,[b°] Thomas W. Rees,[b°] Letizia Liirò-Peluso,[b°] Sergi Riera-Galindo,[a] Peter H. Beton,[c] Mariano Campoy-Quiles,[a] Giuliano Siligardi[d] and David B. Amabilino[a]

a. Institut de Ciència de Materials de Barcelona (ICMAB-CSIC), Carrer dels Til·lers, Bellaterra, 08193 Spain.

b. School of Chemistry and GSK Carbon Neutral Laboratories for Sustainable Chemistry, University of Nottingham, Triumph Road, Nottingham, NG7 2TU, UK.

c. School of Physics and Astronomy, The University of Nottingham, University Park, Nottingham, NG7 2RD.

d. Diamond Light Source, Harwell Science and Innovation Campus, Didcot, Oxfordshire OX11 0DE.

° These authors contributed equally to the research described here.

‡ Present address: The Francis Crick Institute, 1 Midland Road, London NW1 1AT, UK

§ Present address: Université Angers, CNRS, MOLTECH-Anjou, F-49000 Angers, France

Materials and methods

All commercially obtained reagents were used without further purification. Anhydrous solvents were produced using an Inert PureSolv SPS. Column chromatography was carried out using Sigma Aldrich Silica gel (pore size 60Å, particle size 40-63 μm). Melting points were determined on a Stuart SMP20 Melting Point Apparatus. ^{1}H and ^{13}C NMR spectra were recorded in $CDCl_3$ or DMSO-d_6 on a Bruker AVIII HD 400 (400 and 100 MHz) or a Bruker AVIII HD 500 (500 and 126 MHz). Chemical shifts are reported as δ values (ppm) referenced to the following solvent signals: $CHCl_3$, δH 7.26, $CDCl_3$, δC 77.0, $(CH_3)_2SO$, δH 2.50, $(CH_3)_2SO$, δC 39.5. Multiplicity of signals and coupling constants were obtained by processing on MestReNova. Non-equivalent protons with signals that cannot be resolved separately are reported as a "stack". Mass spectra were recorded on a Bruker micrOTOF II spectrometer utilizing electrospray ionization with an MeOH/H_2O mobile phase. Infrared spectra were recorded neat as thin films on a Bruker Vertex 70 spectrometer. UV−Vis spectra were recorded on an Agilent Technologies Cary Series UV-Vis-NIR spectrophotometer in $CHCl_3$ solution. Emission spectra were recorded on an Edinburgh Instruments FLS 980 in $CHCl_3$ solution.

Variable angle spectroscopic ellipsometry (VASE) measurements for the films deposited on quartz substrate. The response of both the neat-chiral and blended films were satisfactory fitted using dielectric functions provided by the JA Woollam CompleteEase (v 6.62) materials library. The films, deposited by spin coating on the quartz substrates, were modelled using Gaussian functions at photon energies between 1.0 eV and 6.0 eV. The samples were measured using focus probes with an elliptical spot that had a minor diameter of 300 microns at 55°, 60°, 65° angles of incidence. To estimate the uniqueness of the model, the thickness of the films was systematically varied from the best fit position and the other fitting parameters refitted to the data. The results suggested that the mean-square error was altered by 10% for the thickness variation of ± 0.2 nm. Therefore, the thickness of the films was estimated to be 86.9 ± 0.2 nm on average over the 300 micron diameter spot size.

Fabrication and Characterisation of electronic devices

Device Preparation

The organic photodetector devices and solar cells were constructed with an inverted structure of ITO/ZnO/Active Layer/MoO_X/Ag (see illustration below).

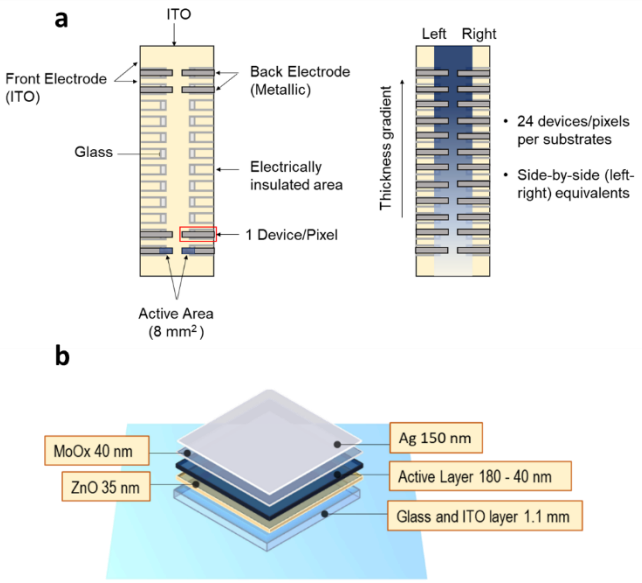

c

Pixel (nº)	Thickness (± 20nm)
1	180
2	160
3	140
4	133
5	120
6	110
7	90
8	80
9	70
10	60
11	50
12	40

Illustration of (a) the device components over the glass slide coated with ITO, (b) the layered structure of each pixel/device with respective thickness of each layer, and (c) the thickness of the (*S,S*)-**1** and **ITIC-4F** blend. The thickness was calculated with a profilometer analysis using Filmetric Profilm3D at B23 beamline, DLS, UK.

The substrates (Ossila S241, ITO Glass Scale Up Substrates PV and OLED- Pixelated Size: 75 x 25 mm) underwent a cleaning process involving consecutive sonication baths in acetone, a 10% Hellmanex solution in water, isopropanol (each for 5 minutes), and a 10% sodium hydroxide (NaOH) solution (for 10 minutes), followed by rinsing with deionized (DI) water. The ZnO layer, serving as the electron transport layer (ETL), was applied using an automatic blade coater Zehntner ZAA 2300 with an aluminum applicator Zehntner ZUA 2000 under air conditions. A droplet volume of 50 µL, a blade gap of 150 µm, a constant speed of 5 mm/s, and a substrate temperature of 40 °C were maintained during deposition, giving a thickness of approximately 35 nm. The ETL layer was then annealed at 100 °C for 10 minutes before transferring to a nitrogen-filled glovebox. A mixture of *(S,S)*-**1** and **ITIC-4F**, with a 1:1 weight ratio and a total solid content of 20 mg/mL, was dissolved in chlorobenzene to prepare the active layer solution. The active layer was then blade-coated in the glovebox with a blade gap of 200 µm, at a substrate temperature of 80 °C, and a decelerating speed ranging from 90 to 10 mm/s across a 75 mm-long direction, resulting in a thickness-gradient layer. The samples were then annealed at 100 °C for 10 minutes. Finally, MoOx (40 nm) and Ag (150 nm) layers were evaporated in an ultra-high vacuum at rates of 0.5 and 1 Å/s, respectively.

Device Characterization

The J–V characteristics were automatically recorded in air using a Keithley 2400 source meter in combination with an Arduino-based multiplexer/switcher to measure up to 24 devices consecutively over 6 minutes. For illumination, a SAN-EI Electric XES-100S1 AAA solar simulator was employed to provide uniform light (AM1.5G) over a 10 × 10 cm area, calibrated with a certified silicon solar cell (Oriel). External Quantum Efficiency (EQE) was measured with a custom-built setup that includes a supercontinuum light source (4 W, Fianium) connected to a monochromator and normalized by the light power, measured by a silicon diode. EQE measurements were taken across wavelengths from 400 to 900 nm, focusing the laser on a 50 mm diameter spot.

SYNTHESIS

The overall synthetic scheme for the preparation of (*S,S*)- **1** is shown below.

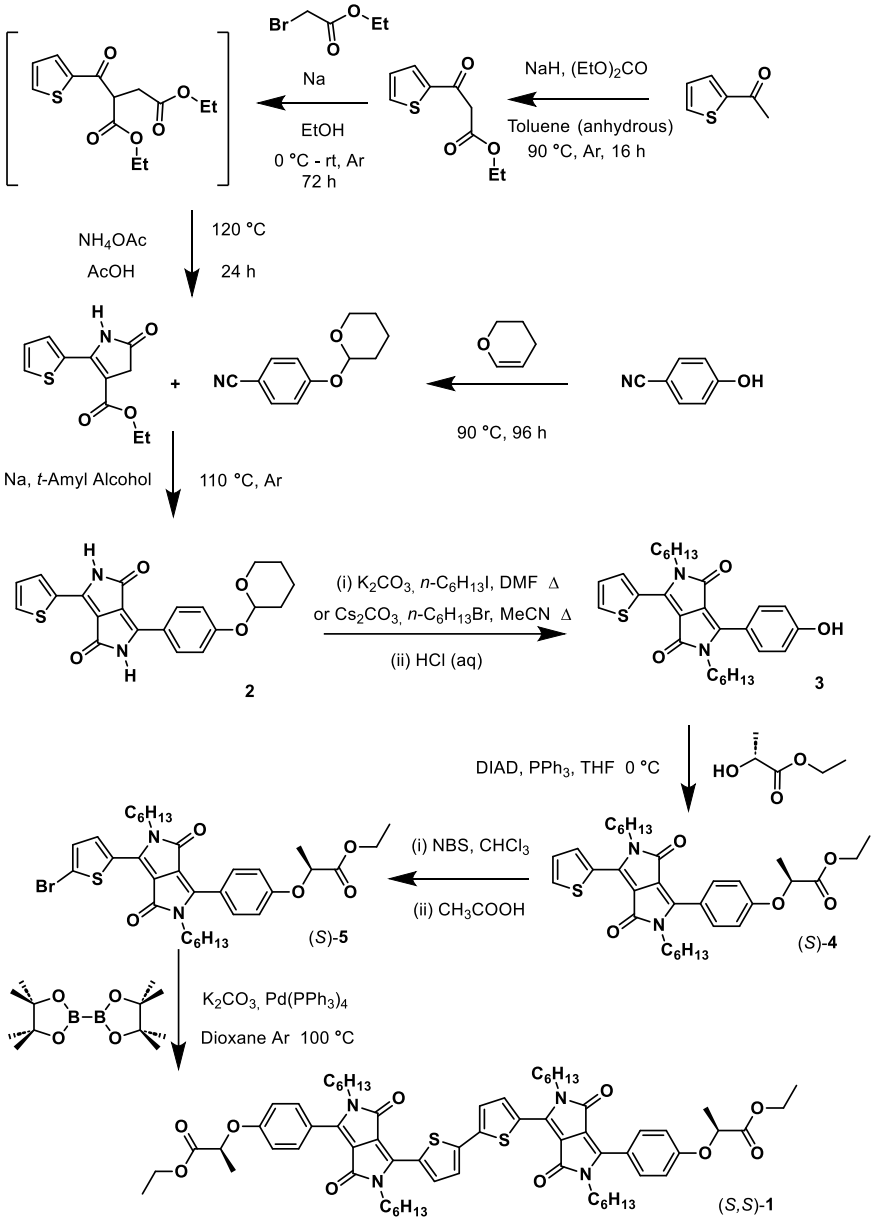

4-((Tetrahydro-2H-pyran-2-yl)oxy)benzonitrile

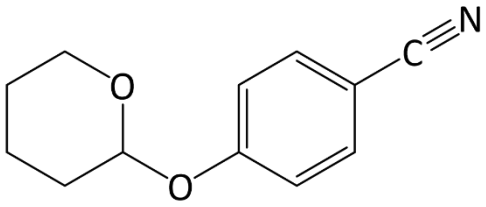

The method follows a literature[1] with minor changes: 4-Cyanophenol (11.1 g, 92.9 mmol) was added to 3,4 dihydropyran (45 mL, 493 mmol). The reaction mixture was stirred at 85 °C for 96 h. Excess 3,4 dihyrdopyran was removed under reduced pressure to give white crystals coated in a viscous yellow oil. The product was recrystallized from a water / ethanol solution (50:50) to give white crystals which were then filtered and washed with water and cold methanol to give the desired product. (8.90 g, 43.8 mmol, 47%); lit mp[1]: 68.5-70 °C; mp 70-72 °C ^{1}H NMR (400 MHz, $CDCl_3$) δ 7.59 (d, *J* = 8.9, 2H), 7.11 (d, *J* = 8.9, 2H), 5.51 (t, *J* = 3.1 Hz, 1H), 3.84 (ddd, *J* = 11.4, 9.8, 3.1 Hz, 1H), 3.64 (dtd, *J* = 11.4, 4.1, 1.5 Hz, 1H), 2.11 – 1.54 (m, 6H) ppm; ^{13}C NMR (101 MHz, $CDCl_3$) δ 160.4, 133.8, 119.2, 116.9, 104.6, 96.2, 62.0, 29.9, 24.9, 18.3 ppm; υ_{max} (ATR-IR) 2943 (CH stretch), 2283 (CH stretch), 2218 (CN stretch), 1603 (CC stretch), 1504, 1243, 1175, 1107, 1037, 1020, 951, 911, 870, 837, 812, 545 cm^{-1}; *m/z*, calcd. for $C_{12}H_{13}NO_2$: 201.08, found MS-ESI $[M+Na]^+$ 226.08.

^{1}H NMR

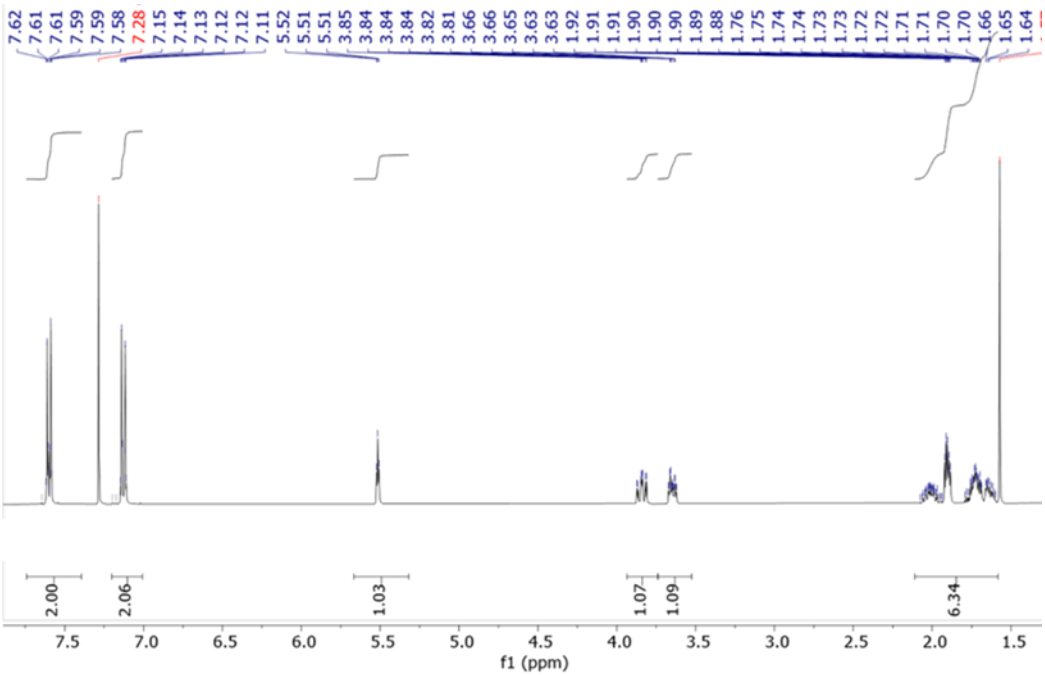

[1] Z. Hao, A. Iqbal, N. Tebaldi and K. Praefcke, US Patent, 5969154, 1999

^{13}C NMR

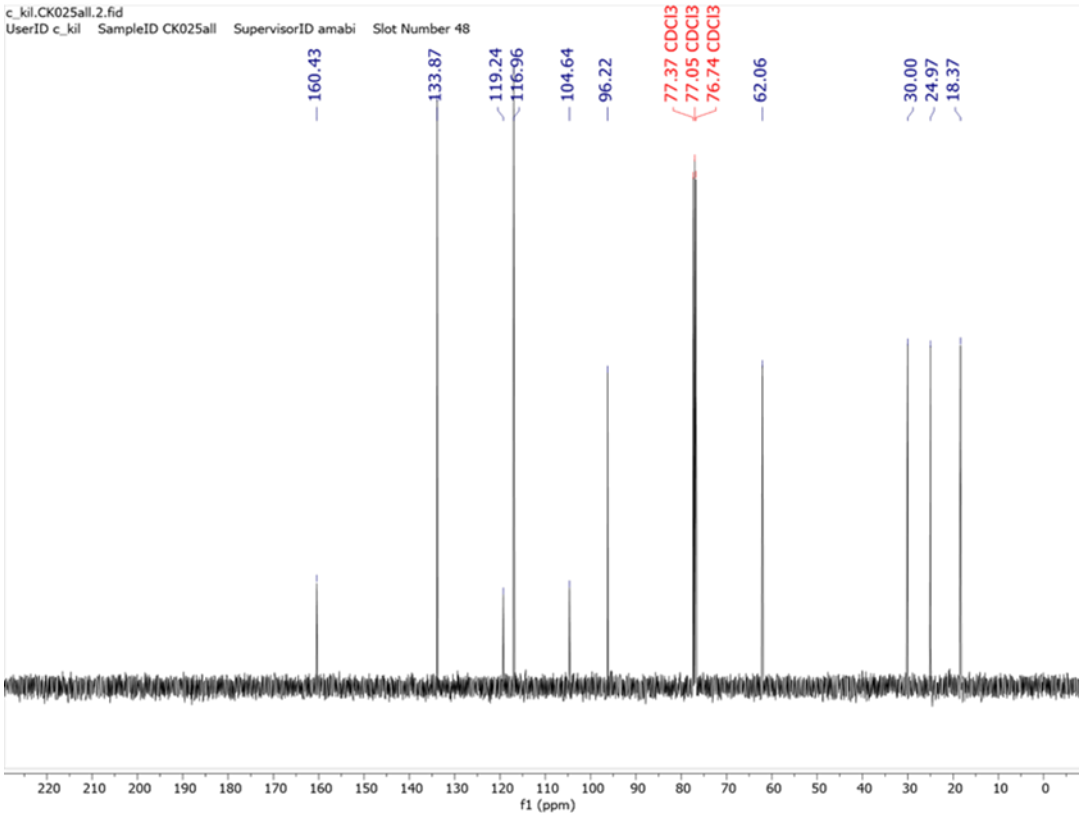
c_kil.CK025all.2.fid
UserID c_kil SampleID CK025all SupervisorID amabi Slot Number 48
160.43
133.87
119.24
116.96
104.64
96.22
77.37 CDCl3
77.05 CDCl3
76.74 CDCl3
62.06
30.00
24.97
18.37
220 210 200 190 180 170 160 150 140 130 120 110 100 90 80 70 60 50 40 30 20 10 0
f1 (ppm)

IR

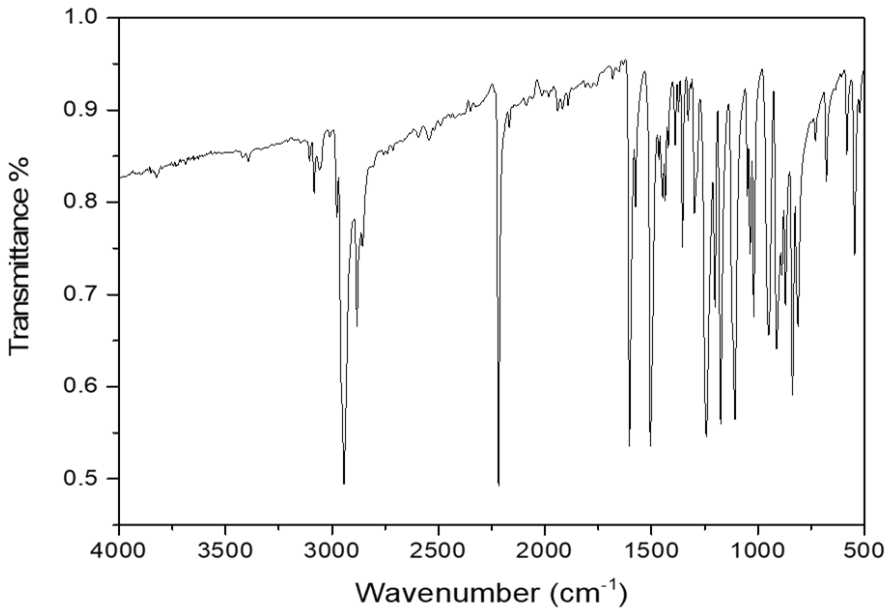
Transmittance %
1.0
0.9
0.8
0.7
0.6
0.5
4000 3500 3000 2500 2000 1500 1000 500
Wavenumber (cm-1)

Ethyl 3-oxo-3(thiophen-2-yl)propanoate

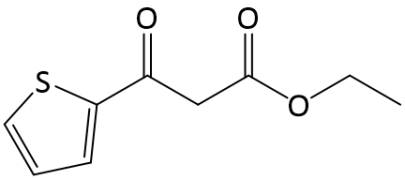

Following a literature procedure,[2] sodium hydride (60% dispersion in mineral oil) (21.4 g, 890 mmol), was suspended in toluene (anhydrous) (400 mL) under argon. Diethyl carbonate (43.1 mL, 355 mmol) was added to the suspension. A solution of 2-acetylthiophene (12.4 mL, 198 mmol) in toluene (anhydrous) (50 mL) was added over 3 hours to the reaction mixture which was stirring at 90 °C. Upon completion of addition the reaction mixture continued to stir at 90 °C for 16 h. The reaction mixture was cooled to room temperature and glacial acetic acid (ca. 50 mL) was added dropwise, followed by ice cold water (300 mL). The solution was extracted with toluene (3 x 30 mL). The organic layers were washed with water (2 x 50 mL), dried over $MgSO_4$ and filtered. The resulting brown oil was distilled via Kugelrohr (155 °C, 78 mbar) to give the desired product as a yellow oil (21.2 g, 106 mmol, 54%) that gave analytical data consistent with the literature.[3] ^{1}H NMR (400 MHz, $CDCl_3$) δ 7.75 (dd, *J* = 3.8, 1.2 Hz, 1H), 7.70 (dd, *J* = 5.0, 1.2 Hz, 1H), 7.15 (dd, *J* = 5.0, 3.8 Hz, 1H), 4.21 (q, *J* = 7.1 Hz, 2H), 3.92 (s, 2H), 1.26 (t, *J* = 7.1 Hz, 3H) ppm; ^{13}C NMR: (400MHz, $CDCl_3$)δ 185.1, 166.9, 135.0, 133.4, 128.5, 61.4, 46.3, 14.0 ppm; υ_{max} (ATR-IR) 3092 (CH stretch) 2984 (CH stretch), 2943 (CH stretch), 1740 (C=O stretch), 1658 (C=O stretch), 1524 (CC stretch), 1417, 1365, 1318, 1262, 1207, 1142, 1030, 914, 842 cm^{-1}; *m/z*, calcd. for $C_9H_{10}O_3S$: 198.04, found MS-ESI $[M+Na]^+$ 221.02.

[2] S. Stag, J.-Y. Balandier, V. Lemaur, O. Fenwick, G. Tregnago, F. Quist, F. Cacialli, J. Cornil, Y.H.Geerts, *Dyes Pigments*, 2013, **97**, 198-208.

[3] J. D. White, R. Juniku, K. Huang, J. Yang and D. T. Wong, *J. Med. Chem*., 2009, **52**, 5872–5879.

^{1}H NMR

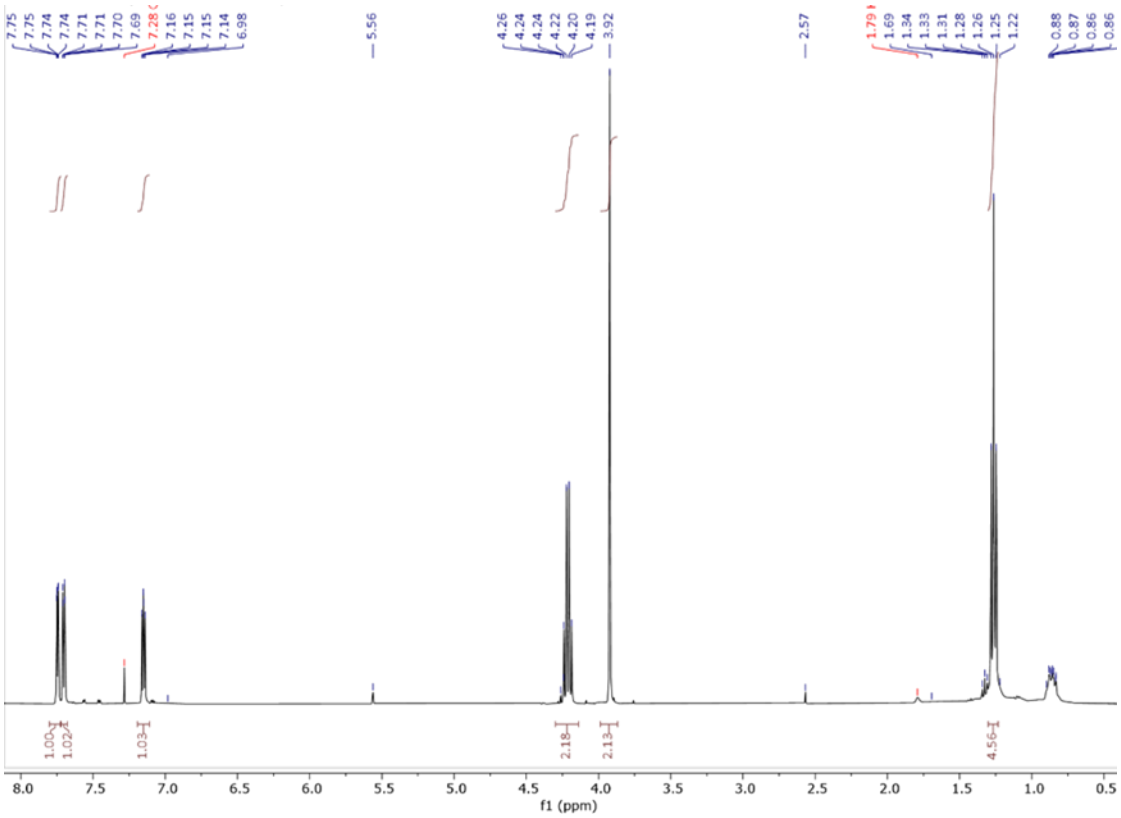

^{13}C NMR

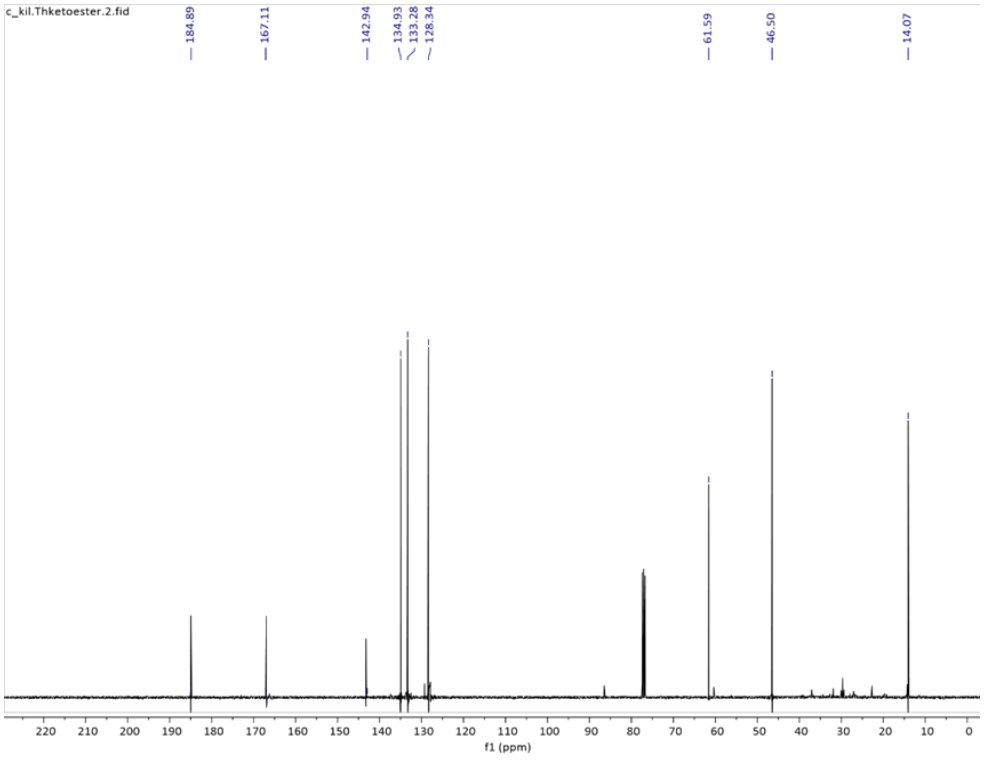

IR

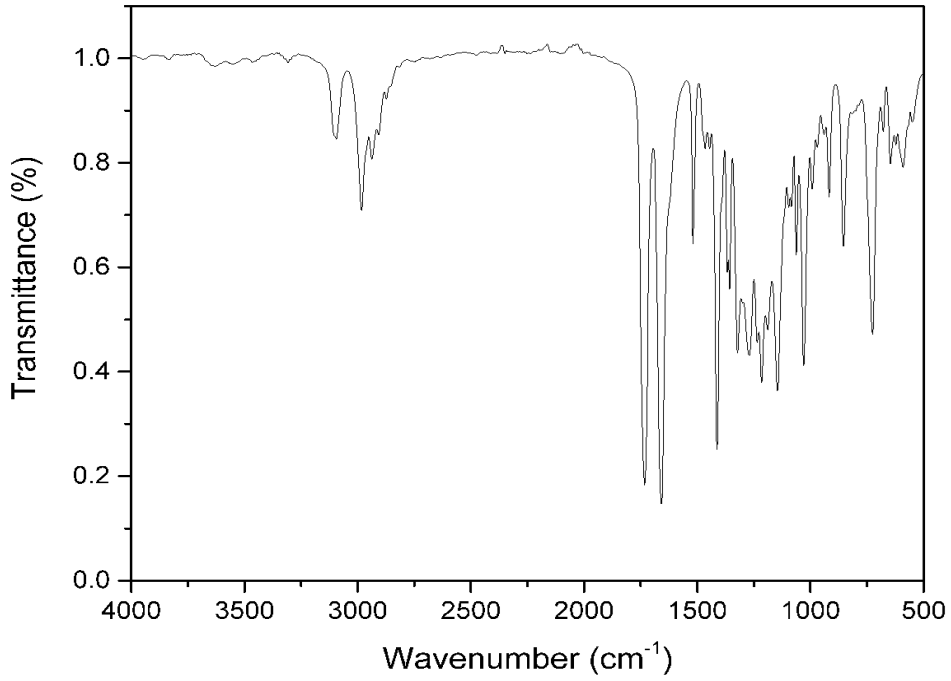

Diethyl 2-(thiophene-2-carbonyl) succinate

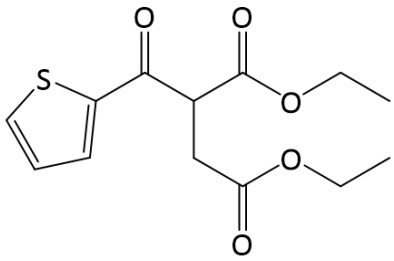

In a flame dried flask, sodium (3.00 g, 130 mmol) was dissolved in absolute ethanol (100 mL). Ethyl 3-oxo-3(thiophen-2-yl)propanoate (4) (20.0 g, 101 mmol) was added to the reaction mixture at 0 °C followed by the dropwise addition of ethyl bromoacetate (23 mL, 201 mmol). The reaction mixture is stirred at room temperature for 72 h. The excess solvent was removed under reduced pressure and the resulting yellow oil and white powder were poured into water (100 mL), whereby the white powder dissolved. The product was extracted into diethyl ether (3 x 30 mL). The organic layer was washed with 2M hydrochloric acid (3 x 30 mL) and dried over $MgSO_4$ and filtered. The diethyl ether was removed under reduced pressure to give the desired product as a yellow oil, which was used in the next step without further purification. (25.0 g, 80 mmol, 79%) ^{1}H NMR (400 MHz, $CDCl_3$) δ 7.93 (dd, *J* = 3.9, 1.1 Hz, 1H), 7.73 (dd, *J* = 5.0, 1.1 Hz, 1H), 7.19 (dd, *J* = 4.9, 3.8 Hz, 1H), 4.71 (t, *J* = 7.3 Hz, 1H), 4.24 – 4.12 (m, 4H), 3.15 – 3.02 (m, 2H), 1.30 – 1.17 (m, 6H) ppm.

^{1}H NMR

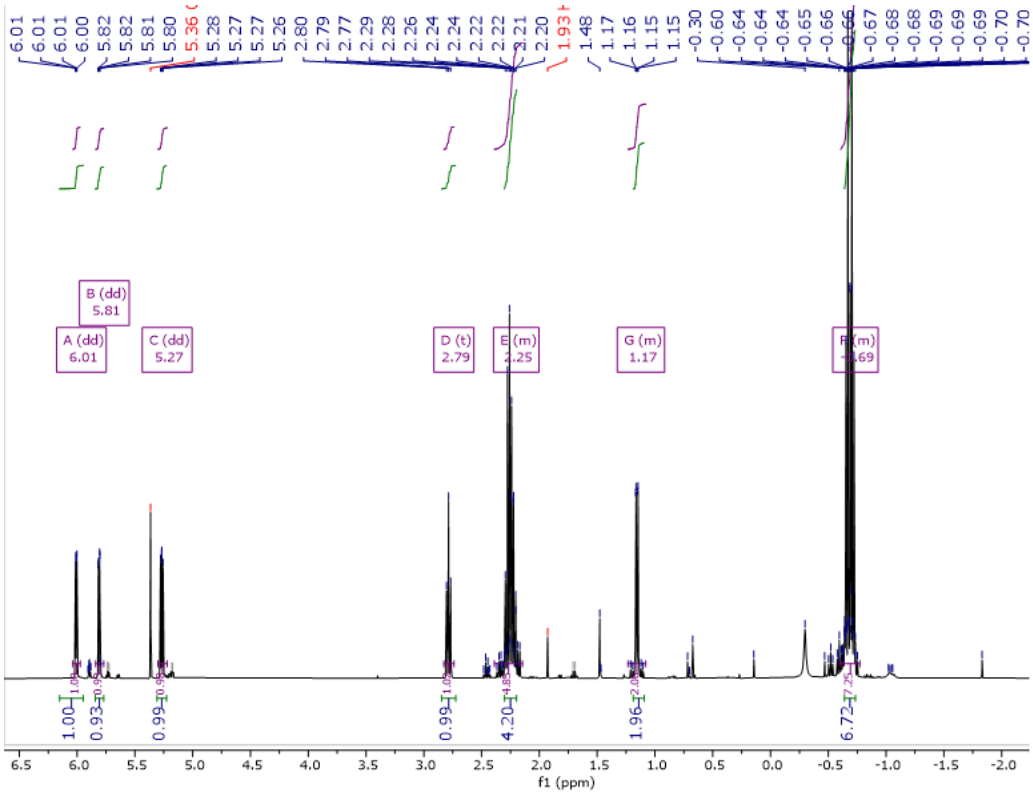

4-Butyryl-5-(thiophen-2-yl)-1,3-dihydro-2H-pyrrol-2-one

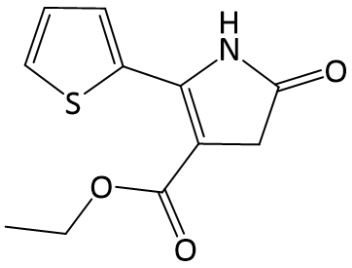

Ammonium acetate (27 g, 352.10 mmol) in glacial acetic acid (60 mL) was added to diethyl 2-(thiophene-2-carbonyl)succinate (5) (10.00 g, 35.21 mmol). The reaction mixture was stirred at 120 °C for 24 h under argon. The reaction mixture was cooled to room temperature and poured into water, the resulting precipitate was filtered and washed with water and ethyl acetate to give the desired product as a blue-black solid (3.17 g, 13.36 mmol, 38 % yield) %); Lit Mp 196 -199 °C, Exp mp 195-197 °C; ^{1}H NMR (400 MHz, $CDCl_3$) δ 8.83 (s, 1H), 7.82 (dd, *J* = 3.9, 1.2 Hz, 1H), 7.61 (dd, *J* = 5.0, 1.2 Hz, 1H), 7.18 (dd, *J* = 5.0, 3.9 Hz, 1H), 4.27 (q, *J* = 7.1 Hz, 2H), 3.57 (s, 2H), 1.34 (t, *J* = 7.1 Hz, 3H) ppm; 13C NMR (101 MHz, $CDCl_3$) δ 176.89, 163.41, 143.93, 131.24, 130.93, 129.83, 127.26, 102.73, 60.32, 38.76, 14.40 ppm; υ_{max} (ATR-IR) 3178 (NH stretch), 3093 (CH stretch), 2975 (CH stretch) 1709 (C=O stretch) 1686 (C=O stretch), 1597 (CC stretch), 1507, 1432, 1314 1253, 1065, 759, 712 cm^{-1} ; *m/z*, calcd. for: $C_{11}H_{11}NO_3S$: 237.05, ESI-MS found: [M+ H] 238.05

^{1}H NMR

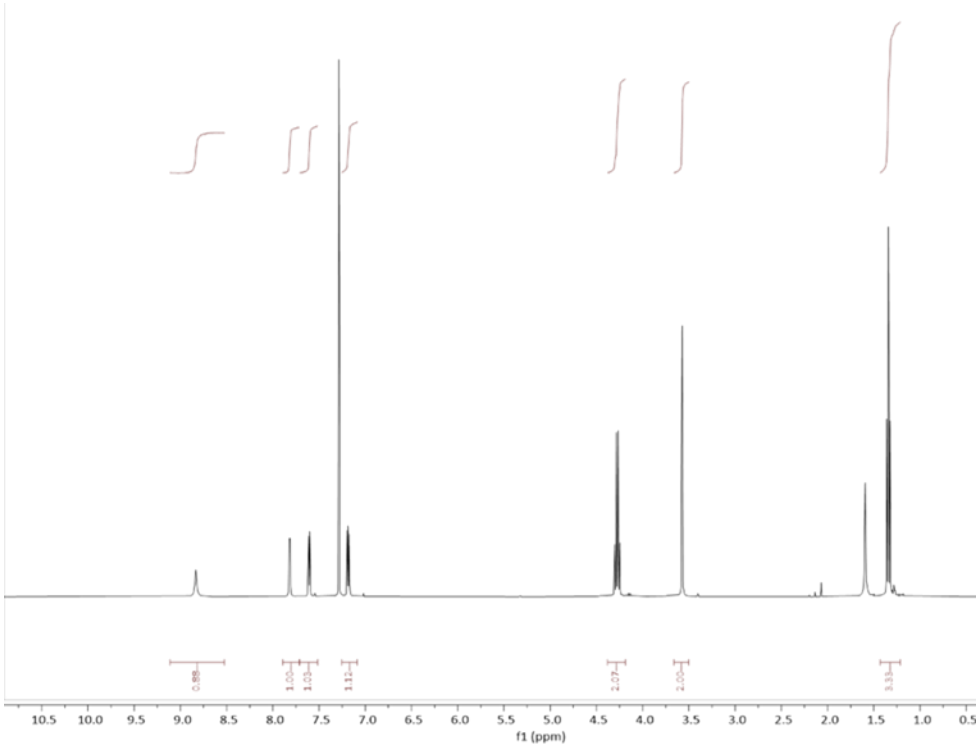

^{13}C NMR

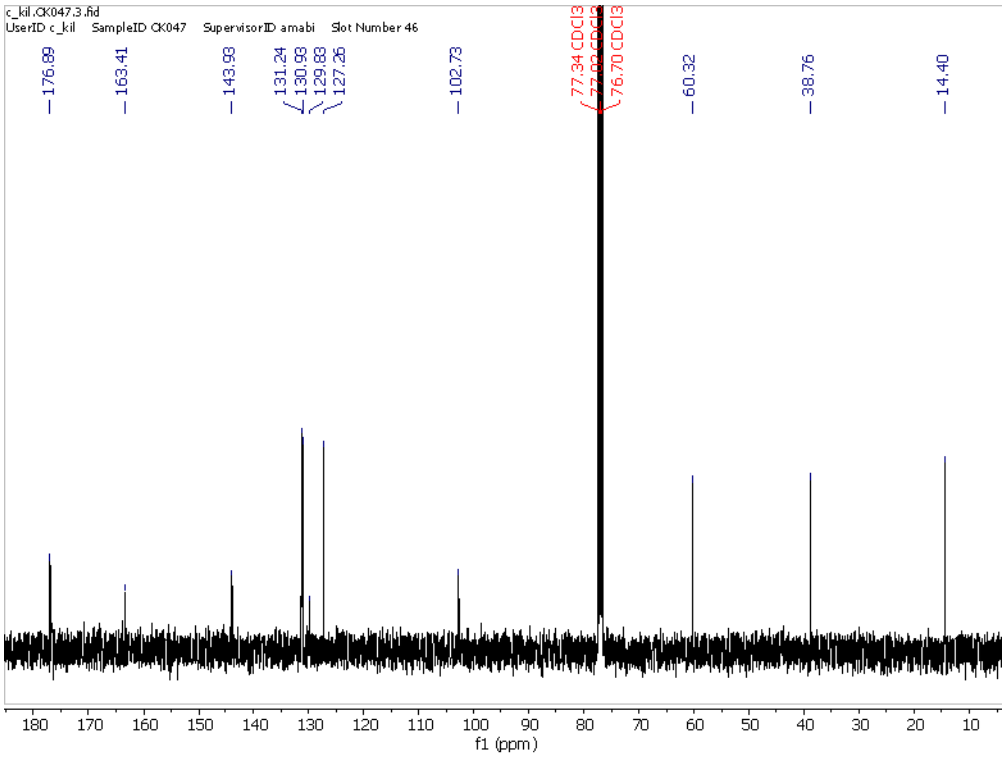

IR

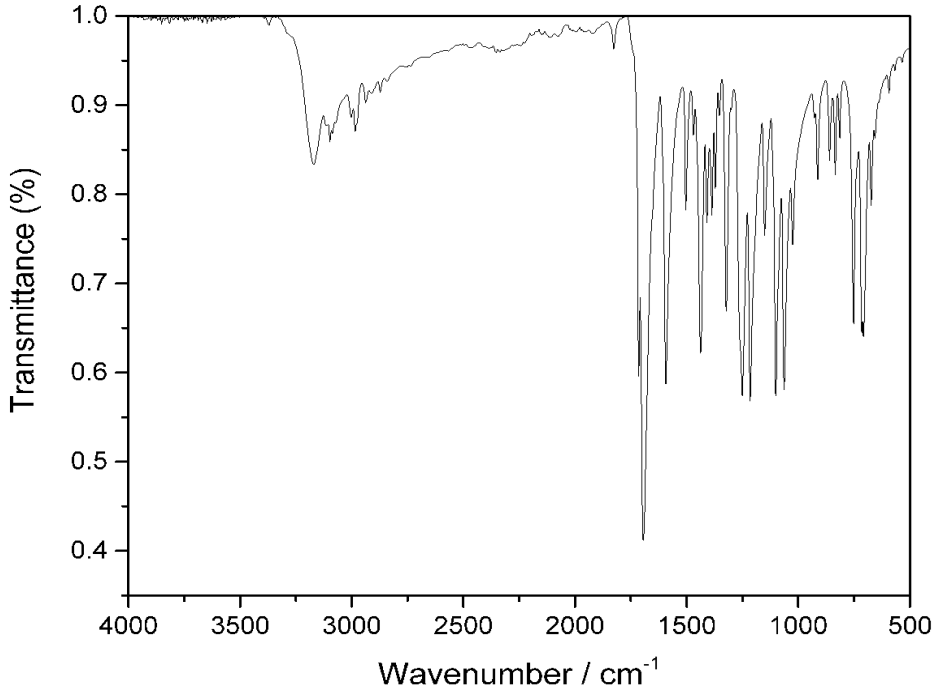

3-(-((tetrahydro-2H-pyran-2-yl)oxy)phenyl-6-(thiophen-2-yl)-2,5-dihydropyrrole[3,4-c]pyrrole-1,4-dione (2)

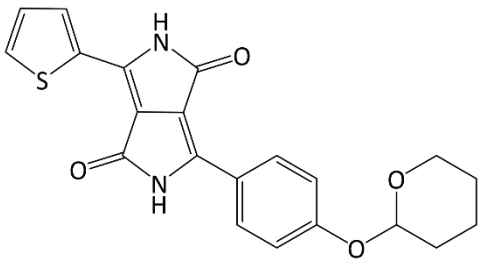

In a flame dried flask, sodium (0.41 g, 17.84 mmol) was stirred in *tert*-amyl alcohol (40 mL) at 100 °C for 2 h until dissolved. The reaction mixture was cooled to room temperature, then ethyl 5-oxo-2- (thiophene-2-yl)-4,5-dihydro-1H-pyrrole-3-carboxylate (3.00 g, 12.6 mmol) and 4- ((tetrahydro-2H-pyran-2-yl)oxy)benzonitrile (2.83 g, 14.0 mmol) were added. The reaction mixture was stirred at 100 °C for 7 h. The reaction mixture was poured into water (ca. 100 mL) and precipitation occurred. The solid was filtered and washed with water, methanol and diethyl ether to the produce the desired product as a deep red solid (2.07 g, 5.23 mmol, 42 %). Mp > 300 °C ^{1}H NMR (400 MHz, DMSO-d_6) δ 11.25 (s, 1H), 11.16 (s, 1H), 8.53 – 8.35 m, 2H), 8.22 (dd, *J* = 3.8, 1.2 Hz, 1H), 7.95 (dd, *J* = 5.0, 1.2 Hz, 1H), 7.30 (dd, *J* = 5.0, 3.8 Hz, 1H), 7.19 (m, 2H), 5.72 – 5.56 (m, 1H), 3.86 – 3.47 (m, 2H), 2.11 – 1.34 (m, 6H) ppm; υ_{max} (ATR-IR) 3108 (NH stretch), 2960 (CH stretch), 2840 (CH stretch), 1632 (CO stretch), 1596,

1503, 1432, 1403, 1241,1176, 1132, 1063, 1024, 946, 899, 830, 784, 737, 711, 621, 514, 478, 425 cm^{-1}; *m/z*, calcd. for $C_{21}H_{18}N_2O_4S$: 394.10, found MS-MALDI-TOF [M- H] 385.31; Elemental analysis: calcd for $C_{21}H_{18}N_2O_4S$: C, 63.95; H, 4.60; N, 7.10%; found: C, 63.58; H, 4.97; N, 6.82%.

^1H NMR

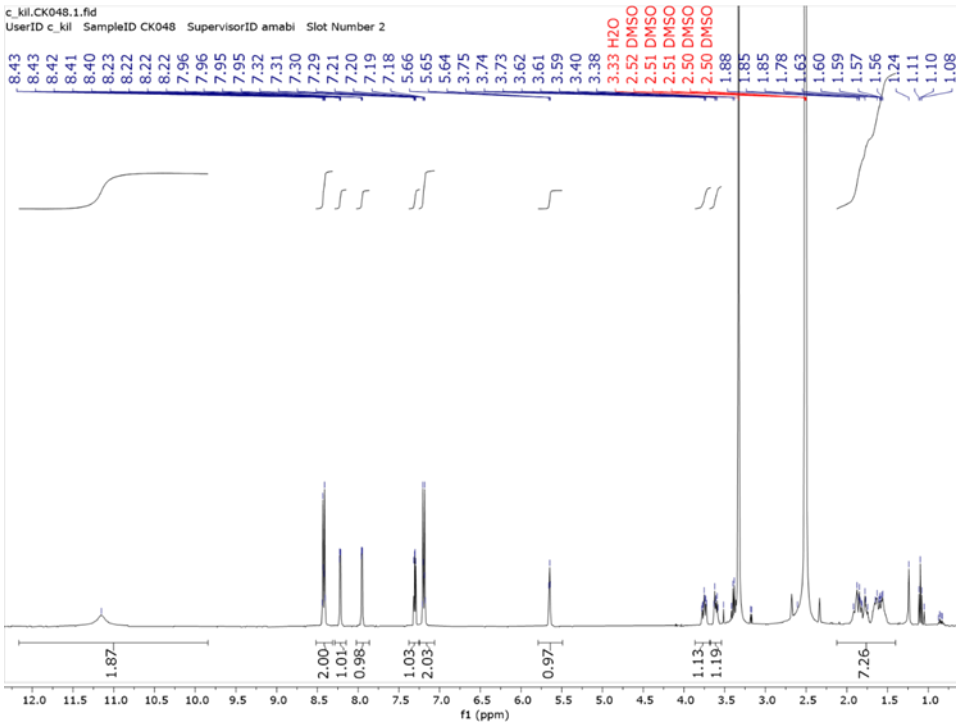

IR

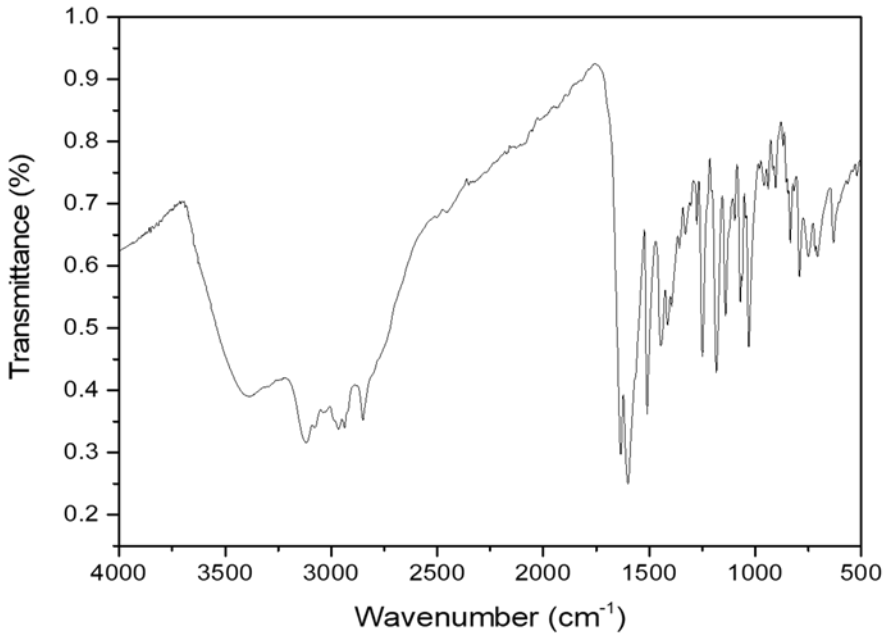

2,5-Dihexyl-3-(4-hydroxyphenyl)-6-(thiophen-2-yl)-2,5-dihydropyrrolo[3,4-c]pyrrole-1,4-dione (3)

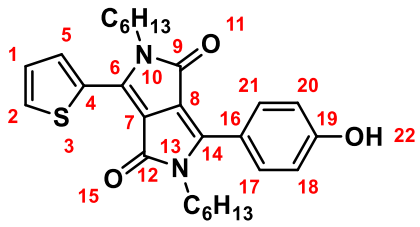

Compound **2** (500 mg, 1.27 mmol, 1 eq., prepared according to a literature procedure[4]), K_2CO_3 (526 mg, 3.81 mmol, 3 eq), and *N*,*N*-dimethylformamide (anhydrous, 50 mL) were combined under argon in a flame dried 100 mL two-neck round bottom flask fitted with reflux condenser. The resulting mixture was heated to 40 °C for 1 h. Hexyliodide (808 mg, 3.81 mmol, 3 eq) was then added dropwise *via* syringe. The resulting mixture was stirred under argon at 40 °C for 16 h. After cooling to room temperature, the solvent was removed under reduced pressure and the resulting solid was dissolved in minimal amount of acetonitrile before pouring into HCl (6 M, 100 mL). The resulting suspension was stirred for 4 h at rt. The solid was collected by filtration and washed with H_2O before drying under air. The crude product was subjected to column chromatography on silica (dry load, cyclohexane:ethyl acetate, 8:2 → 7:3) followed by precipitation from ethyl acetate (0.5 mL) and cyclohexane (5 mL) to give a red solid (147 mg, 307 µmol, 24%). *Rf* 0.30 (cyclohexane:ethyl acetate, 7:3, silica).

Alternatively, compound **2** (500 mg, 1.27 mmol, 1 eq.) and caesium carbonate (1.66 g, 5.08 mmol, 4 eq) were stirred at 90 °C in acetonitrile (resulting conc. ~50 mmol of DPP) for 15 min. Hexyl bromide (839 mg, 5.08 mmol) was then added to the reaction mixture, which was stirred at 90 °C for 24 h. The reaction mixture was cooled to room temperature and stirred in 6 M HCl until precipitation occurred. The solid was filtered and washed with water, methanol and diethyl ether. After drying *in vacuo*, the crude product was purified as above, to give a red solid (237 mg, 495 µmol, 39%). Both products gave the same analysis.

Mp: 220-222 °C;

[4] C.E. Killalea, M. Samperi, G. Siligardi and D.B. Amabilino, *Chem. Commun*., 2022, **58**, 4468-4471.

^{1}H NMR (400 MHz, DMSO) δ 10.34 (s, 1H, H^{22}), 8.76 (dd, *J* = 3.8, 1.0 Hz, 1H, H^{5}), 8.07 (dd, *J* = 5.0, 1.0 Hz, 1H, H^{2}), 7.77 (d, *J* = 8.7 Hz, 1H, $H^{17/21}$), 7.40 (dd, *J* = 4.9, 4.0 Hz, 1H, H^{1}), 6.94 (d, *J* = 8.7 Hz, 1H, $H^{18/20}$), 4.00-3.86 (m, 2H, CH_2N), 3.80 (t, *J* = 7.4 Hz, 2H, CH_2N), 1.68-1.52 (m, 2H, CH_2), 1.51-1.42 (m, 2H, CH_2), 1.36-1.11 (stack, 12H, CH_2), 0.89-0.75 (stack, 6H, CH_3);

^{13}C NMR (101 MHz, DMSO) δ 161.34, 160.75, 147.32, 139.09, 134.22, 132.46, 130.81, 129.18, 128.57, 118.32, 115.77, 106.99, 106.79, 41.18, 41.12, 30.73, 30.51, 29.25, 28.44, 25.84, 25.64, 21.93, 21.85, 13.83, 13.78;

IR (thin film, cm^{-1}): 3228 (O-H), 3084 (C-H), 2953 (C-H), 2926 (C-H), 2854 (C-H), 1683 (C=O), 1641 (C=O), 1608 (C=C), 1587 (C=C), 1564 (C=C), 1514 (C=C), 1448 (C=C), 1400 (C=C);

MS TOF (ESI+): m/z: 479.2 $[M+H]^+$, 501.2 $[M+Na]^+$;

HRMS (ESI+): $[M+H]^+$ calcd. for $C_{28}H_{35}N_2O_3S$, 479.2363; found, 479.2368.

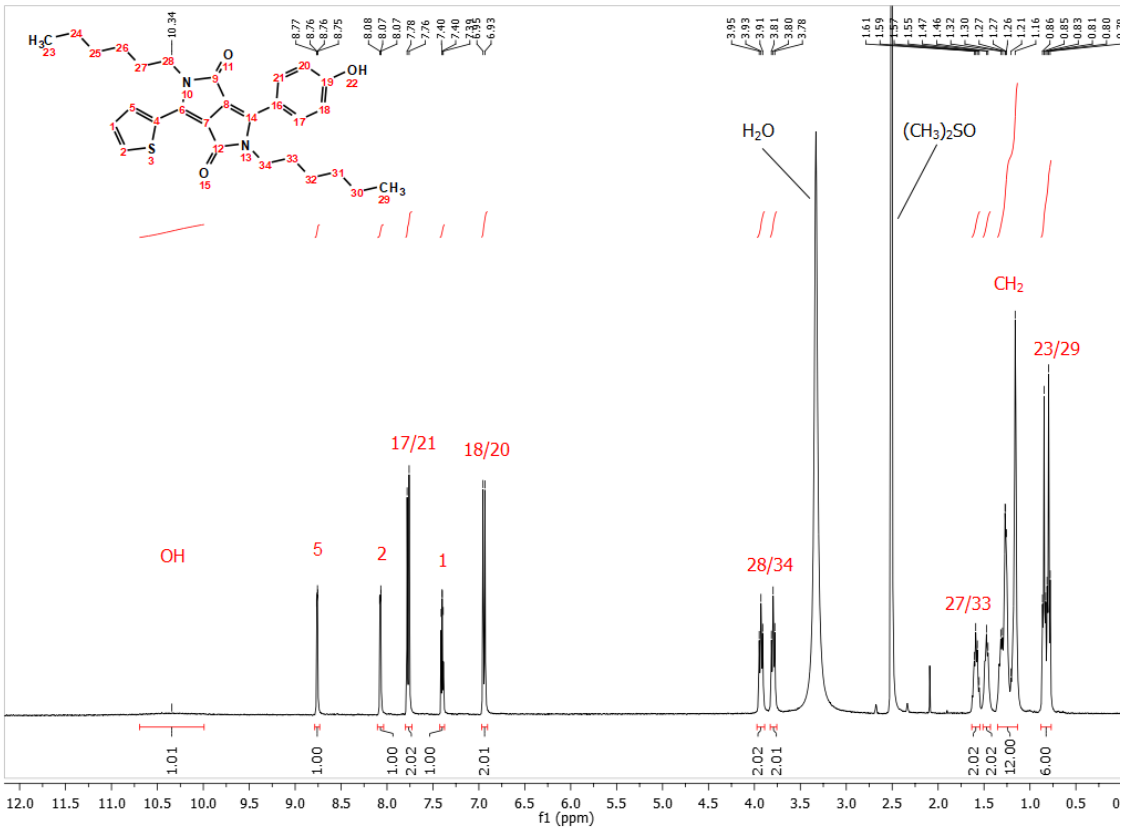

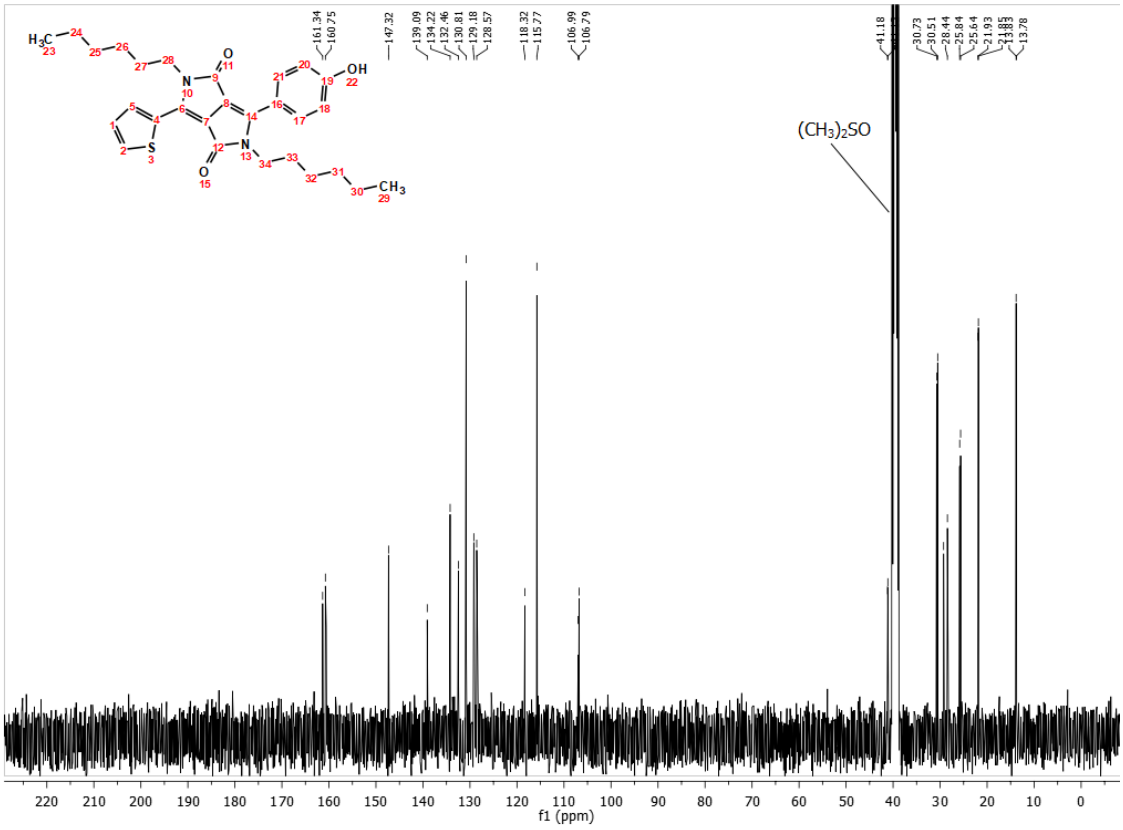
161.34
160.75
147.32
139.09
134.22
132.46
130.81
129.18
128.57
118.32
115.77
106.99
106.79
41.18
30.73
30.51
28.44
25.84
25.64
21.93
21.85
13.83
13.78
(CH3)2SO
220 210 200 190 180 170 160 150 140 130 120 110 100 90 80 70 60 50 40 30 20 10 0
f1 (ppm)

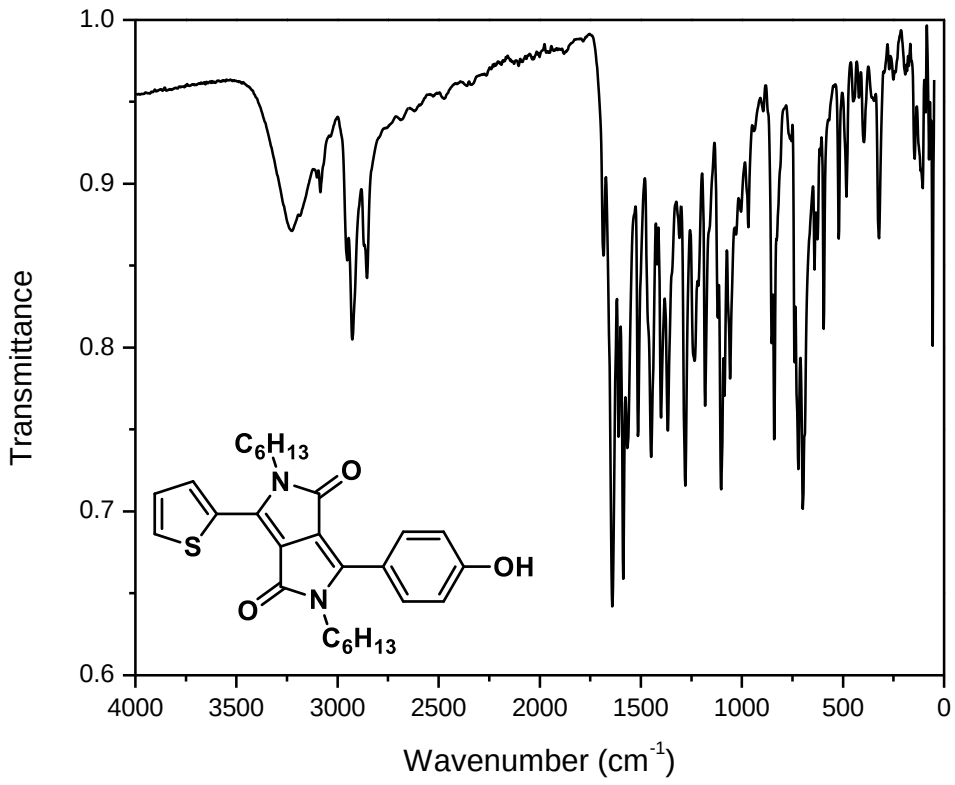
Transmittance
1.0
0.9
0.8
0.7
0.6
4000 3500 3000 2500 2000 1500 1000 500 0
Wavenumber (cm-1)
C6H13
N
O
S
OH
O
N
C6H13

Ethyl (S)-2-(4-(2,5-dihexyl-3,6-dioxo-4-(thiophen-2-yl)-2,3,5,6-tetrahydropyrrolo[3,4-c]pyrrol-1-yl)phenoxy)propanoate ((*S*)-4)

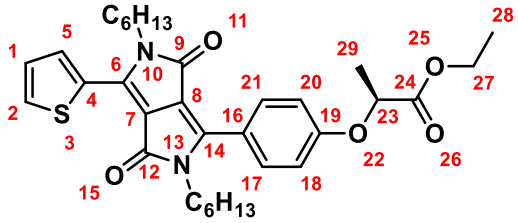

To a flame dried flask with septum (flask 1) containing triphenylphosphine (1.10 g, 4.18 mmol, 4 eq) and THF (anhydrous, 10 mL) under argon at 0 °C, diisopropylazodicarboxylate (978 mg, 4.18 mmol, 4 eq) was added. The resulting mixture was sonicated at 0 °C for 30 min. In a separate flame dried flask with septum (flask 2) compound **3** (500.0 mg, 1.04 mmol, 1 eq), (+)-ethyl D lactate (493 mg, 4.18 mmol, 4 eq), and toluene (anhydrous 10 mL) were combined under argon and cooled to 0 °C. The contents of flask 1 was transferred to flask 2 which was kept at 0 °C. A further portion of toluene (2 mL) was used to wash remnants of flask 1 and added to flask 2. The resulting mixture in flask 2 was allowed to warm to 50 °C over 1 h while sonicated. After cooling to rt solvent was removed under reduced pressure. The crude product was dissolved in CH_2Cl_2 (100 mL) and washed with H_2O (100 mL). The organic phase was dried ($MgSO_4$) and solvent removed under reduced pressure. The product was purified by column chromatography on silica (cyclohexane:ethyl acetate, 8:2) to give a red solid (590 mg, 1.02 mmol, 98%). *Rf*: 0.32 (cyclohexane:ethyl acetate, 8:2, silica).

Mp: 89-90 °C;

^{1}H NMR (400 MHz, $CDCl_3$) δ 8.89 (dd, *J* = 3.9, 1.1 Hz, 1H, H^{5}), 7.82 (d, *J* = 8.9 Hz, 2H, $H^{17/21}$), 7.63 (dd, *J* = 5.0, 1.0 Hz, 1H, H^{2}), 7.28 (dd, *J* = 5.0, 4.0 Hz, 1H, H^{1}), 7.00 (d, *J* = 8.9 Hz, 2H, $H^{18/20}$), 4.82 (q, *J* = 6.8 Hz, 1H, H^{23}), 4.25 (q, *J* = 7.1 Hz, 2H, H^{27}), 4.08-3.93 (m, 2H, C*H*$_2$N), 3.86-3.72 (m, 2H, C*H*$_2$N), 1.76-1.58 (stack, 7H, C*H*$_2$/C*H*$_3$), 1.44-1.21 (stack, 15H, C*H*$_2$/C*H*$_3$), 0.93-0.77 (stack, 6H, C*H*$_3$);

^{13}C NMR (101 MHz, $CDCl_3$) δ 171.77, 162.43, 162.08, 159.84, 146.96, 140.88, 135.36, 130.82, 130.79, 129.93, 128.71, 121.66, 115.46, 108.95, 107.92, 72.81, 61.68, 42.37, 42.18, 31.55, 31.39, 30.03, 29.64, 26.67, 26.59, 22.68, 22.65, 18.63, 14.29, 14.14, 14.10;

IR (thin film, cm^{-1}): 3072 (C-H), 2953 (C-H), 2924 (C-H), 2858 (C-H), 1745 (C=O), 1654 (C=O), 1604 (C=C), 1556 (C=C), 1504 (C=C), 1469 (C=C), 1450 (C=C);

MS TOF (ESI+): m/z: 579.3 $[M+H]^+$, 601.3 $[M+Na]^+$;

HRMS (ESI+): $[M+H]^+$ calcd. for $C_{33}H_{43}N_2O_5S$, 579.2887; found, 579.2868.

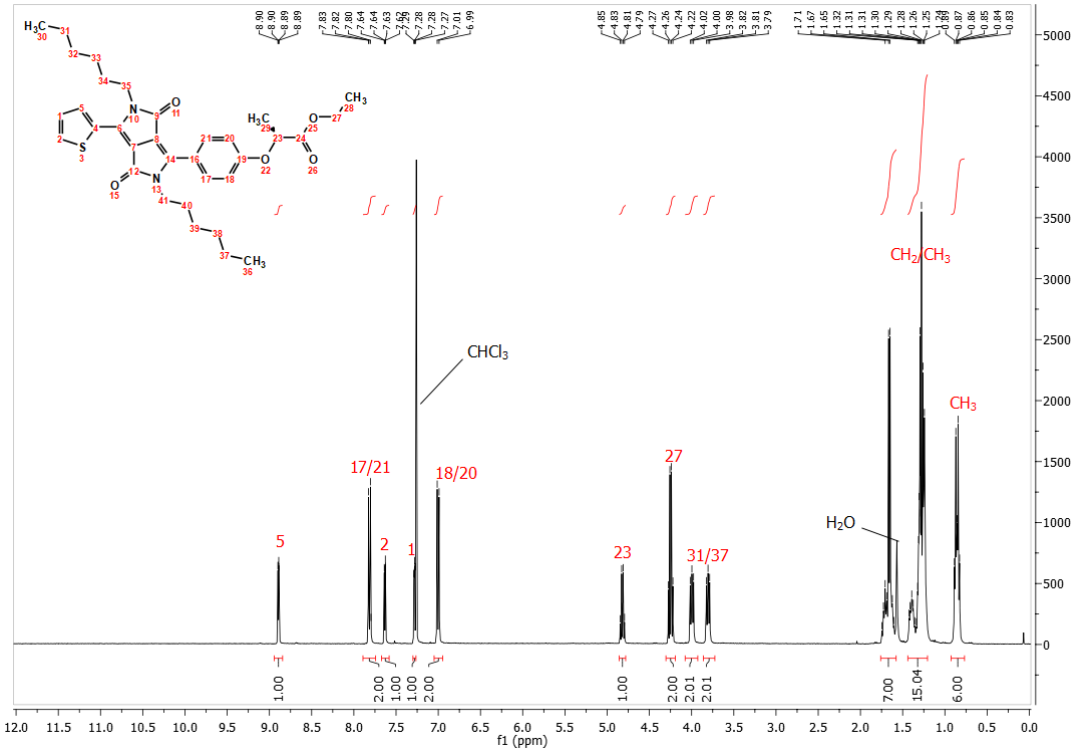

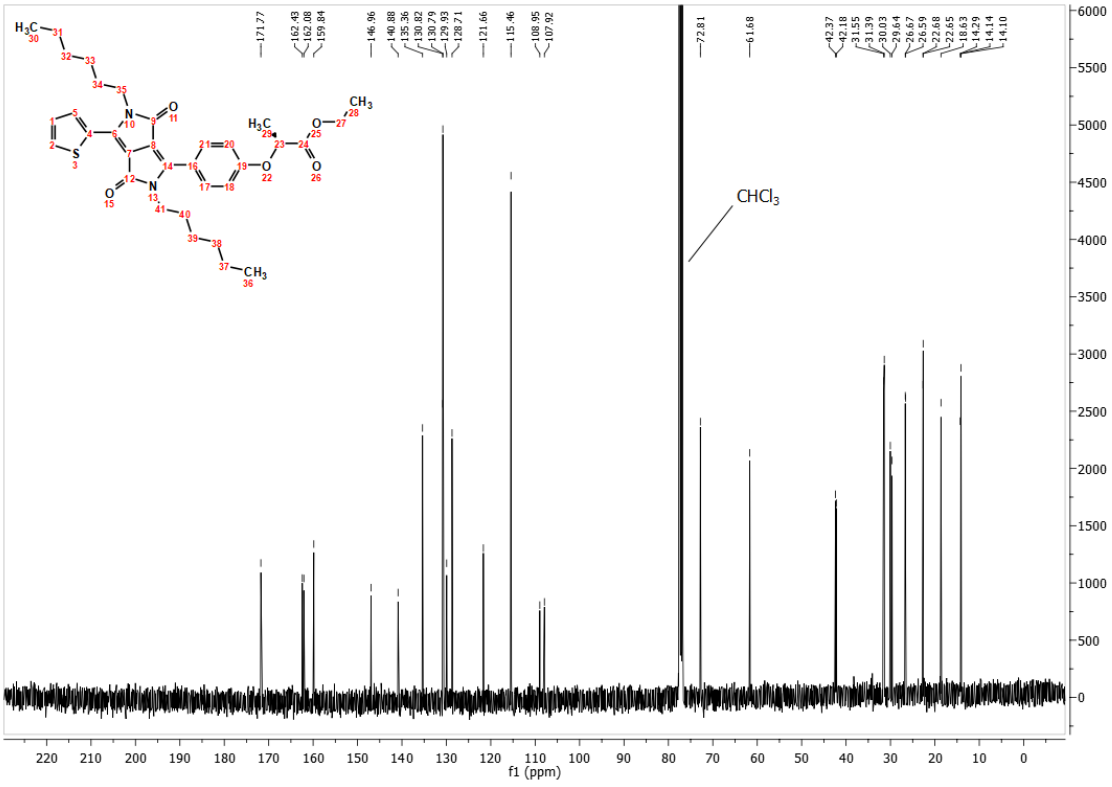
171.77
162.43
162.08
159.84
146.96
140.88
135.36
130.92
130.79
129.93
128.71
121.66
115.46
108.95
107.92
72.81
61.68
42.37
42.18
31.55
31.39
30.03
29.84
26.67
26.59
22.68
22.65
18.83
14.29
14.14
14.10
CHCl3
f1 (ppm)

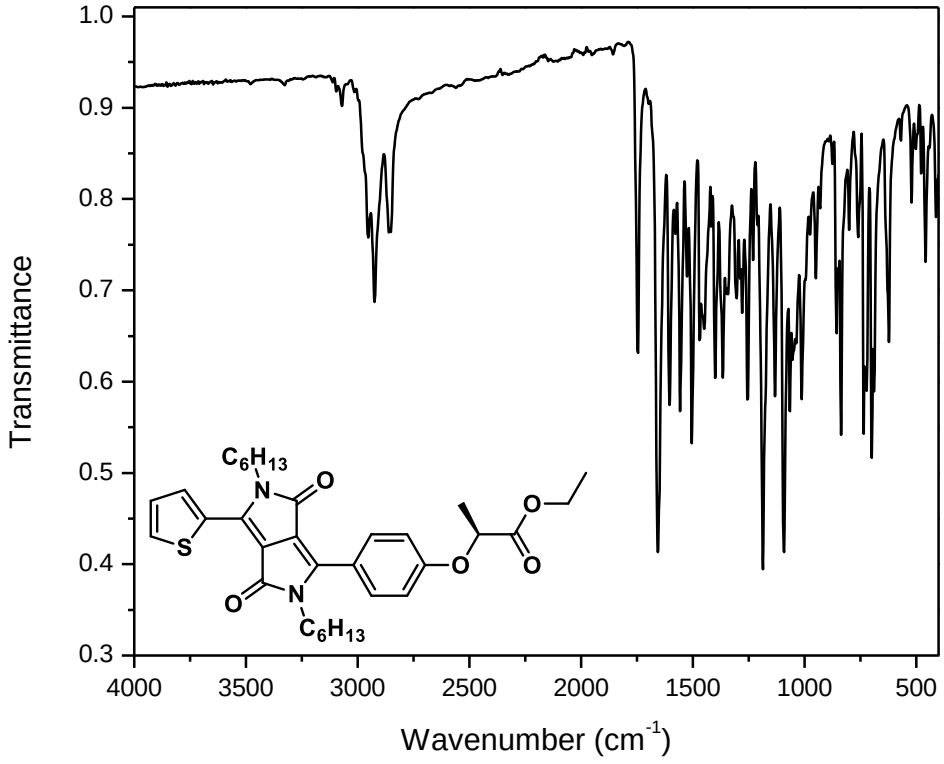
Transmittance
Wavenumber (cm-1)
C6H13
C6H13

Ethyl (S)-2-(4-(4-(5-bromothiophen-2-yl)-2,5-dihexyl-3,6-dioxo-2,3,5,6-tetrahydropyrrolo[3,4-c]pyrrol-1-yl)phenoxy)propanoate ((*S*)-5)

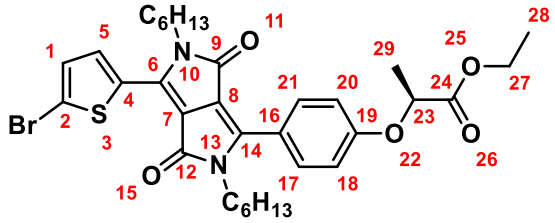

Compound (*S*)-**4** (500 mg, 864 µmol, 1 eq), $CHCl_3$, (85 mL) and *N*-bromosuccinimide (185 mg, 1.04 µmol, 1.2 eq) were combined in a 250 mL round bottom flask under darkness. The resulting mixture was stirred for 30 min in the dark before the addition of acetic acid (glacial, 10 drops). The reaction mixture was stirred in the dark at rt for 24 h. Solvent was removed under reduced pressure in the dark, and the crude solid dried further *in vacuo* and under darkness. The product was purified by column chromatography on silica (Cyclohexane:ethyl acetate, 9:1 → 8:2) To give a dark red solid (341 mg, 518 µmol, 60%). *Rf*: 0.41 (Cyclohexane:ethyl acetate, 8:2, silica).

Mp: 106-108 °C;

^{1}H NMR (400 MHz, $CDCl_3$) δ 8.64 (d, *J* = 4.2 Hz, 1H, H^5), 7.81 (d, *J* = 8.9 Hz, 2H, $H^{17/21}$), 7.23 (d, *J* = 4.2 Hz, 1H, H^1), 7.00 (d, *J* = 8.9 Hz, 2H, $H^{18/20}$), 4.82 (q, *J* = 6.8 Hz, 1H, H^{23}), 4.25 (q, *J* = 7.1 Hz, 2H, H^{27}), 3.99-3.85 (m, 2H, C*H*$_2$N), 3.84-3.71 (m, 2H, C*H*$_2$N), 1.76-1.57 (stack, 7H, C*H*$_2$/C*H*$_3$), 1.44-1.17 (stack, 15H, C*H*$_2$/C*H*$_3$), 0.95-0.77 (stack, 6H, C*H*$_3$);

^{13}C NMR (101 MHz, $CDCl_3$) δ 171.73, 162.33, 161.82, 159.96, 147.45, 139.46, 135.21, 131.68, 131.34, 130.81, 121.53, 118.93, 115.48, 108.84, 108.16, 72.81, 61.69, 42.42, 42.19, 31.51, 31.38, 30.08, 29.62, 26.64, 26.58, 22.65, 18.62, 14.28, 14.14, 14.10;

IR (thin film, cm^{-1}): 2945 (C-H), 2927 (C-H), 2868 (C-H), 2854 (C-H), 1748 (C=O), 1660 (C=O), 1602 (C=C), 1583 (C=C), 1506 (C=C), 1454 (C=C);

MS TOF (ESI+): *m*/*z*: 657.2 $[M+H]^+$, 679.2 $[M+Na]^+$;

HRMS (ESI+): $[M+H]^+$ calcd. for $C_{33}H_{42}BrN_2O_5S$, 657.1992; found, 657.1970

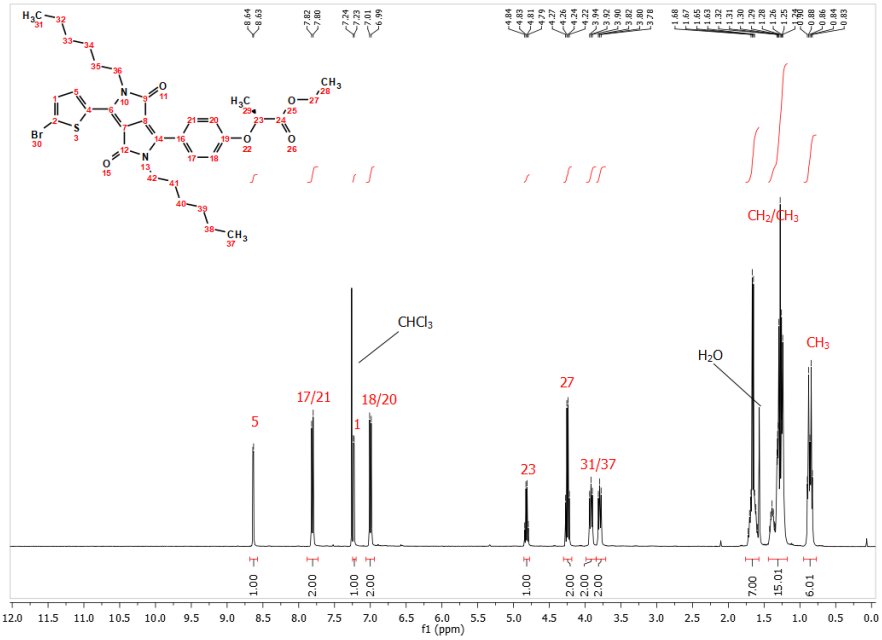
CHCl3
H2O
CH2/CH3
CH3
5
17/21
18/20
1
27
23
31/37
f1 (ppm)

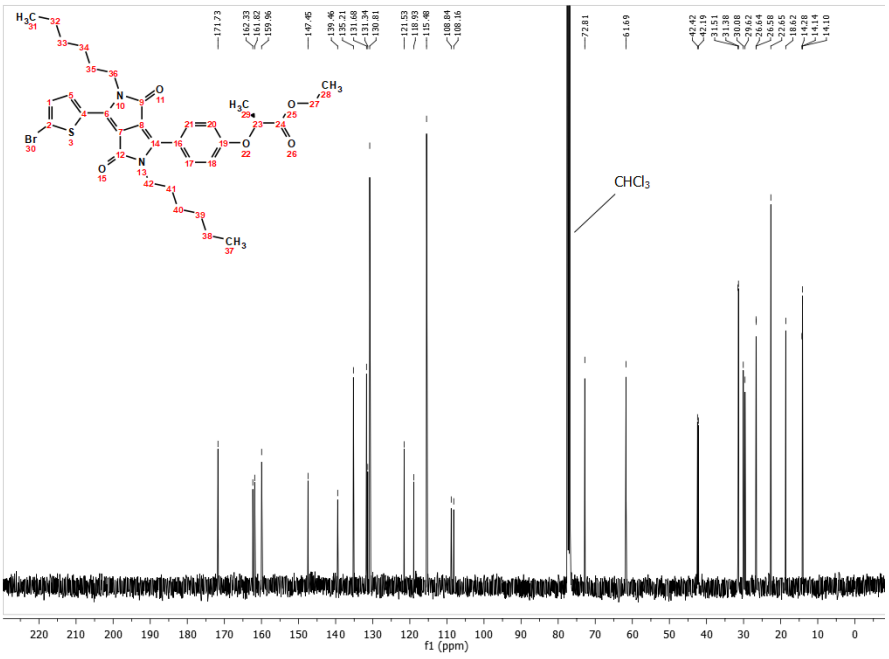
CHCl3
f1 (ppm)

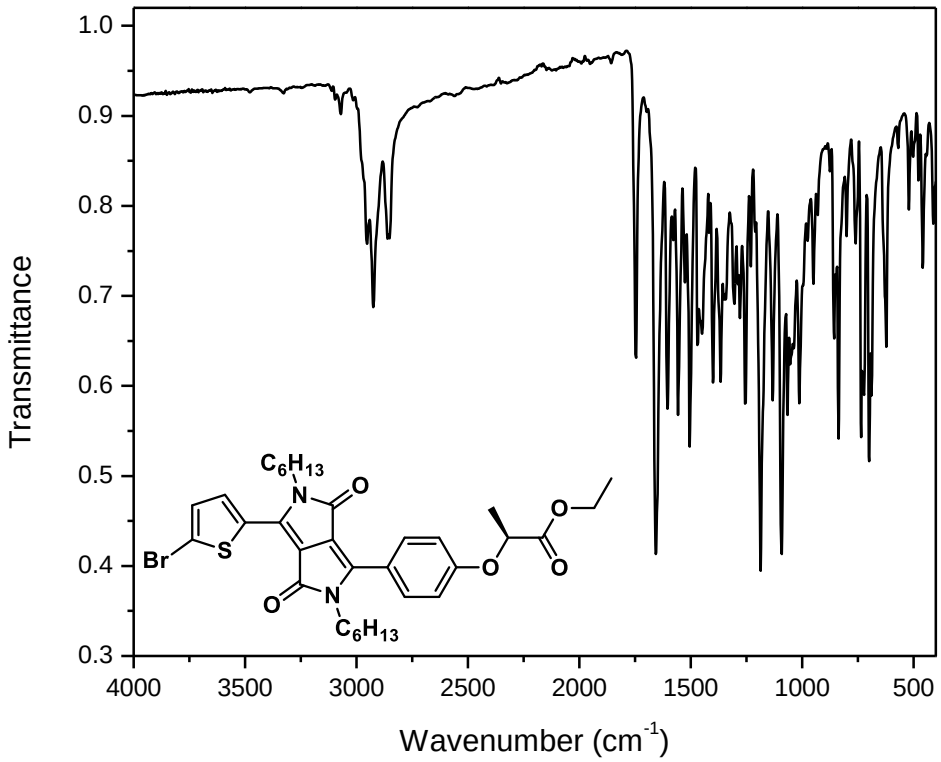

Diethyl 2,2'-((([2,2'-bithiophene]-5,5'-diylbis(2,5-dihexyl-3,6-dioxo-2,3,5,6-tetrahydropyrrolo[3,4-c]pyrrole-4,1-diyl))bis(4,1-phenylene))bis(oxy))(2S,2'S)-dipropionate ((*S*,*S*)-1)

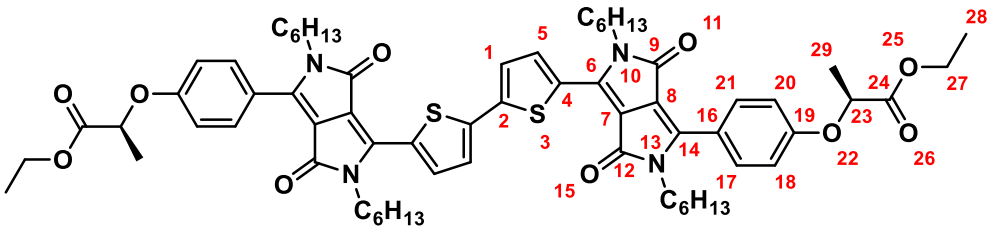

A 50 mL two-neck round bottom flask fitted with reflux condenser was charged with compound (*S*)-**5** (250 mg, 380 µmol, 1 eq), bis(pincolato)diboron (96.5 mg, 380 µmol, 1 eq), K_2CO_3, (210 mg, 1.52 mmol, 4 eq), tetrakis(triphenylphosphine)palladium(0) (22.0 mg, 19.0 µmol, 5 mol%) and 1,4-dioxane (25 mL). The resulting mixture was degassed with argon for 30 min, before heating to 100 °C in the dark for 24 h. After cooling to rt solvent was removed under reduced pressure and the product purified by recrystallisation from acetonitrile,

filtered, and washed with acetonitrile, water and acetone before drying *in vacuo* to give a blue/black solid (165 mg, 143 µmol, 75%). *Rf*: 0.10 (CH_2Cl_2, silica).

Mp: 186-188 °C;

^{1}H NMR (400 MHz, $CDCl_3$) δ 8.94 (d, *J* = 4.2 Hz, 2H, H^5), 7.85 (d, *J* = 8.9 Hz, 4H, $H^{17/21}$), 7.47 (d, *J* = 4.2 Hz, 2H, H^1), 7.02 (d, *J* = 8.9 Hz, 4H, $H^{18/20}$), 4.85 (q, *J* = 6.8 Hz, 2H, H^{23}), 4.28 (q, *J* = 7.1 Hz, 4H, H^{27}), 4.11-3.98 (m, 4H, C*H*$_2$N), 3.91-3.77 (m, 4H, C*H*$_2$N), 1.81-1.72 (m, 4H, C*H*$_2$), 1.70-1.61 (stack, 10H, C*H*$_2$), 1.53-1.15 (stack, 30H, C*H*$_2$/C*H*$_3$), 1.03-0.73 (stack, 12H, C*H*$_3$);

^{13}C NMR (101 MHz, $CDCl_3$) δ 171.61, 162.19, 161.81, 159.82, 147.07, 140.98, 139.53, 136.41, 130.73, 129.72, 126.25, 121.40, 115.34, 109.04, 108.77, 72.67, 61.55, 42.31, 42.07, 31.39, 31.26, 29.97, 29.51, 26.53, 26.46, 22.52, 18.49, 14.15, 14.04, 13.97;

IR (thin film, cm^{-1}): 3068 (C-H), 2927 (C-H), 2855 (C-H), 1748 (C=O), 1655 (C=O), 1600 (C=C), 1552 (C=C), 1504 (C=C), 1436 (C=C).

MS (MALDI-TOF+): $[M+H]^+$ calcd. for $C_{66}H_{82}N_4O_{10}S_2$, 1155.56; found, 1155.47

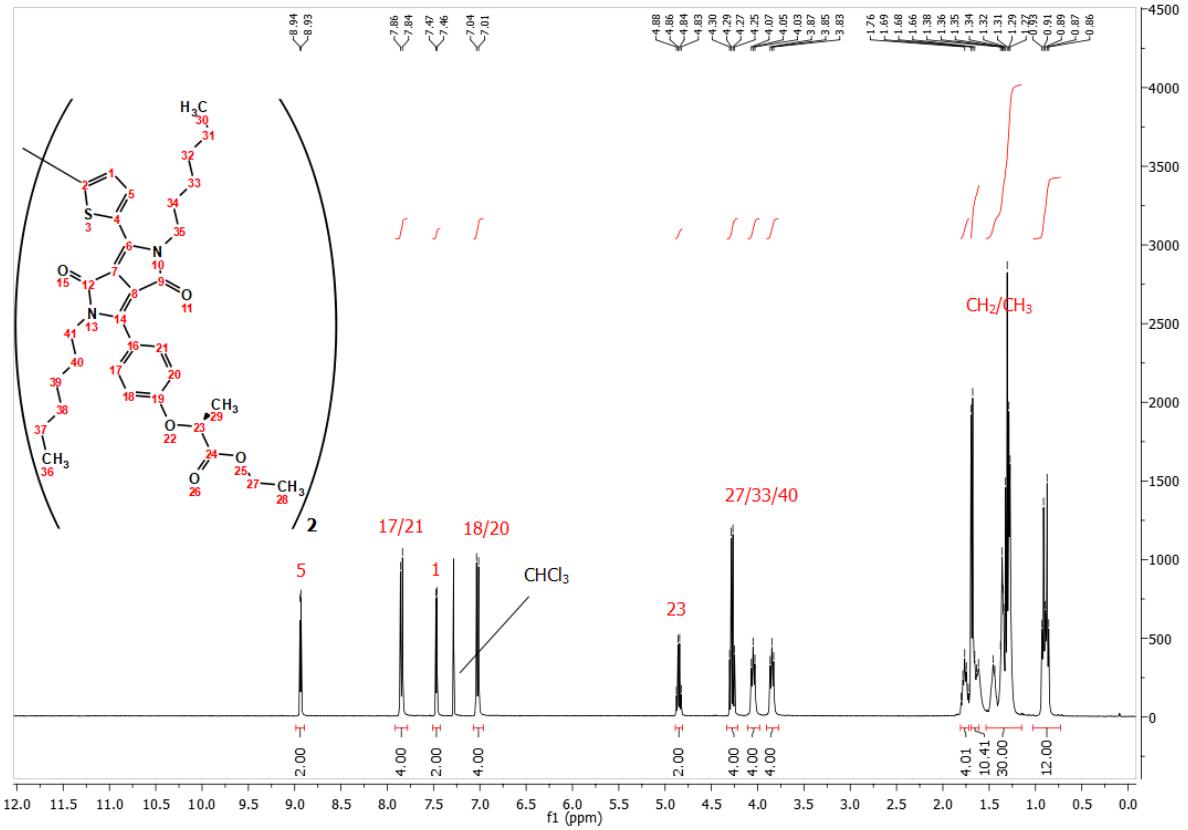

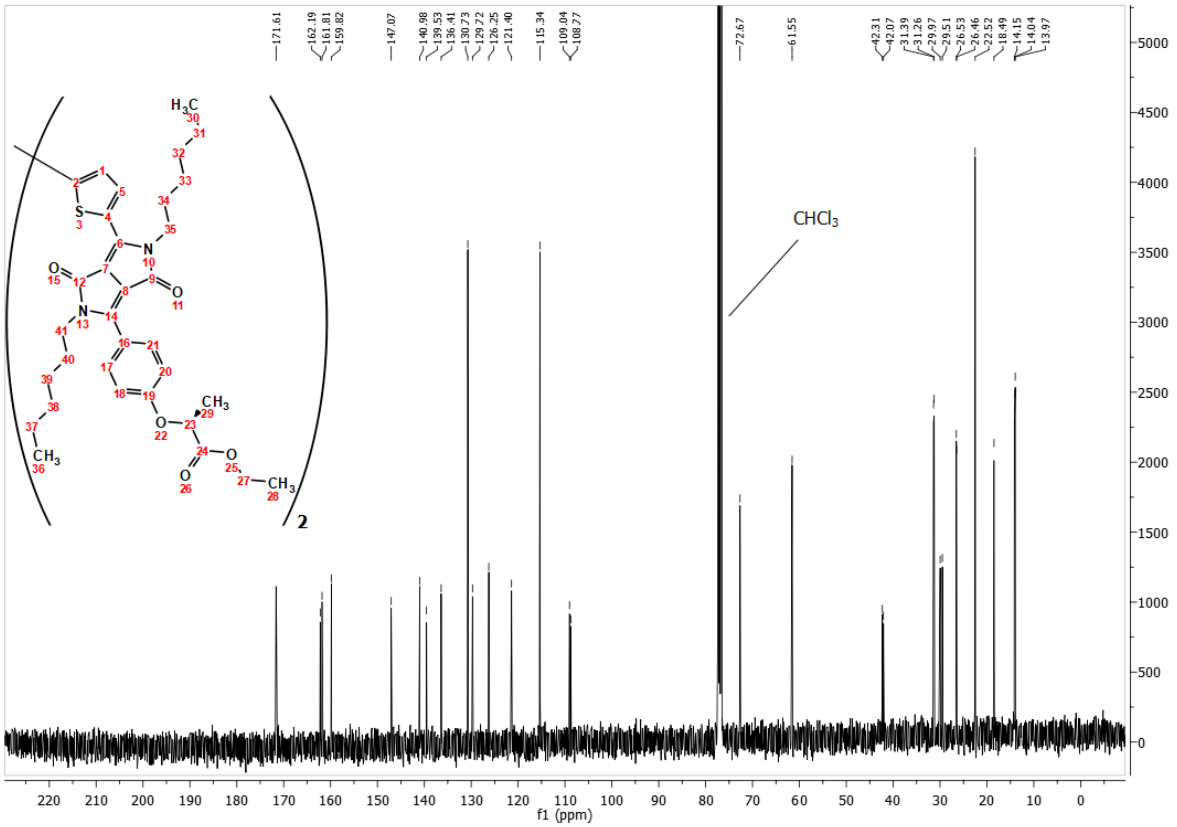
171.61
162.19
161.81
159.82
147.07
140.98
139.53
136.41
130.73
129.72
126.25
121.40
115.34
109.04
108.77
72.67
61.55
42.31
42.07
31.39
31.26
29.97
29.51
26.53
25.46
22.52
18.48
14.15
14.04
13.97
CHCl3
2
f1 (ppm)

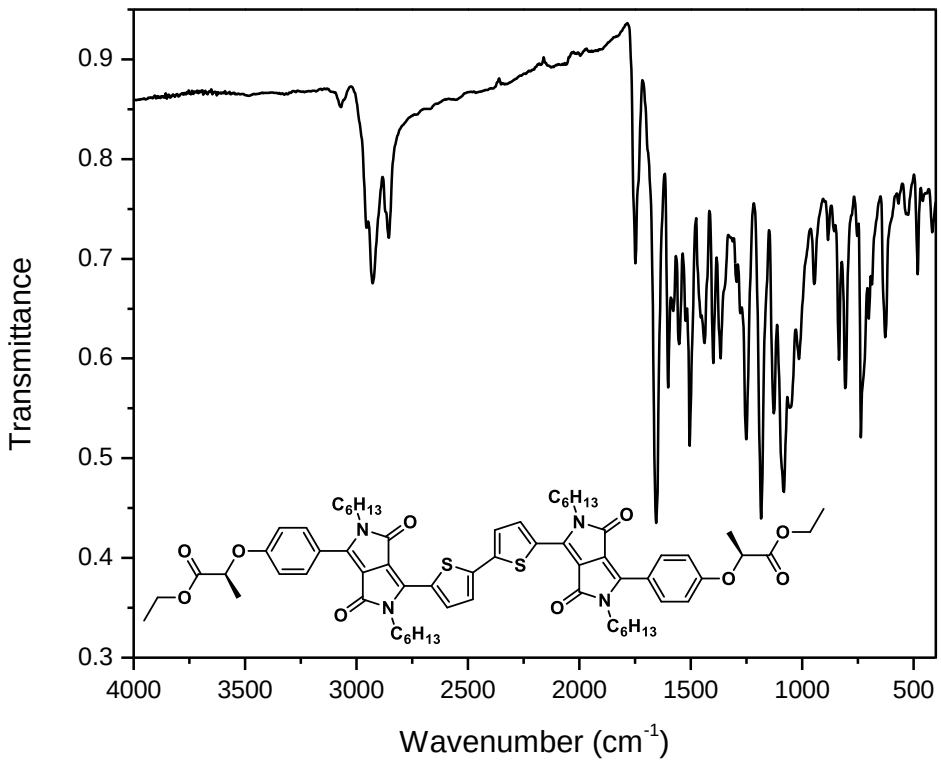
Transmittance
Wavenumber (cm-1)

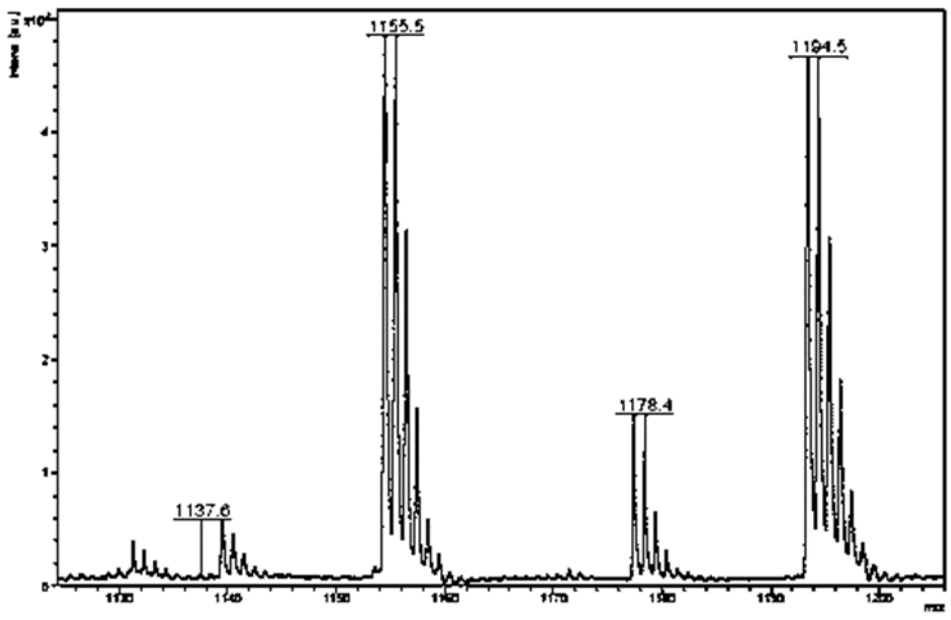

m/z	Rel. Intens.
1194.450	92
1178.434	26
1156.473	71
1155.472	100
1137.643	12
1092.317	4
1067.932	43
995.788	5
981.691	3
967.343	7
896.065	4

Absorption and emission spectroscopy

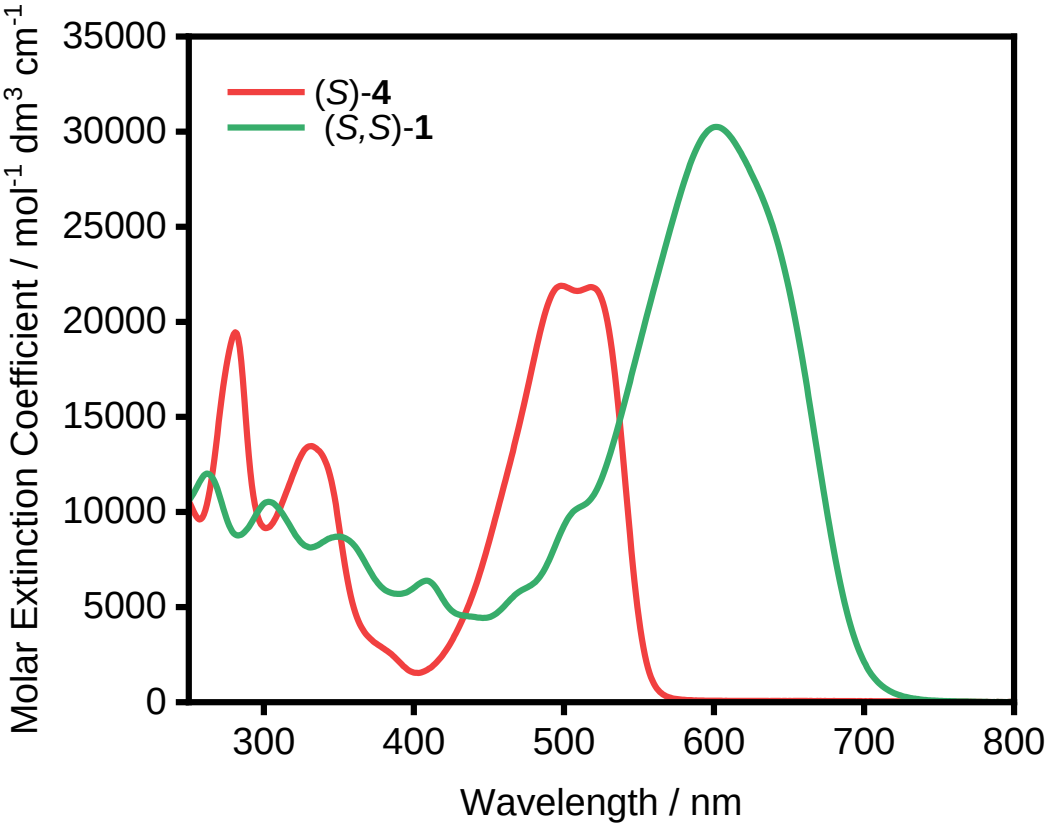

Fig. S1: Electronic absorption of single and dimer DPP compounds in chloroform.

Table S1*. Absorption maxima and molar extinction coefficients of synthesised novel diketopyrrolopyrrole derivatives. All spectra were collected from solutions of chloroform.*

	λ_{max} / nm	ε / M^{-1} cm^{-1}
(*S*)-4	499, 518	24600
(*S,S*)-1	603	32800

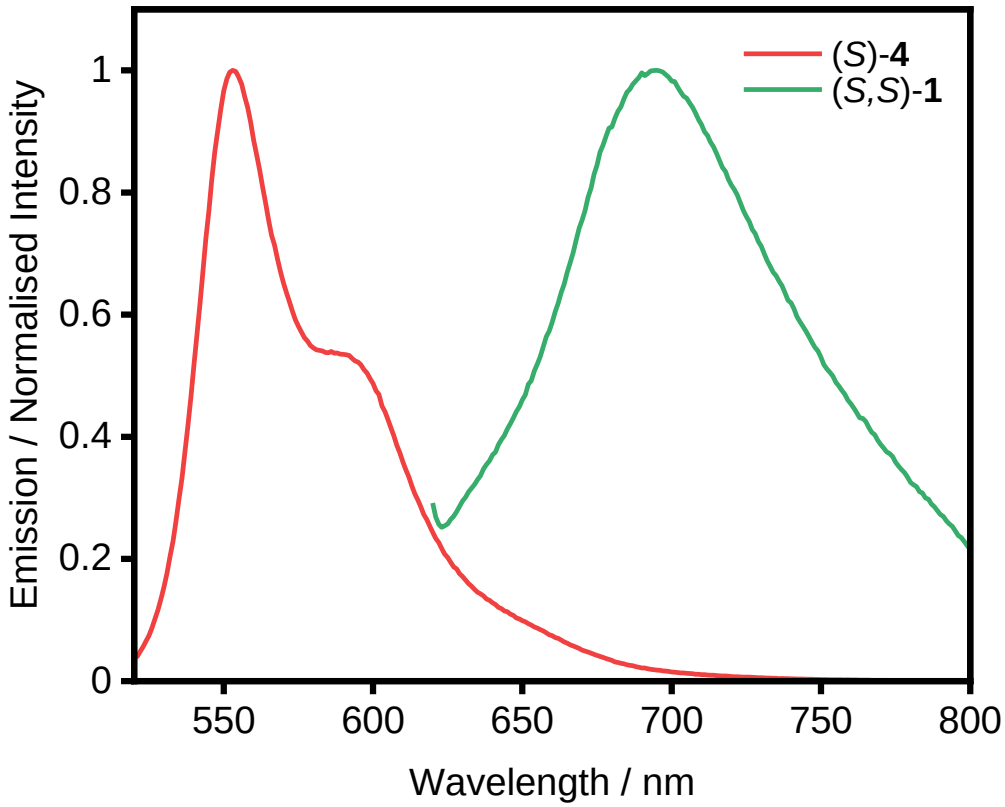

Fig. S2: Fluorescence spectra of single and dimer DPP compounds in chloroform. λ_{exc}=510 nm and 610 nm

***Table S2**: Stokes shifts and quantum yields of synthesised novel diketopyrrolopyrrole derivatives.*

	Stokes Shift (nm)	**Φ (%)**
(*S*)-4	35	29
(*S,S*)-1	98	21

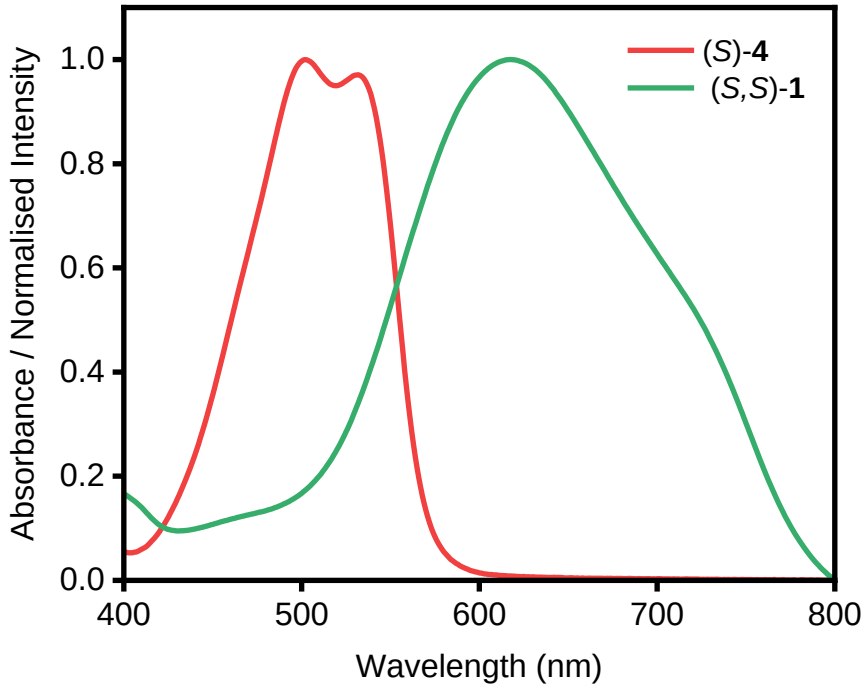

Fig. S3: Electronic absorption of thin films of single and dimer DPP compounds (cast from chloroform).

Table S3*. Absorption maxima of solution and thin film absorption spectra, the onset of absorption in the thin film samples, and the calculated optical band gaps. All thin films were cast from solutions of chloroform.*

	λ_{max} (solution)/ nm	**λ_{max} (thin film)/ nm**	**λ_{onset} / nm**	**Optical band gap / eV**
(*S*)-4	499, 518	502, 533	576	2.15
(*S,S*)-1	603	618	780	1.59

Electrochemistry

Cyclic voltammetry was performed under dry nitrogen in 1 mM solutions with 0.1 M *n*-Bu_4NPF_6 in nitrogen-degassed $CHCl_3$ using a CHI600E Series Electrochemical Analyzer with a glassy carbon disk as working electrode, Ag reference and Pt counter electrode. The ferrocene/ferrocenium couple (Fc/Fc+) was used as an internal standard.

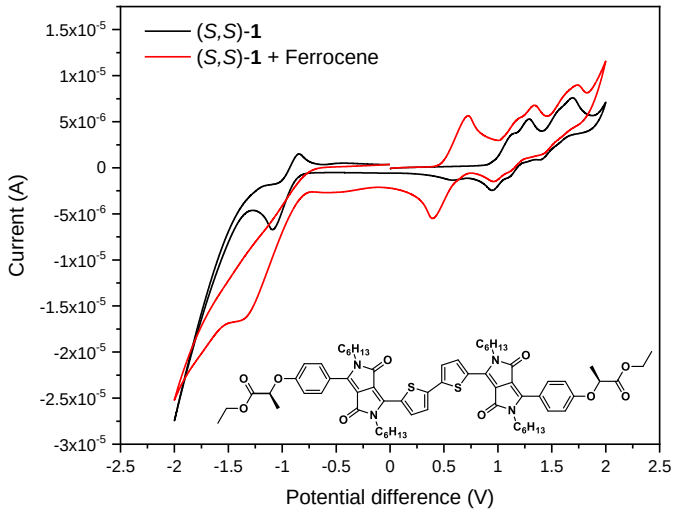

Fig. S4: Cyclic voltammogram of (*S,S*)-**1** in chloroform with 0.1 M *n*-Bu_4NPF_6 as electrolyte.

***Table S4**. Anodic and cathodic peak potentials for the first and second oxidation and reduction processes of (S,S)-**1**, referenced against the potential of Fc/Fc^{+}.*

Scan Rate	E_{pa} (1st ox)	E_{pc} (1st ox)	E_{pa}-E_{pc} (1st ox)	E_{pa} (2nd ox)	E_{pc} (2nd ox)	E_{pa}-E_{pc} (2nd ox)
0.1	0.5025	0.8565	-0.354	0.9455	1.2405	-0.295
0.05	0.5205	0.8235	-0.303	0.9505	1.1825	-0.232
0.025	0.5185-	0.7985	-0.28	0.9425	1.165	-0.223

Scan Rate	E_{pa} (1st red)	E_{pc} (1st red)	E_{pa}-E_{pc} (1st red)
0.1	-1.6835	n/a	n/a
0.05	-1.6085	n/a	n/a
0.025	-1.5725	n/a	n/a

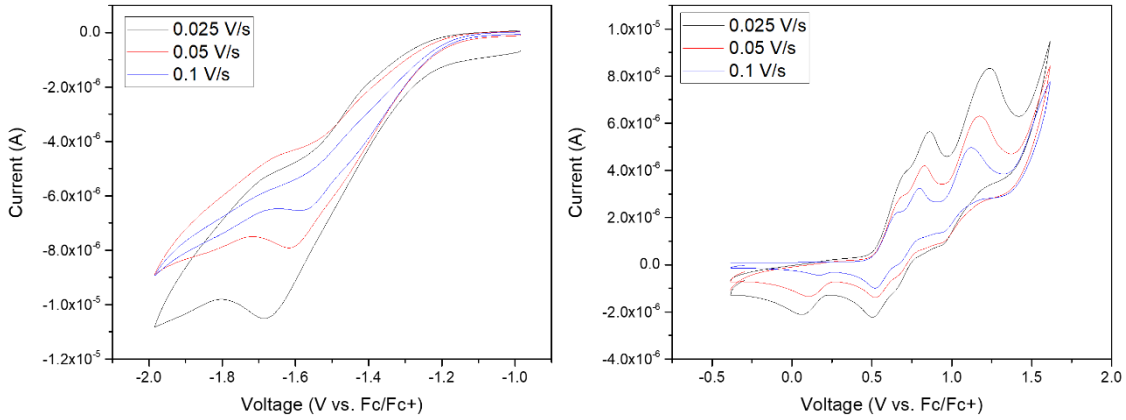

Fig. S5. Scan rate dependence of the reduction process (left) and oxidation processes (right) of (*S,S*)-**1** referenced against the potential of Fc/Fc^{+}.

Solution state aggregation of enantiomers of 1 as a function of concentration and temperature

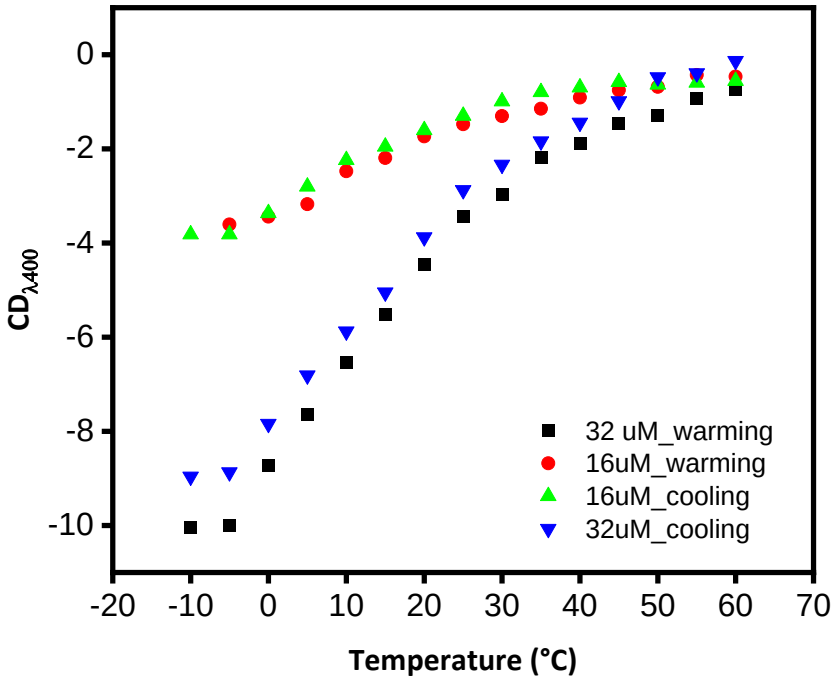

Fig. S6. Intensity of the CD signal of (*S,S*)-**1** in chloroform:heptane (1:5) at 580 nm as a function of concentration, temperature, and temperature cycle.

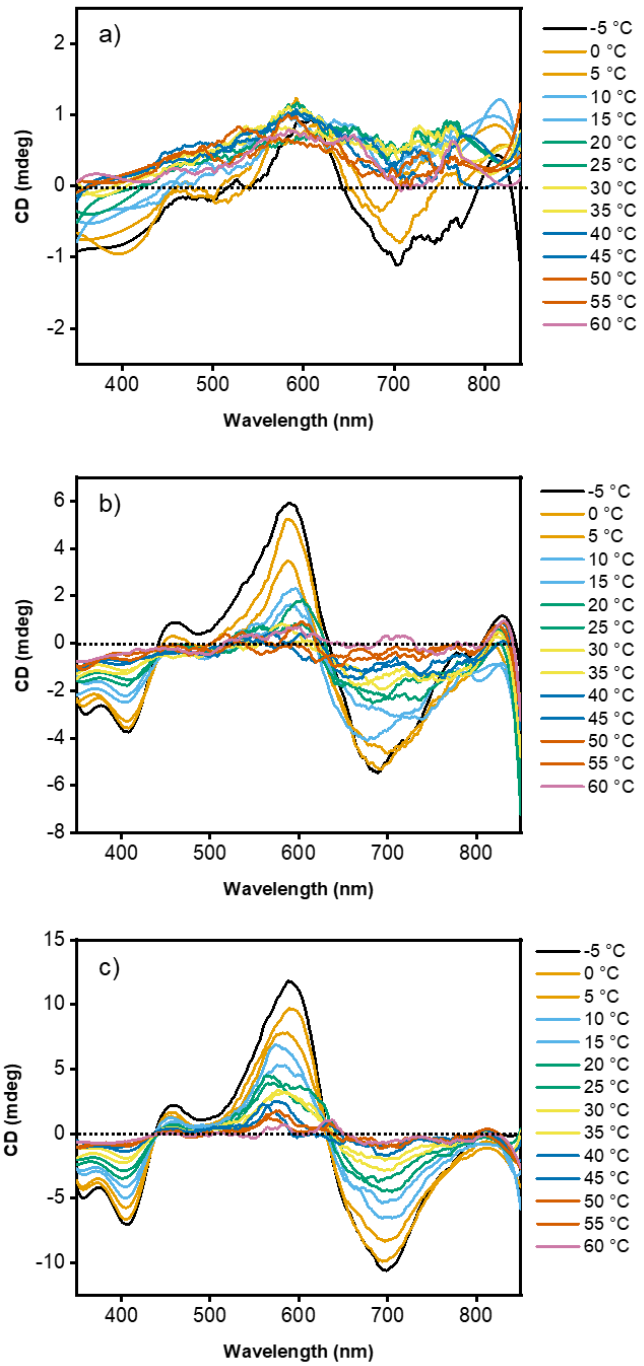

Fig. S7. Variable temperature warming CD spectra of (*S,S*)-**1** in chloroform:heptane (1:5) at different concentrations a) 8 µM, b) 16 µM, c) 32 µM

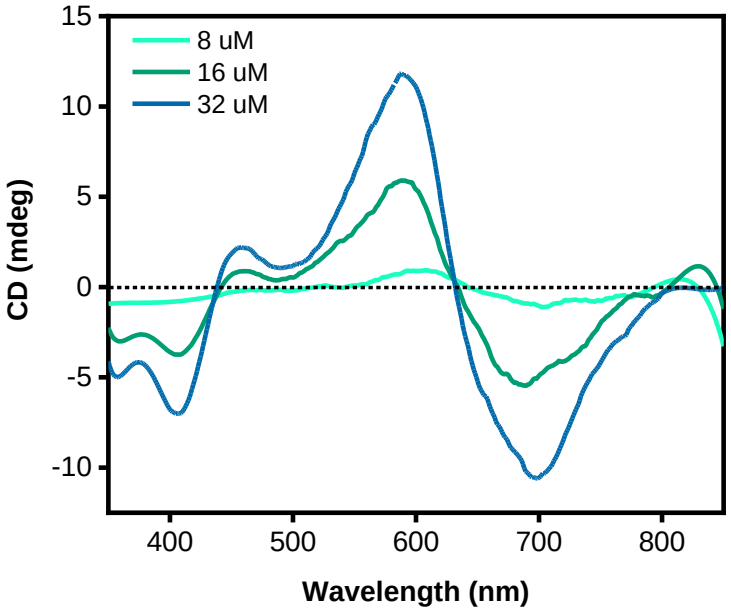

Fig. S8. CD spectra of (*S,S*)-**1** in chloroform:heptane (1:5) at different concentrations and all at -5 °C, showing an isodichroic point indicative of very similar aggregation processes at all concentrations.

Optical Activity of Films of the enantiomers of 1 and their Composites with ITIC-4F

Table S5 *g-factors related to the pure (R,R)- and (S,S)-**1** films and to the blends with the **ITIC-4F**.*

	θ (+)	**θ (-)**	**Δθ**	**ΔA = Δθ/32982**	**A (au)**	***g* = ΔA/A**
(*R,R*)-**1**	93.9	−48.9	142.8	$4.3x10^{-3}$	0.99	$4.3x10^{-3}$
(*S,S*)-**1**	47.2	−103.3	150.5	$4.6x10^{-3}$	0.92	$5.0x10^{-3}$
(*R,R*)-**1**:**ITIC-4F**	28.1	−13.5	41.7	$1.3x10^{-3}$	0.50	$2.5x10^{-3}$
(*S,S*)-**1**:**ITIC-4F**	6.35	−14.5	20.9	$6.3x10^{-4}$	0.45	$1.4x10^{-3}$

Intermittent contact Atomic Force Microscopy of Films

Atomic force microscopy (AFM) images were acquired in Intermittent contact mode under ambient conditions using an Asylum Cypher S AFM (Oxford Instruments-Asylum Research, Santa Barbara, USA). The images were collected using a Scout 70R cantilever from Nunano (spring constant of 2 N/m and a fundamental resonant frequency of 70 kHz) driven at its fundamental resonance frequency. Raw data were processed from .ibw files with Gwyddion.

Scans were taken ranging between 10 µm and 1 µm with three different profiles extracted from the topography channel using 128 pixels. The surface was analysed on various positions relatively close to the areas where the MMP analysis was performed.

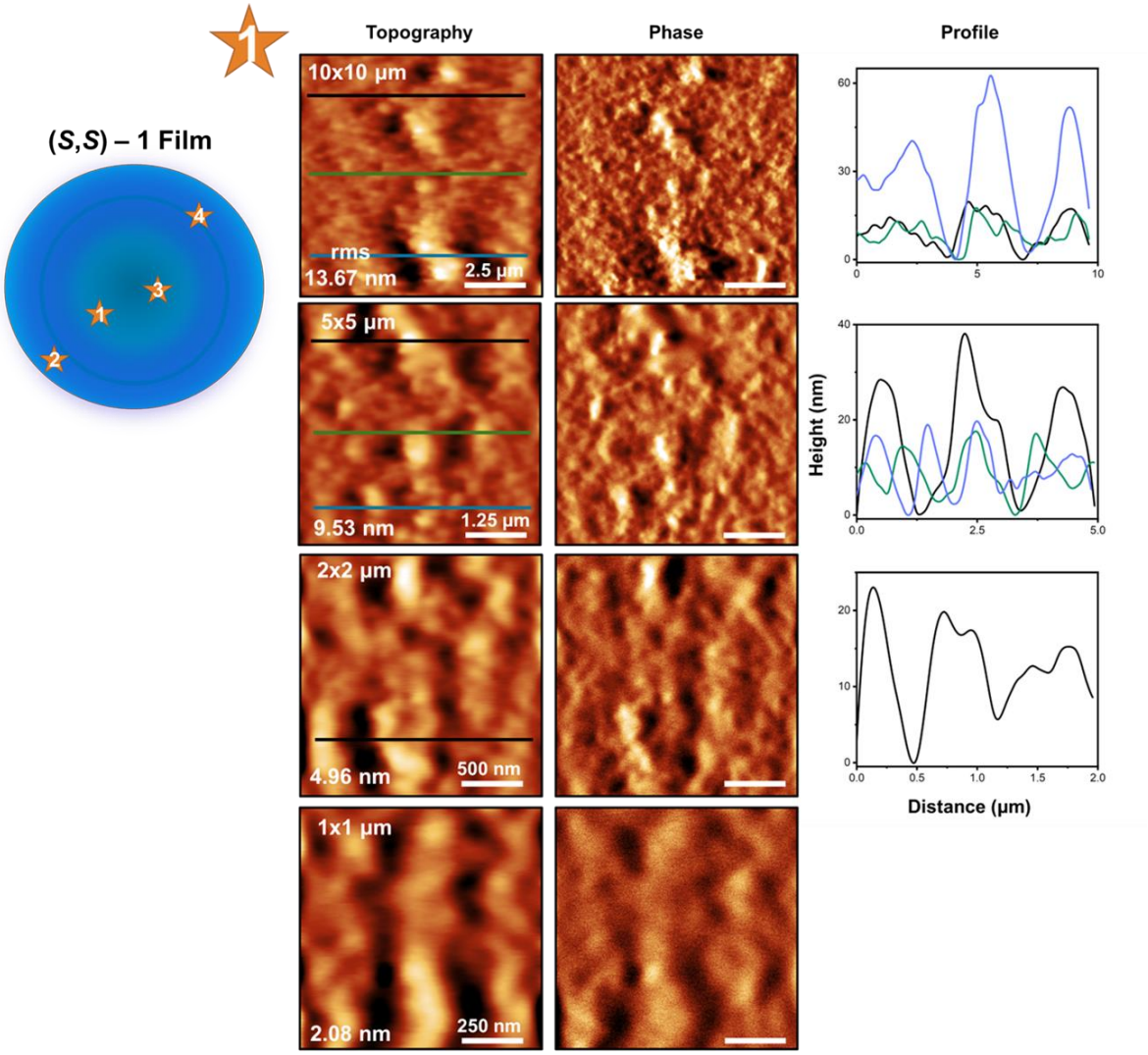

Fig. S9a. Intermittent contact AFM images of (*S,S*)-**1** (20 mg/ml, chlorobenzene solution). The solution was spin coated on a pre-cleaned quartz disc (conditions 1300 rpm, 36 seconds) and dried in air. A drawing of the quartz disc (top left) shows the top view of the blue film and region 1, indicated with a star and number, where the analysis was conducted. Scale sizes: 10x10 µm (top row), 5x5 µm (middle row), 2x2 µm (lower middle row), 1x1 µm (bottom row). Images acquired using the first eigenmode of a standard Scout 70 RAl cantilever.

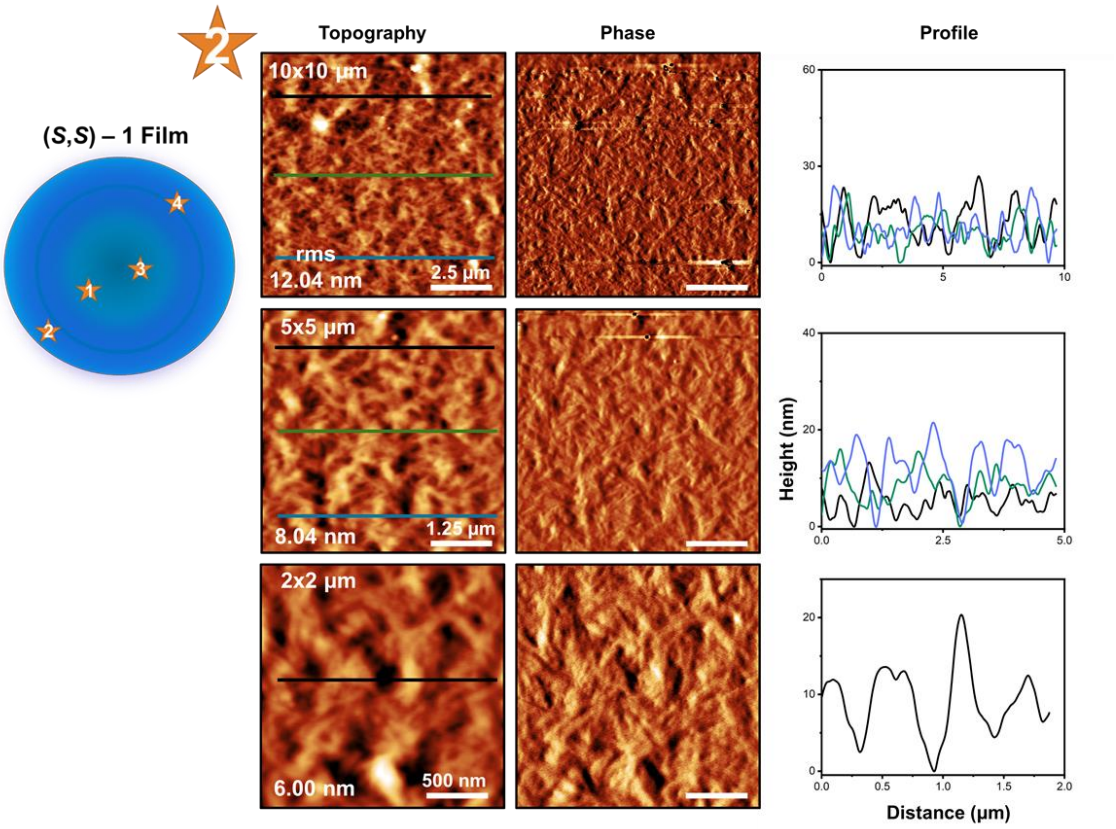

Fig. S9b. Intermittent contact AFM images of (*S,S*)-**1** (20 mg/ml, chlorobenzene solution). The solution was spin coated on a pre-cleaned quartz disc (conditions 1300 rpm, 36 seconds) and dried in air. A drawing of the quartz disc (top left) shows the top view of the blue film and region 2, indicated with a star and number, where the analysis was conducted. Scale sizes: 10x10 µm (top row), 5x5 µm (middle row), 2x2 µm (bottom row). Images acquired using the first eigenmode of a standard Scout 70 RAl cantilever.

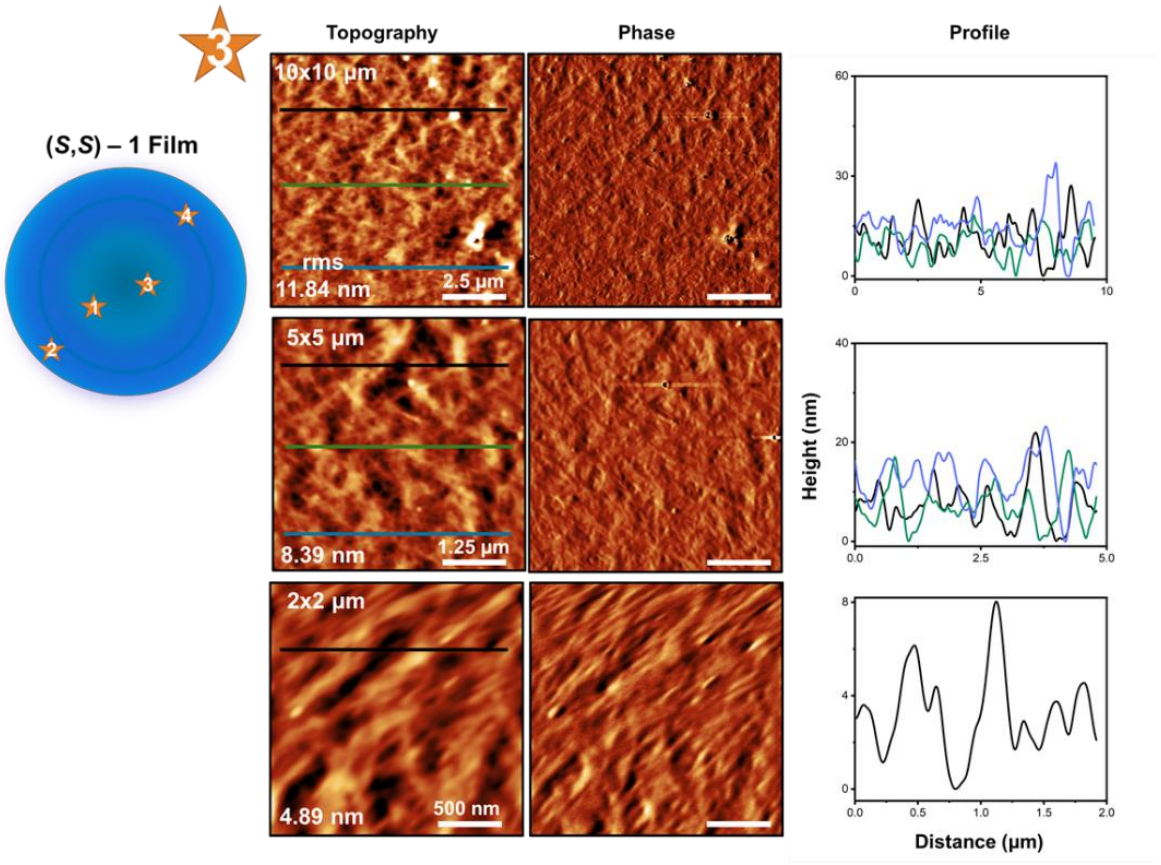

Fig. S9c. Intermittent contact AFM images of (*S,S*)-**1** (20 mg/ml, chlorobenzene solution). The solution was spin coated on a pre-cleaned quartz disc (conditions 1300 rpm, 36 seconds) and dried in air. A drawing of the quartz disc (top left) shows the top view of the blue film and region 3, indicated with a star and number, where the analysis was conducted. Scale sizes: 10x10 µm (top row), 5x5 µm (middle row), 2x2 µm (bottom row). Images acquired using the first eigenmode of a standard Scout 70 RAl cantilever.

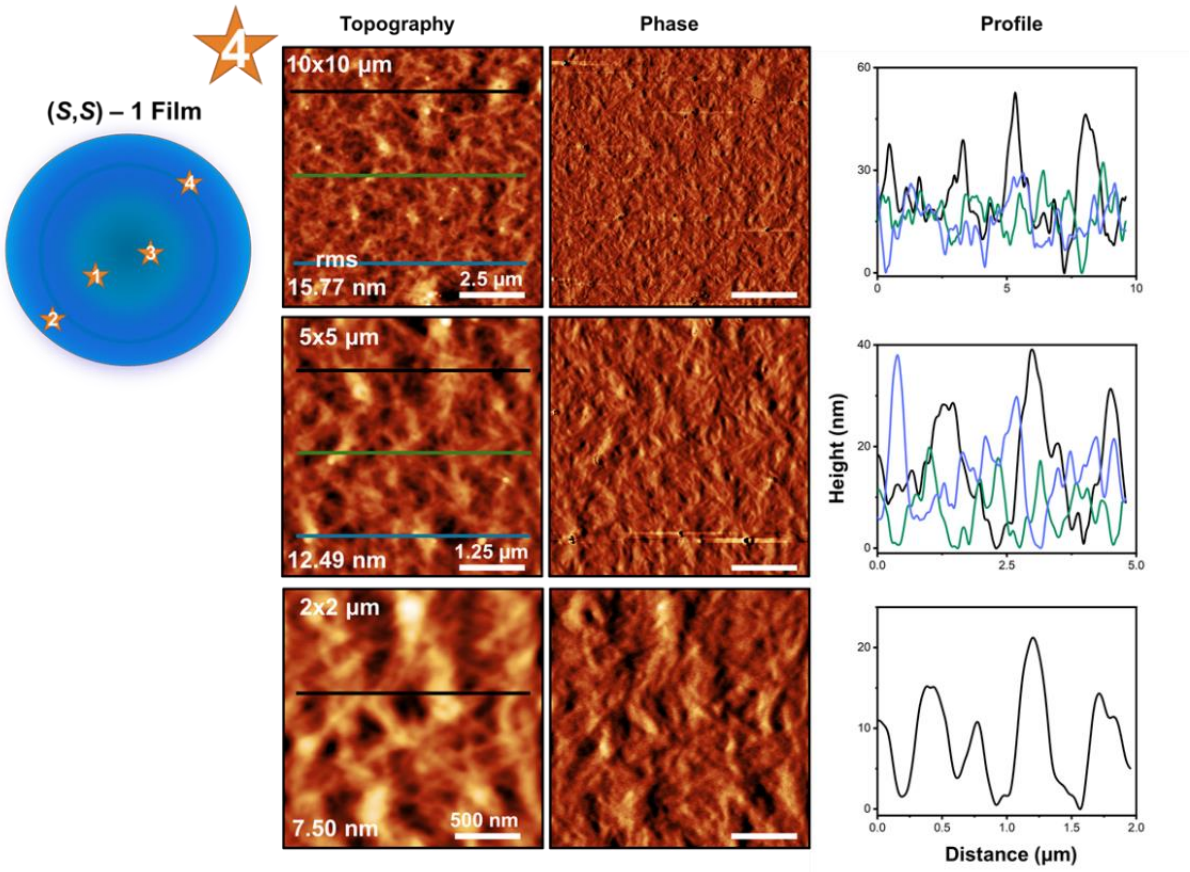

Fig. S9d. Intermittent contact AFM images of (*S,S*)-**1** (20 mg/ml, chlorobenzene solution). The solution was spin coated on a pre-cleaned quartz disc (conditions 1300 rpm, 36 seconds) and dried in air. A drawing of the quartz disc (top left) shows the top view of the blue film and region 4, indicated with a star and number, where the analysis was conducted. Scale sizes: 10x10 µm (top row), 5x5 µm (middle row), 2x2 µm (bottom row). Images acquired using the first eigenmode of a standard Scout 70 RAl cantilever.

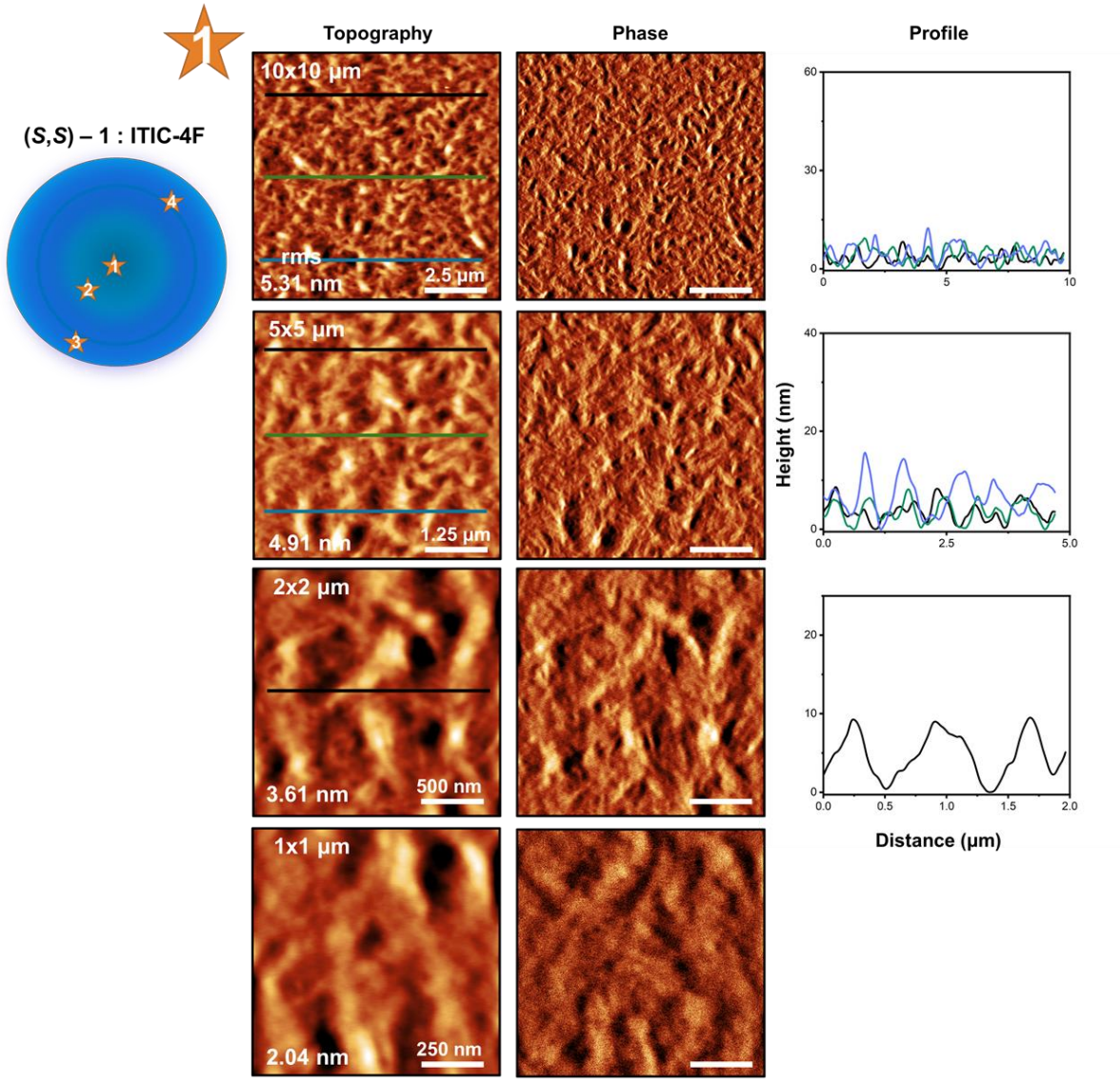

Fig. S10a. Intermittent contact AFM images of (*S,S*)-**1**:**ITIC-4F** (20 mg/ml, ratio 1:1, chlorobenzene solution). The solution was spin coated on a pre-cleaned quartz disc (conditions 1500 rpm – 36 seconds) and dried in air. A drawing of the quartz disc (top left) shows the top view of the blue film and numbered spot, indicated with a yellow star, where the analysis was conducted. Topography (left column) and phase (middle column) images with coloured line profiles extracted from the corresponding topography images. Scale sizes: 10x10 µm (top row), 5x5 and 2x2 µm (middle rows), 1x1 µm (bottom row). Images acquired using the first eigenmode of a standard Scout 70 RAl cantilever.

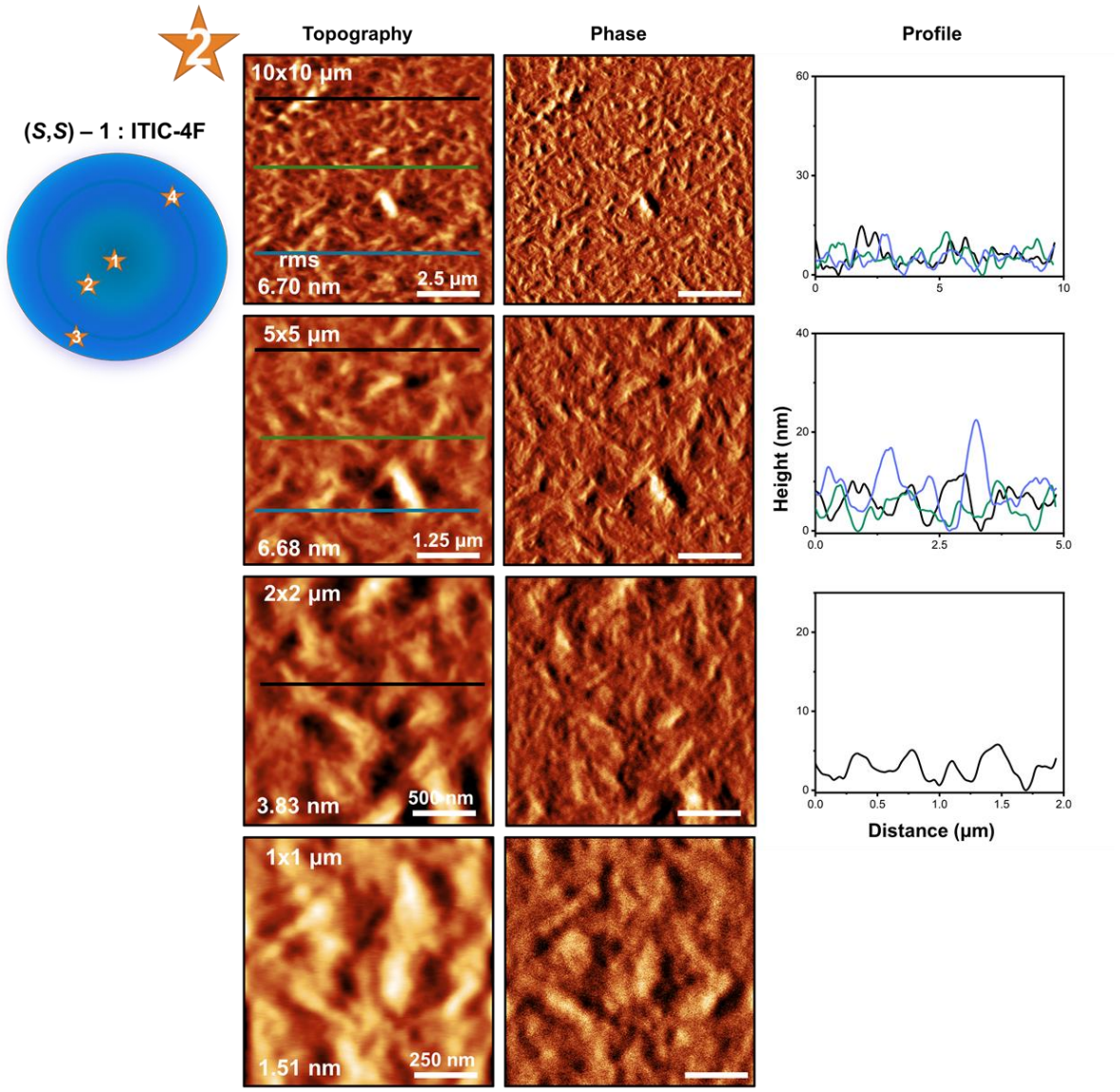

Fig. S10b. Intermittent contact AFM images of (*S,S*)-**1**:**ITIC-4F** (20 mg/ml, ratio 1:1, chlorobenzene solution). The solution was spin coated on a pre-cleaned quartz disc (conditions 1500 rpm – 36 seconds) and dried in air. A drawing of the quartz disc (top left) shows the top view of the blue film and numbered spot, indicated with a yellow star, where the analysis was conducted. Topography (left column) and phase (middle column) images with coloured line profiles extracted from the corresponding topography images. Scale sizes: 10x10 µm (top row), 5x5 and 2x2 µm (middle rows), 1x1 µm (bottom row). Images acquired using the first eigenmode of a standard Scout 70 RAl cantilever.

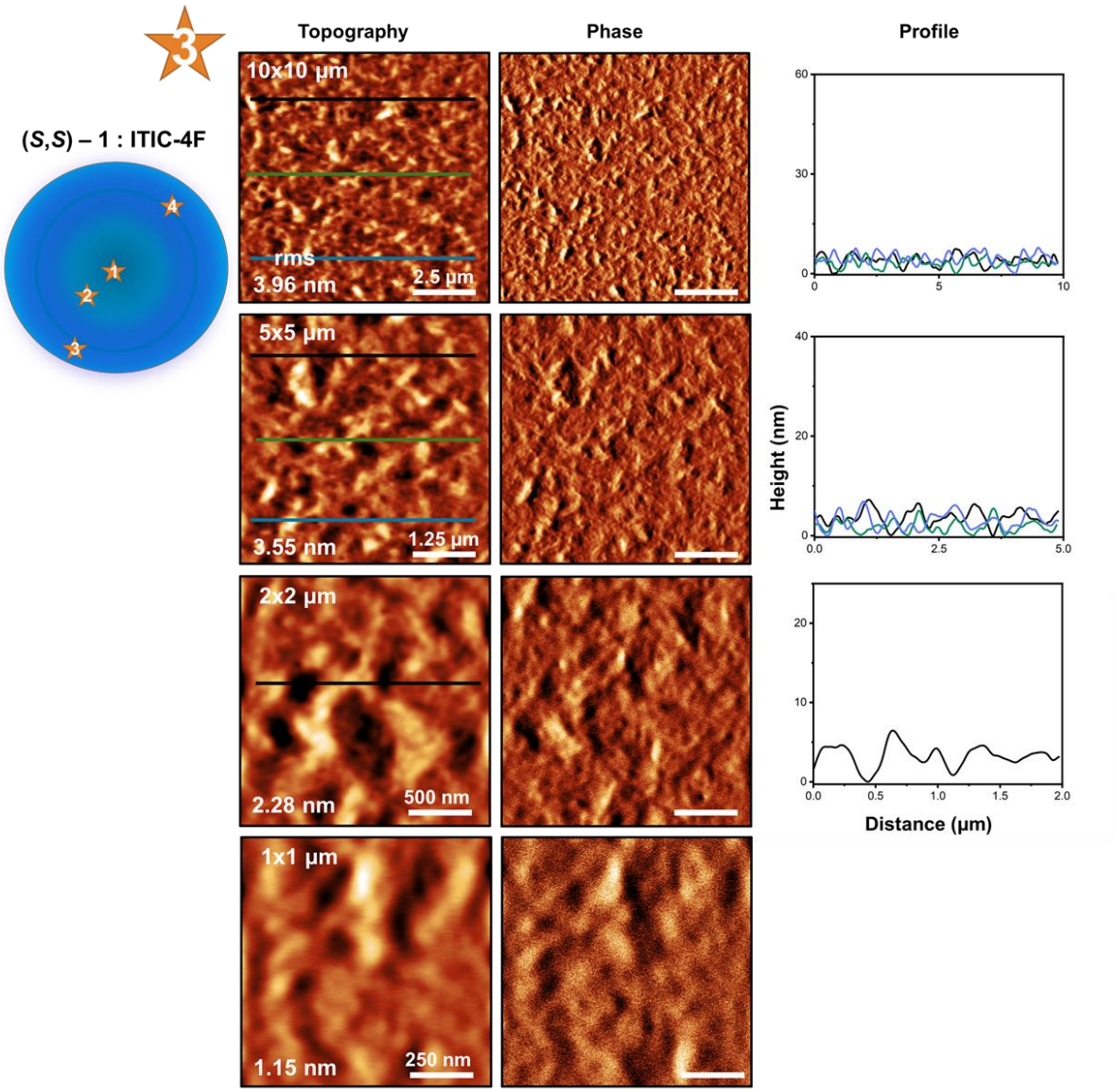

Fig. S10c. Intermittent contact AFM images of (*S,S*)-**1**:**ITIC-4F** (20 mg/ml, ratio 1:1, chlorobenzene solution). The solution was spin coated on a pre-cleaned quartz disc (conditions 1500 rpm – 36 seconds) and dried in air. A drawing of the quartz disc (top left) shows the top view of the blue film and numbered spot, indicated with a yellow star, where the analysis was conducted. Topography (left column) and phase (middle column) images with coloured line profiles extracted from the corresponding topography images. Scale sizes: 10x10 µm (top row), 5x5 and 2x2 µm (middle rows), 1x1 µm (bottom row). Images acquired using the first eigenmode of a standard Scout 70 RAl cantilever.

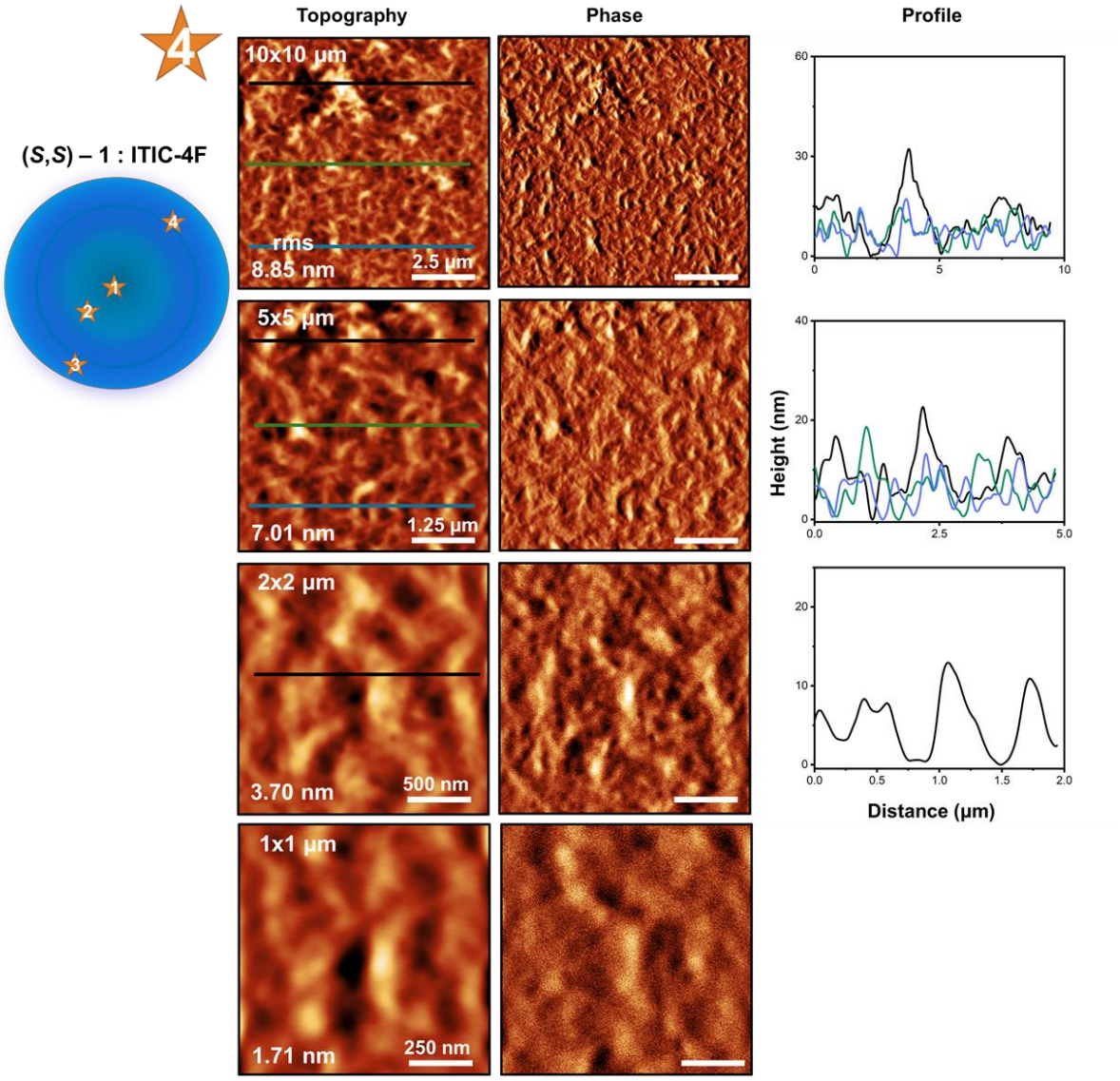

Fig. S10d. Intermittent contact AFM images of (*S,S*)-**1**:**ITIC-4F** (20 mg/ml, ratio 1:1, chlorobenzene solution). The solution was spin coated on a pre-cleaned quartz disc (conditions 1500 rpm – 36 seconds) and dried in air. A drawing of the quartz disc (top left) shows the top view of the blue film and numbered spot, indicated with a yellow star, where the analysis was conducted. Topography (left column) and phase (middle column) images with coloured line profiles extracted from the corresponding topography images. Scale sizes: 10x10 µm (top row), 5x5 and 2x2 µm (middle rows), 1x1 µm (bottom row). Images acquired using the first eigenmode of a standard Scout 70 RAl cantilever.

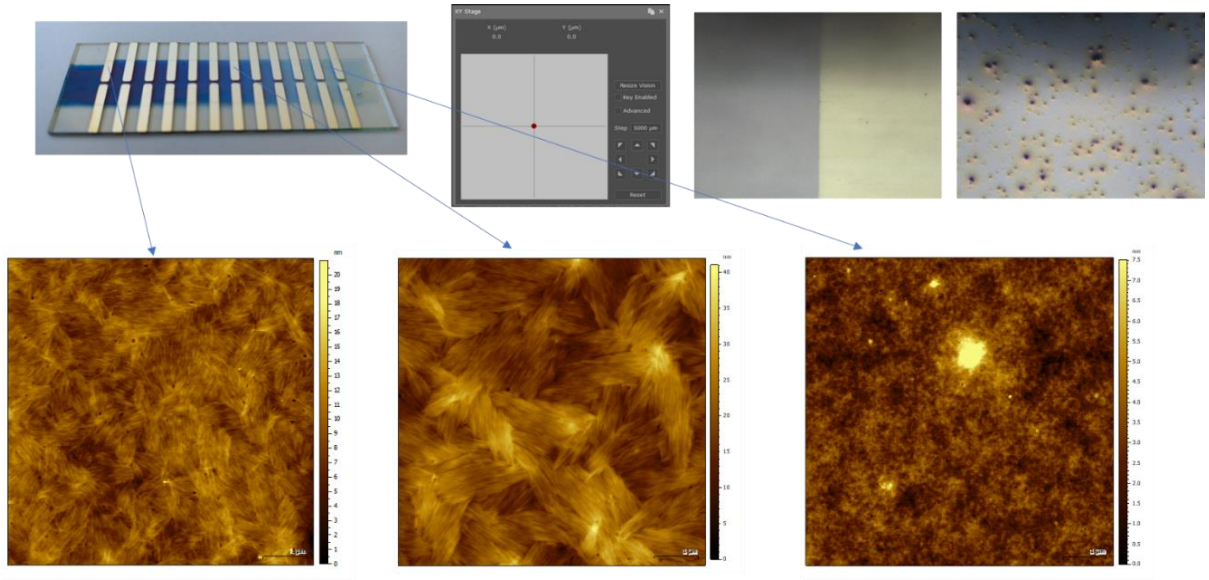

Fig. S11. Intermittent contact AFM images at different areas along the gradient of (*S,S*)-**1**:**ITIC-4F** (20 mg/ml, ratio 1:1, chlorobenzene solution), gradient blade-coated device on ZnO-coated ITO on glass with aluminium contacts. The three positions correspond to approximate sample thicknesses of 180, 90 and 40 nm.

ALBA MIRAS 01 IR Image

Spectroscopic mapping was performed at the BL01MIRAS beamline of ALBA synchrotron.

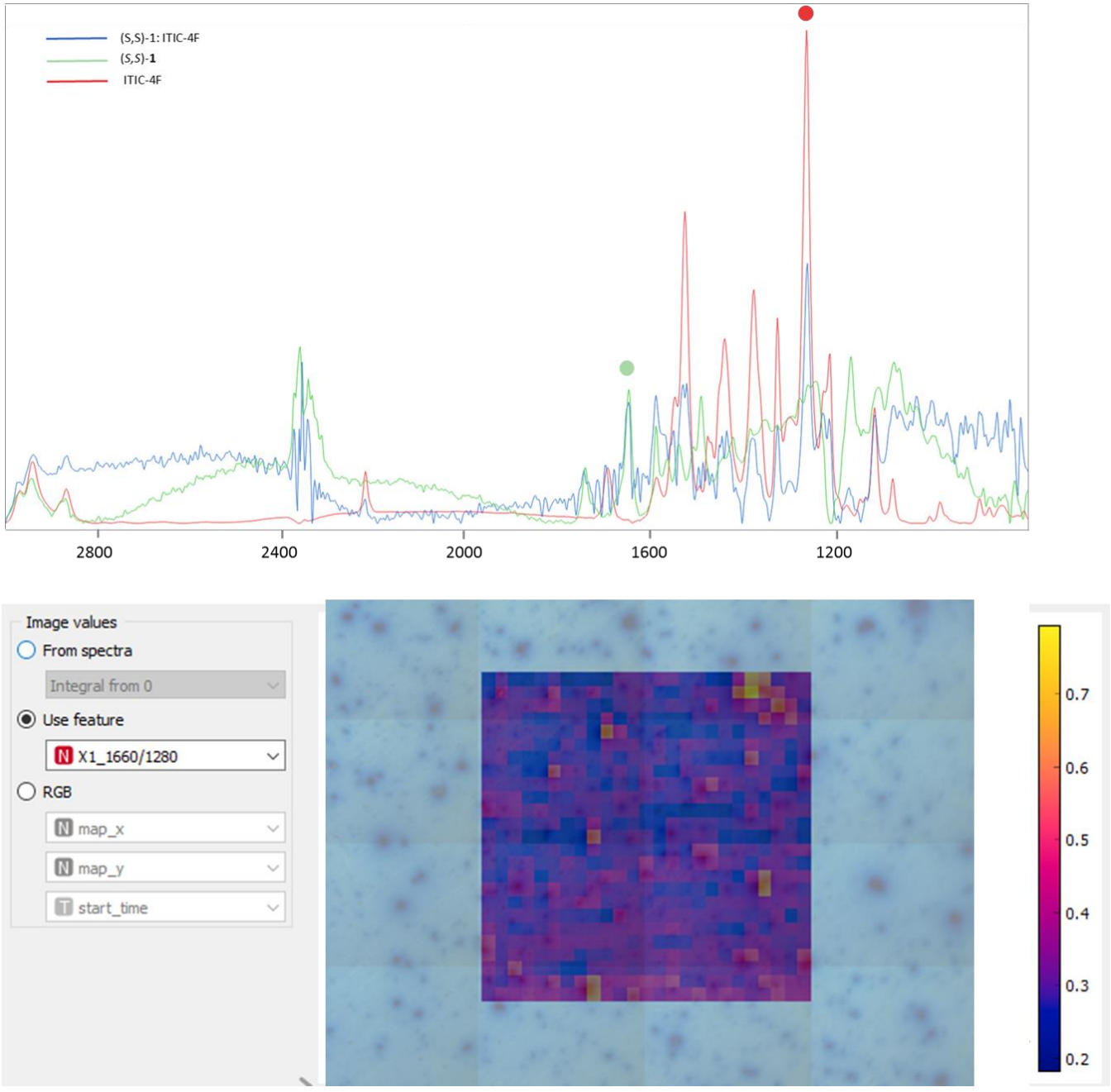

Figure S12. IR spectra of the donor and acceptor components and their mixture: From the spectra above it was possible to identify peaks of (*S,S*)-**1** (1660 cm^{-1}) and **ITIC-4F** (1280 cm^{-1}). The ratio of the area those peaks was calculated and overlapped to microscopy image with an overlaid heatmap of the IR map probing (bottom). Each pixel corresponds to a single measurement with a 10x10 µm2 area. The colour scale indicates the ratio of the area under the representative peaks at 1660 and 1280 cm^{-1}. Yellow corresponds to an excess of **ITIC-4F** and dark blue to an excess of the DPP.

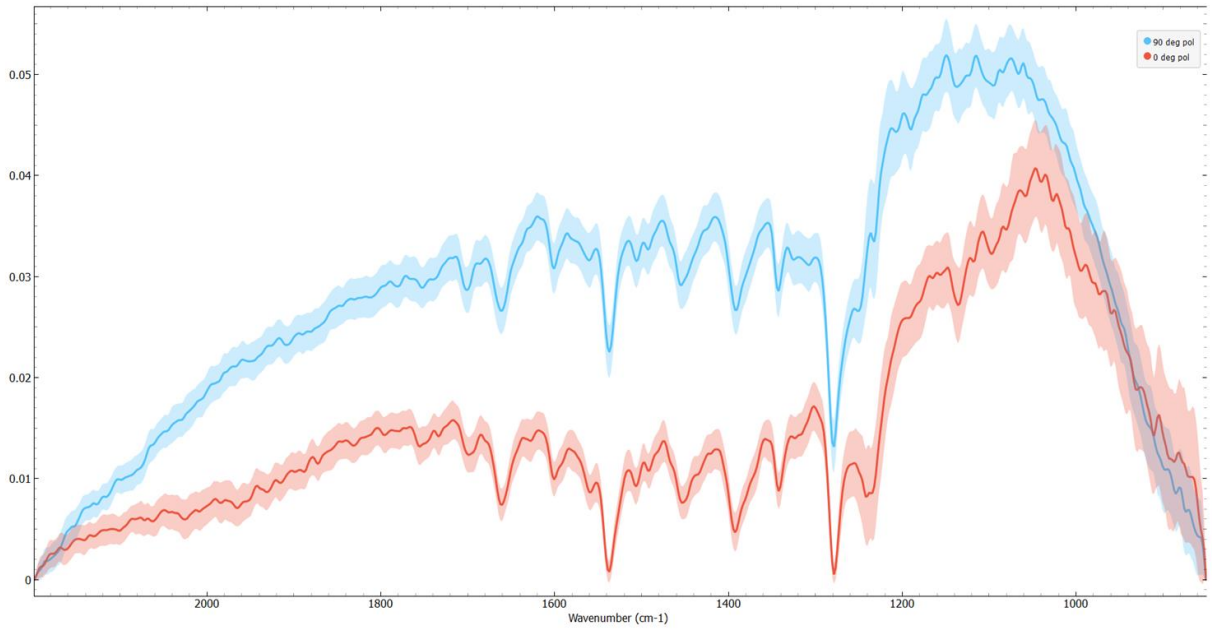

Figure S13 IR spectra recorded in reflection on a solar cell of the mixture of (*S,S*)-**1** and **ITIC-4F** at different polarisation angles in the MIRAS beamline.

Analysis on thin films with Mueller Matrix Polarimetry imaging measurements

Mueller Matrix Polarimetry imaging (MMP*i*) experiments of thin films were recorded using Module B spectrophotometer at B23 beamline for Synchrotron Radiation CD (SRCS) of Diamond Light Source (see Fig. S14). Module B employs an Olis DSM20 Monochromator and Photomultiplier tube detector. The beam light was positioned in a vertical measurement chamber using a motorized XY stage. UV and CD spectra were recorded simultaneously in the wavelength range 400-650 nm with 251 increments (1 nm step).

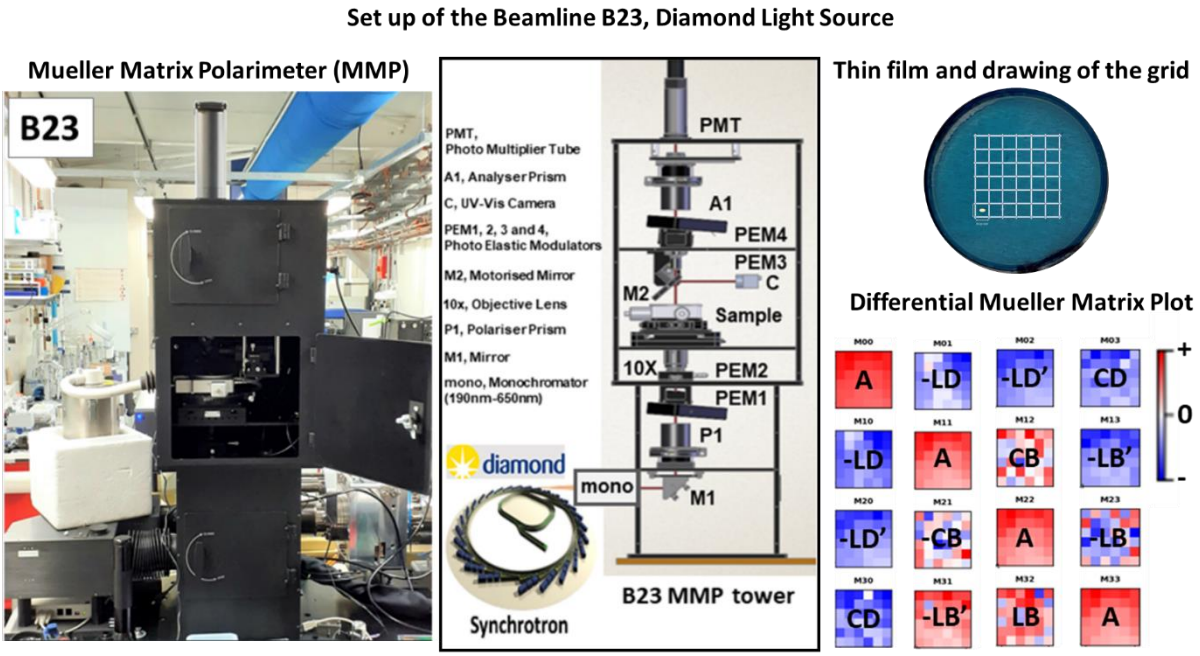

Fig. S14. The experimental set-up for Mueller Matrix Polarimetry imaging measurements at beamline B23 of the Diamond Light Source (Harwell, UK).

MMP data

The generation of artefacts-free CD spectra of solid-state samples is extremely important to efficiently characterize thin films of chiral molecules and unveil ordered aggregated forms. The Müller Matrix Polarimeter (MMP), developed at Diamond Light Source, allows fine study of solid state optically active materials with an exceptionally improved spatial resolution and with the advantage of isolating the true CD signal from the other linear and circular components. The system allows (1) The acquisition of spectra in a single spot over the sample surface;(2) The investigation of areas with the acquisition of 2D maps of the different signals in a specific range of wavelength from multiple spots, known as Spectrogrid; and (3) The acquisition of 2D maps at a specific wavelength, which we refer to as a Heatmap.

Calculation of the depolarisation index was performed using the equation:

$$\mathrm{DI} = \sqrt{\frac{1}{3m_{00}^2}\left(\sum_{i,j=0}^{3} m_{ij}^2 - m_{00}^2\right)}$$

From: J.J. Gill and E. Bernabeu, A depolarization criterion in Mueller matrices, *Optica Acta*, 1985, **32**, 259-261.

Optimisation of integration time for Diamond Synchrotron B23 imaging

An area of a spin-coated film of (*S,S*)-**1**:**ITIC-4F** (ratio 1:1, w/w from a heat treated mixture) was used to generate optical activity component intensity maps as a function of integration time (Fig.). Note the increase in uniformity of the *g* factor signal.

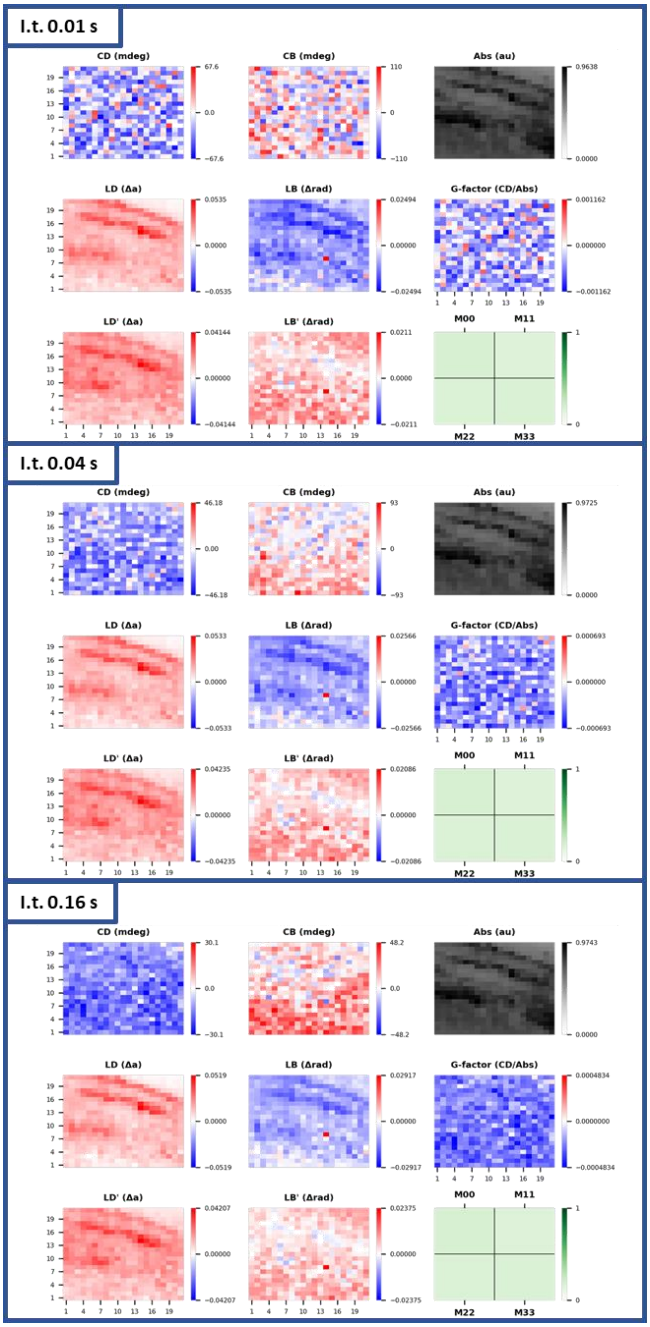

Fig. S15. An area of a spin-coated film of (*S,S*)-**1**:**ITIC-4F** (ratio 1:1, w/w from a heat treated mixture) showing MMP intensity maps 2x2 mm (21x21 steps) with a spatial resolution of 100 μm^2 (integration cycles 16) at 600 nm, and the integration time was varied as noted.

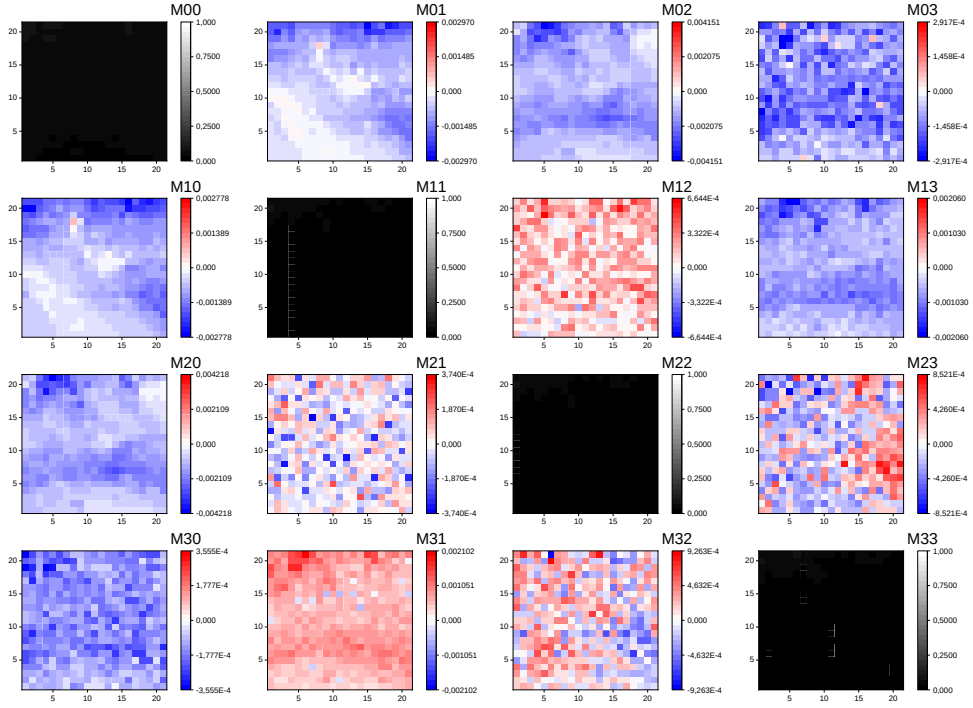

Fig. S16. Full MMPi data at 600 nm of a 0.5x0.5 mm area of 21x21 steps with a spatial resolution of 25 µm^2 at 600 nm performed on the spin coated film of (*S,S)* **1**.

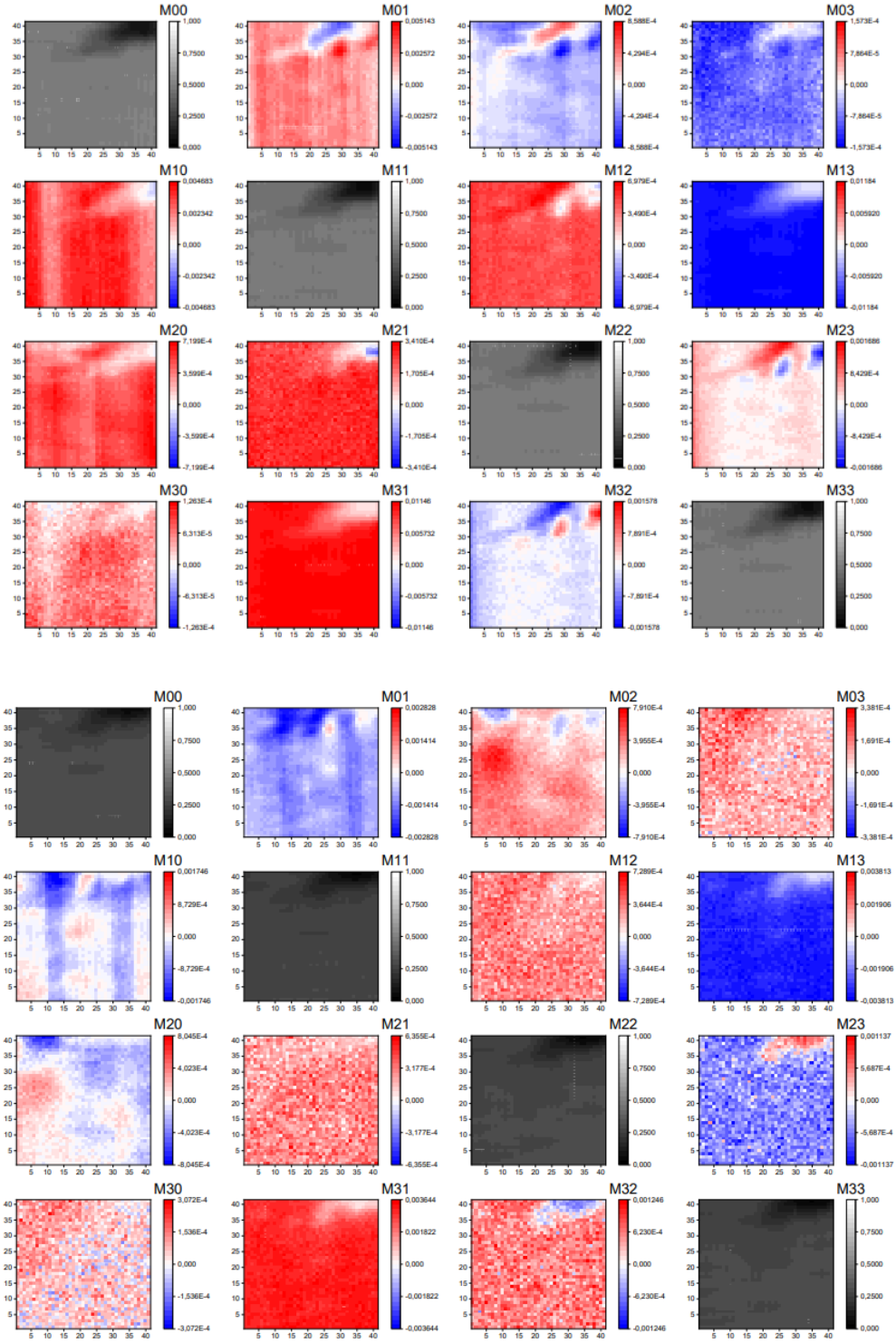

Fig. S17. Full MMPi data at 630 nm (top) and 350 nm (bottom) of a 1x1 mm area of 41x41 steps with a spatial resolution of 25 µm^2 at 600 nm performed on the spin coated film of (*S,S)* **1**:**ITIC-4F** from a heat treated mixture.

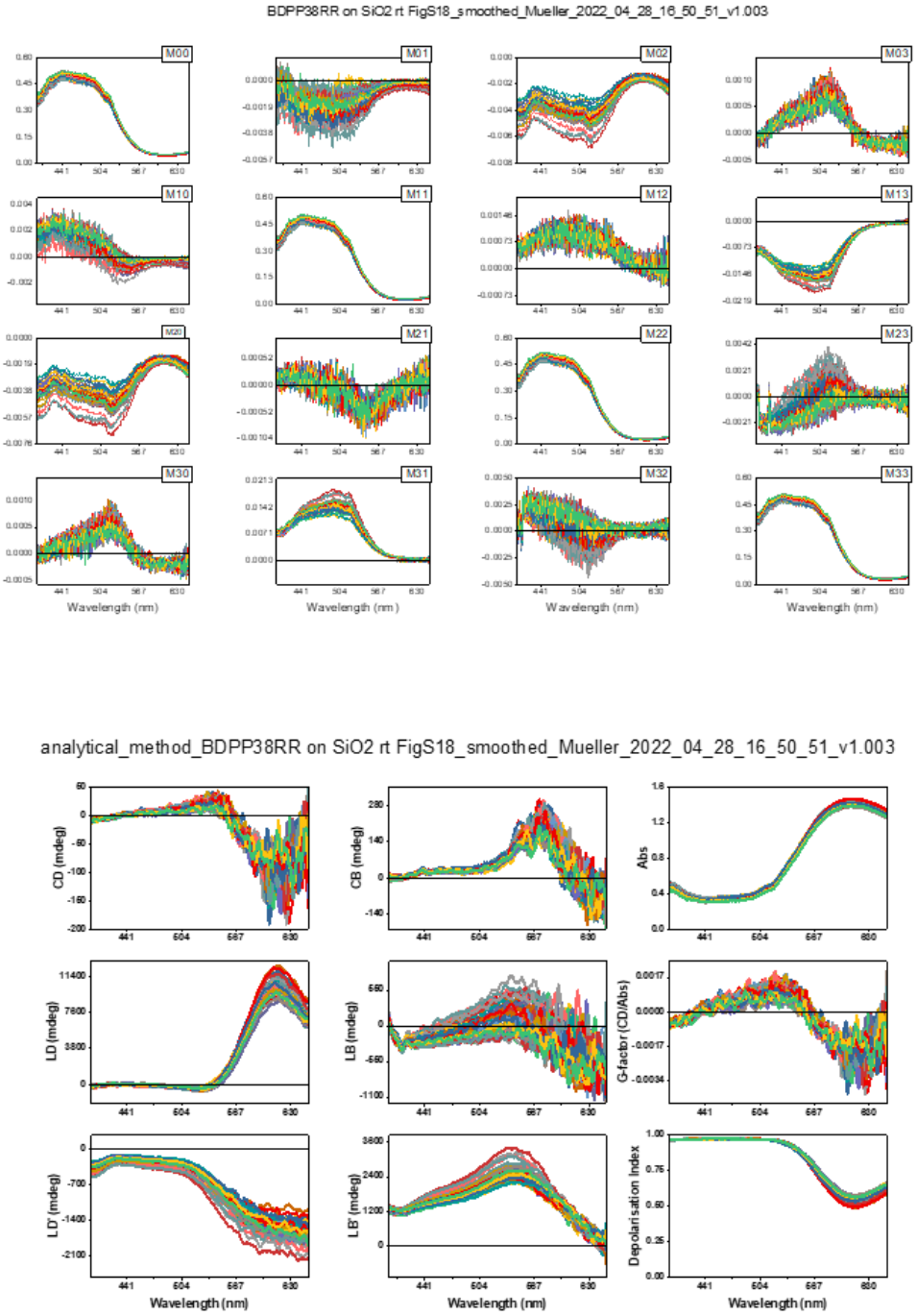

Fig. S18. Optical activity MMP spectroscopic map data of a 0.5x0.5 mm area (21x21 steps) with a lateral resolution of 25 µm of a spin coated film of (*S,S*)-**1**.

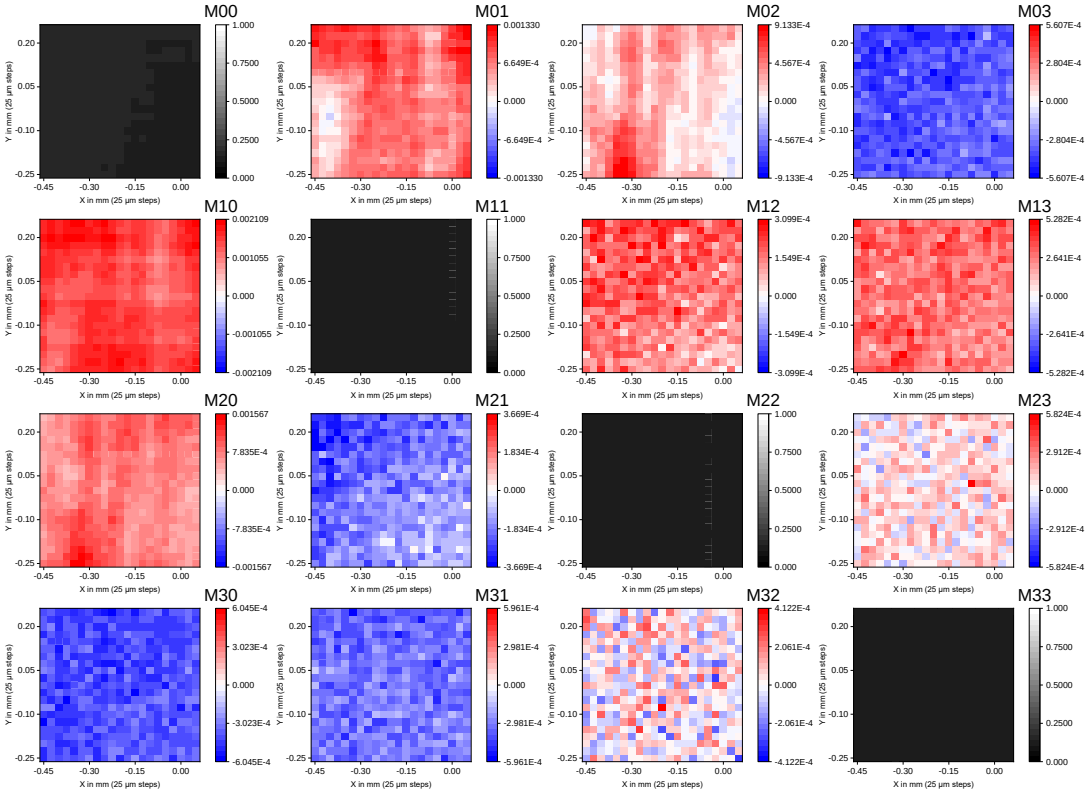

Fig. S19. Full MMPi data of a 0.5x0.5 mm area of 21x21 steps with a spatial resolution of 25 µm^2 at 600 nm performed on the blade coated film of (*S,S)*-**1** Figure 7 in the main paper.

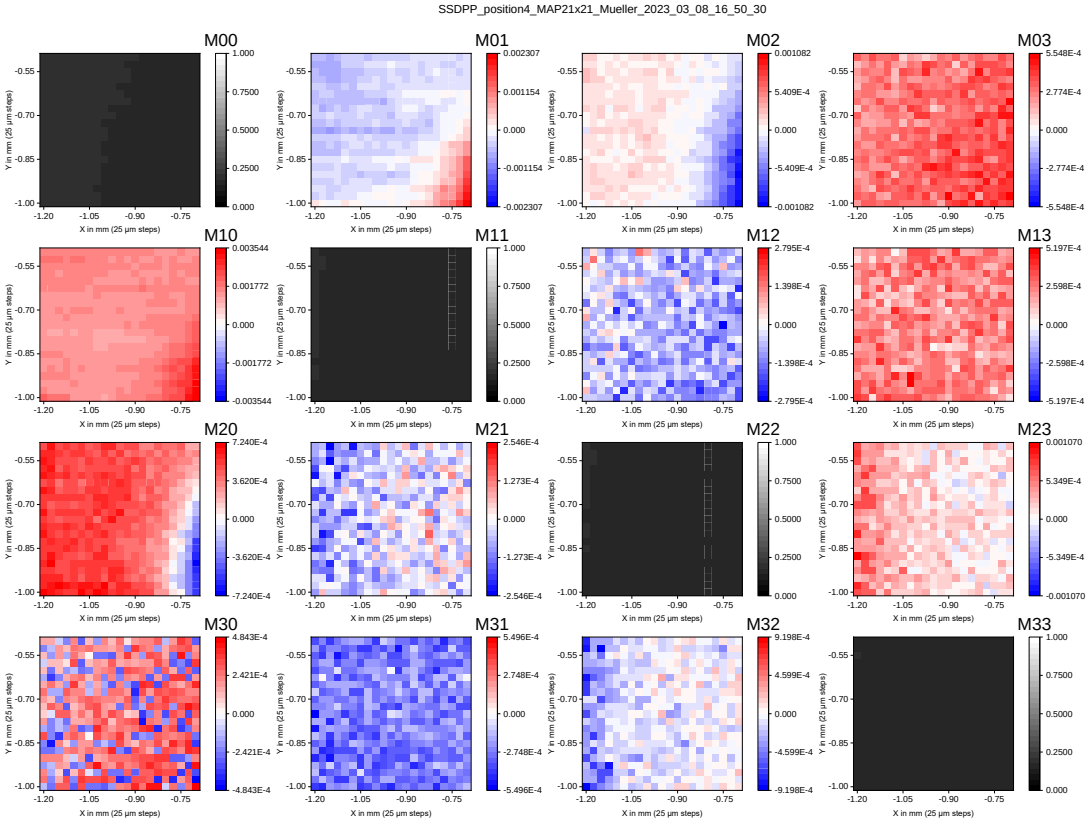

Fig. S20. Full MMPi data of a 0.5x0.5 mm area of 21x21 steps with a spatial resolution of 25 µm^2 at 600 nm performed on the blade coated film of (*S,S)*-**1**:**ITIC-4F** Figure 8 in the main paper.

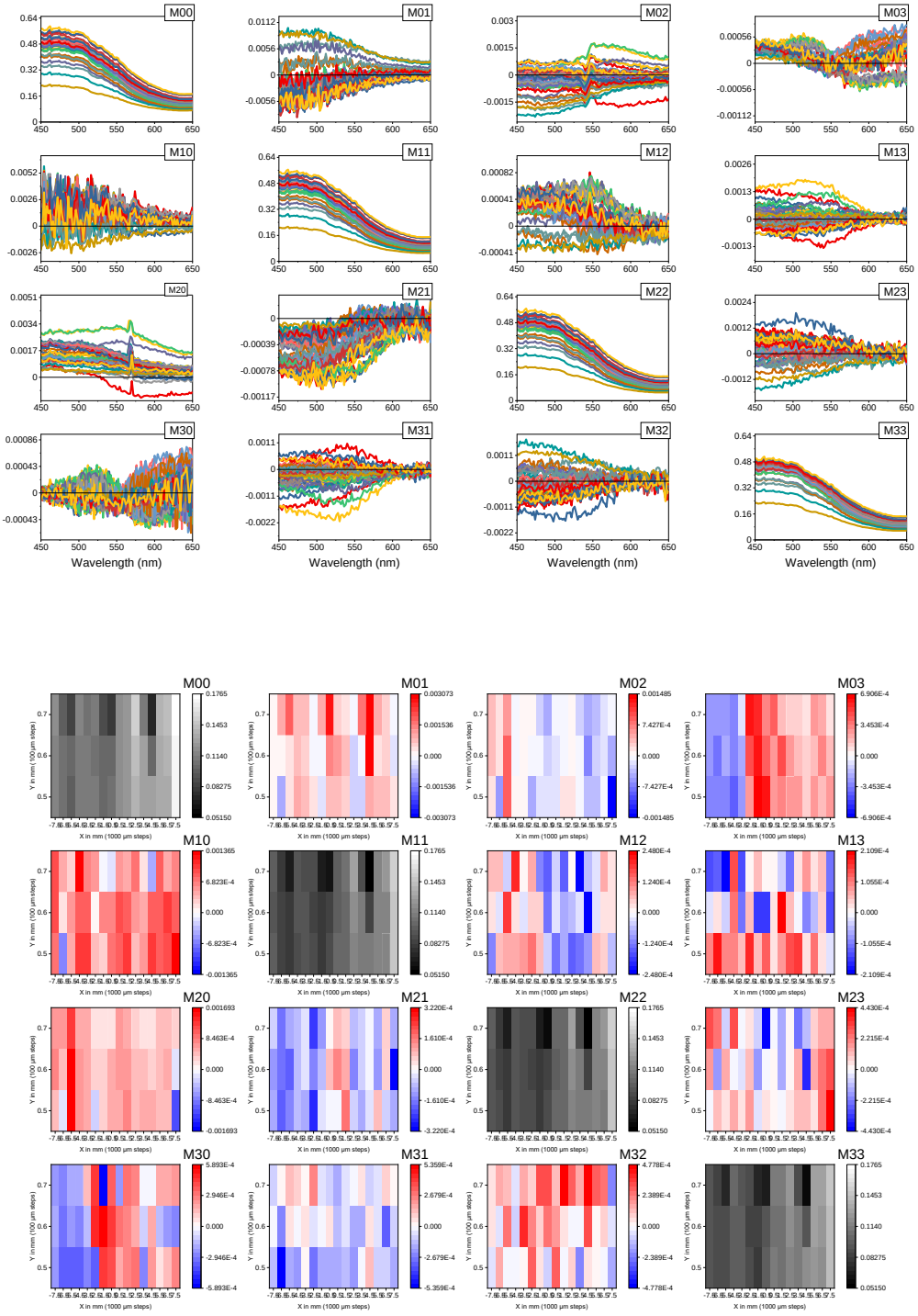

Figure S21a. Full spectroscopic MMP data and 630 nm map for the gradient blade-coated device formed from of (*S,S*)-**1**:**ITIC-4F** on ZnO-coated ITO on glass with aluminium contacts, corresponding to the data in Figure 9 in the main paper.

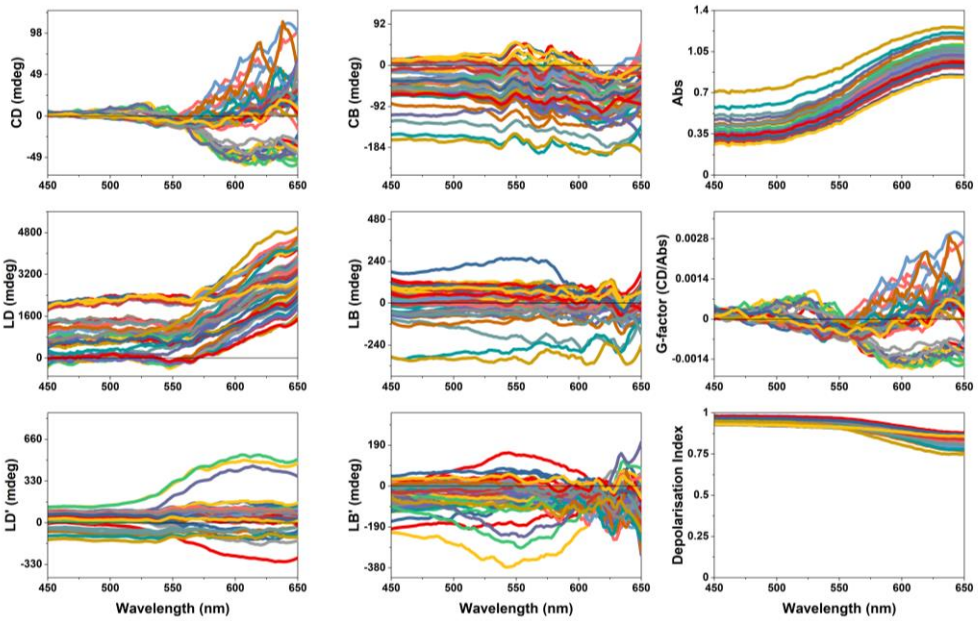

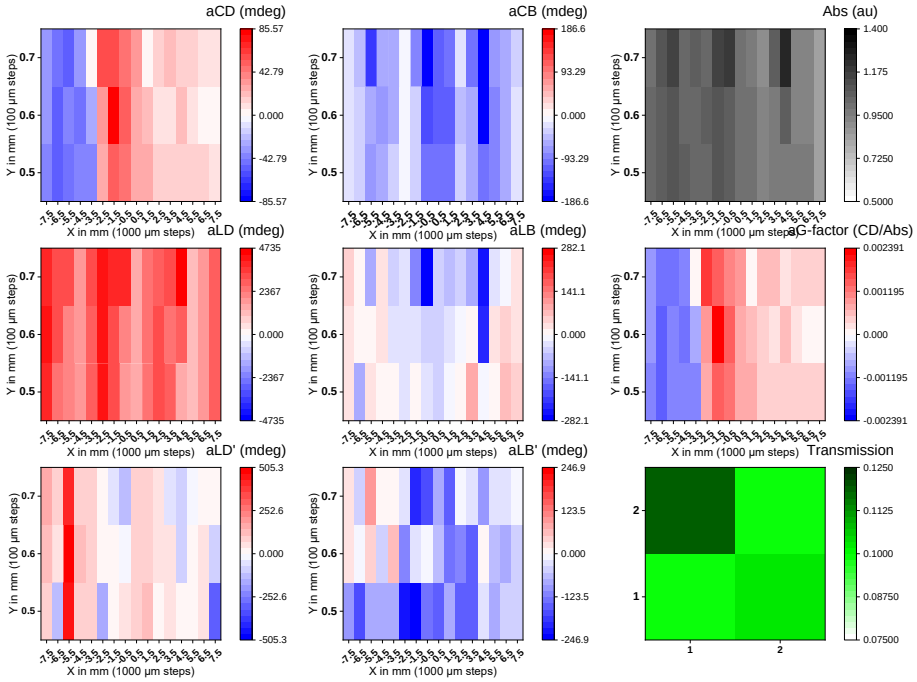

Figure S21b. MMP data from Fig. S21a and 630 nm map for the gradient blade-coated device formed from of (*S,S*)-**1**:**ITIC-4F** on ZnO-coated ITO on glass with aluminium contacts, corresponding to the data in Figure 3 in the main paper.

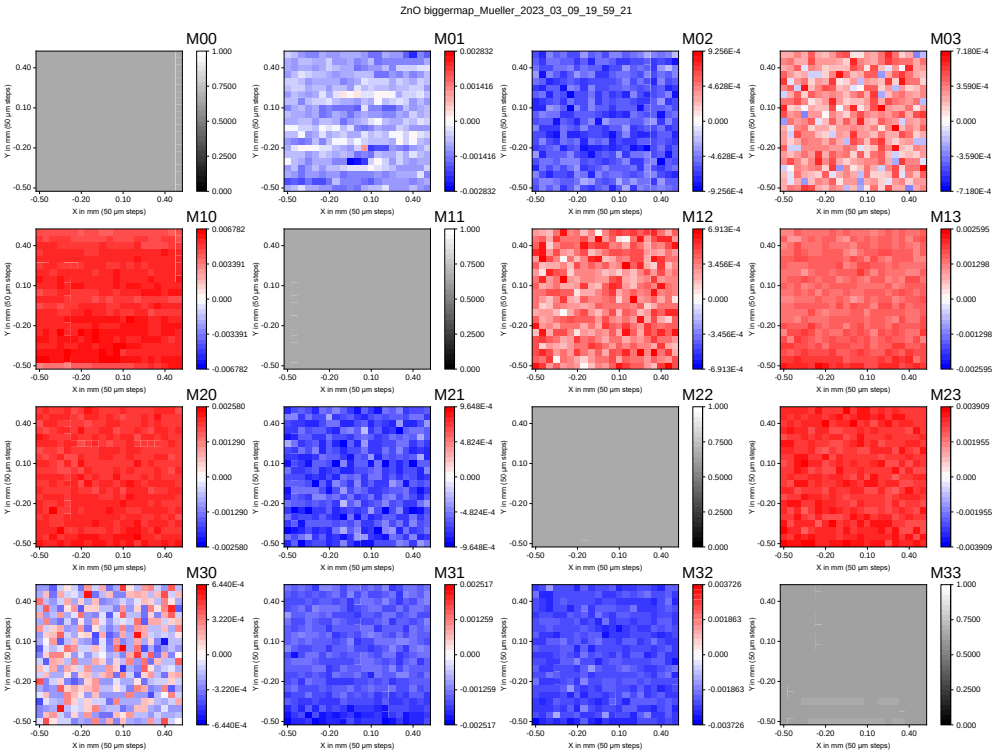

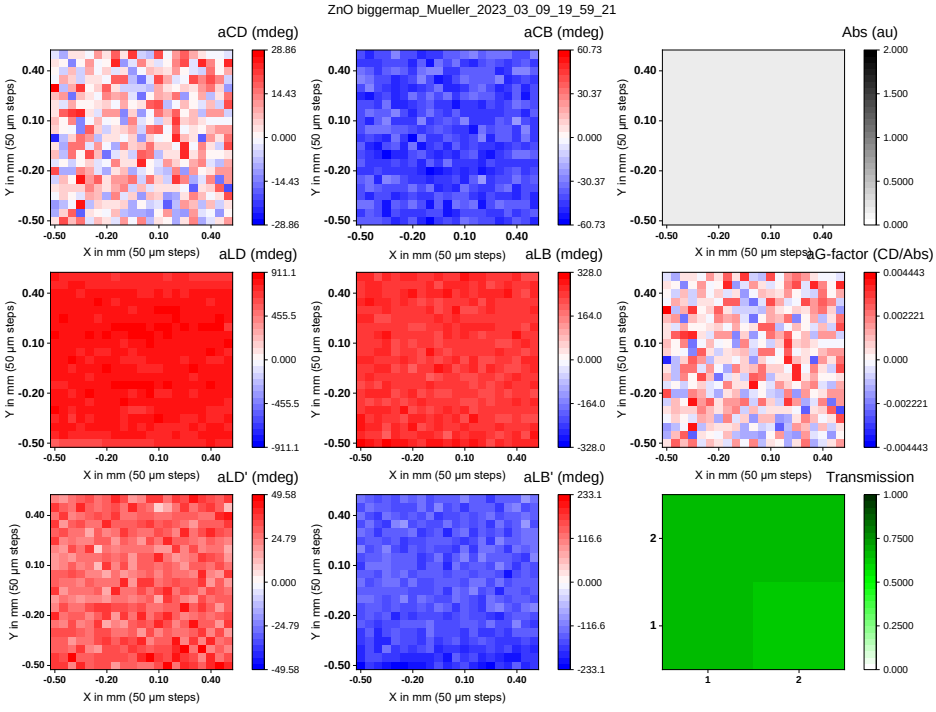

Figure S22. Full spectroscopic MMP data for ZnO-coated ITO on glass 21x21 steps with a spatial resolution of 25 µm^2 at 600 nm

Optical Micrographs

The images were acquired with Optical Microscope B-600 MET from OPTIKA with 100x magnification and polarizer filter, the scale bar is 10 µm.

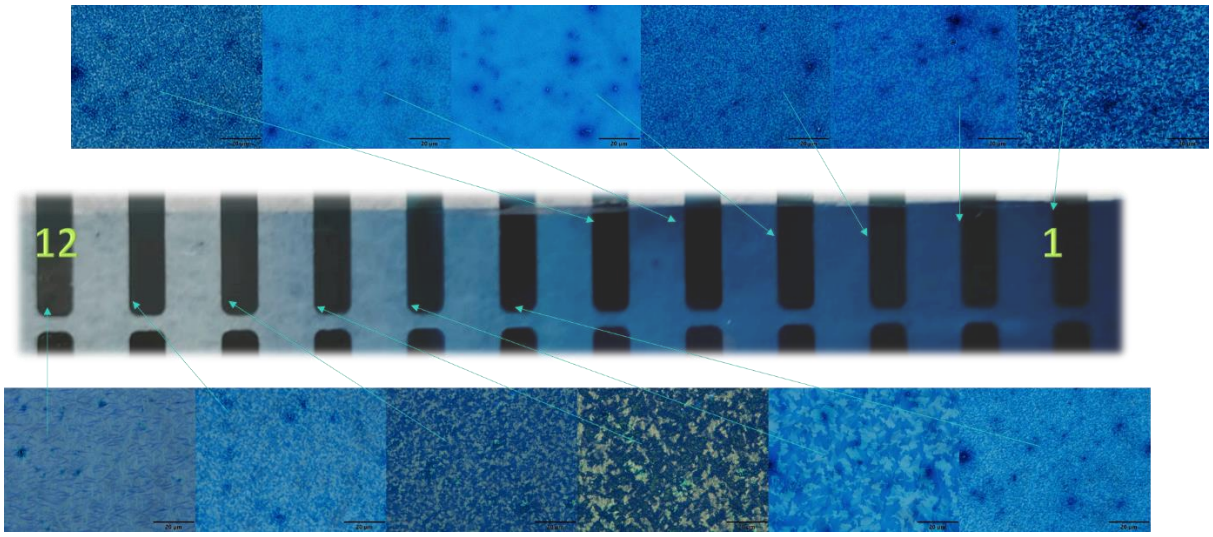

Fig. S23. Optical microscopy image with crossed polarizers of (*S,S*)-**1**:**ITIC-4F** film all along the bladed coated organic solar cell.

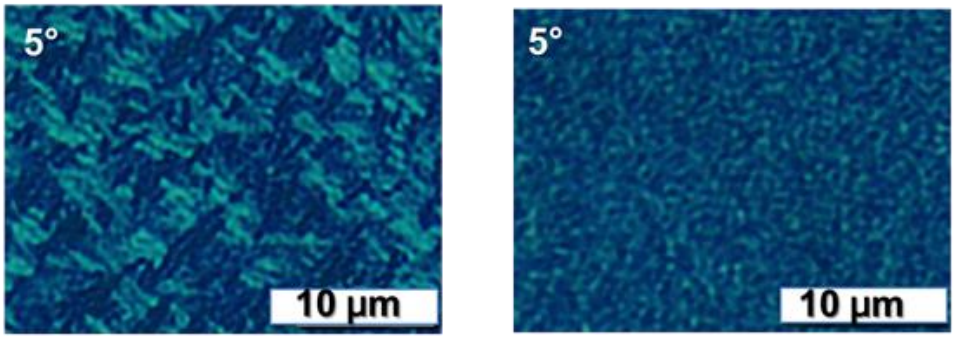

Fig. S24. Right) Optical microscopy image with crossed polarizers of (*S,S*)-**1**:ITIC-4F film after annealing 120°C ; left) Optical microscopy image with crossed polarizers of (*S,S*)-**1**:ITIC-4F as a cast film (approximately 150 nm thick).

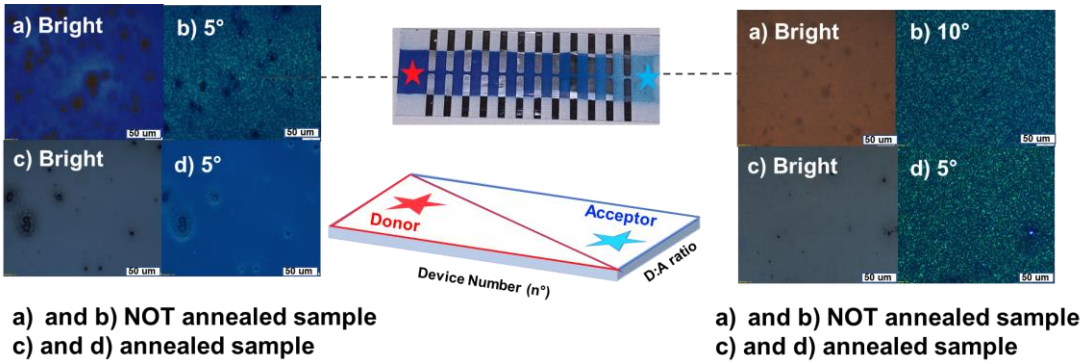

Fig. S25. Right) Optical microscopy image with crossed polarizers of bilayer (*S,S*)-**1**:ITIC-4F film after annealing 120°C; left) Optical microscopy image with crossed polarizers of (*S,S*)-**1**:ITIC-4F as deposited bilayer film (approximately 200 nm thick).

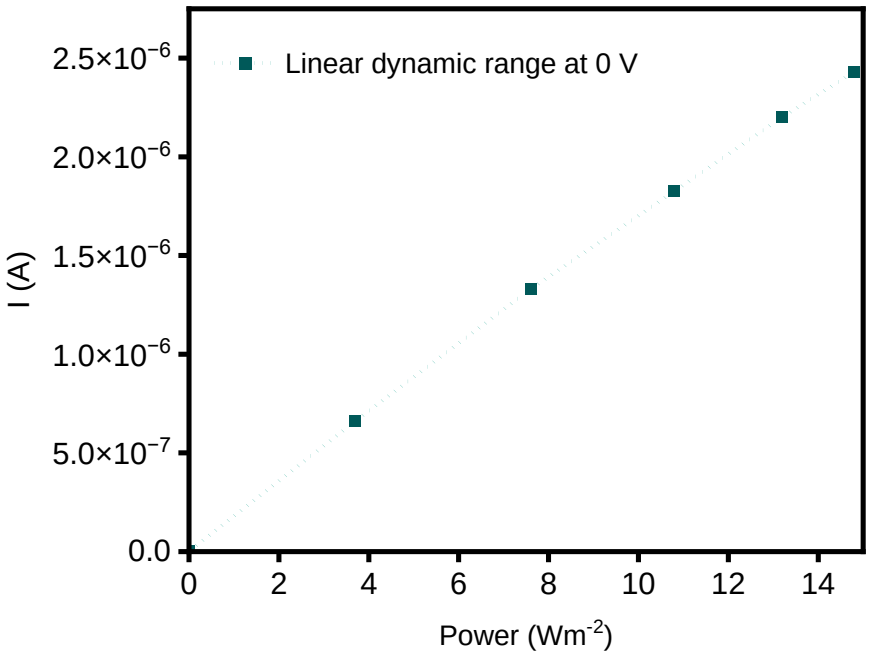

Fig. S26. Linear dynamic response at 0 V of the OPV device no. 6 (approximately 110 nm thick) under illumination at 709 nm with unpolarised light.

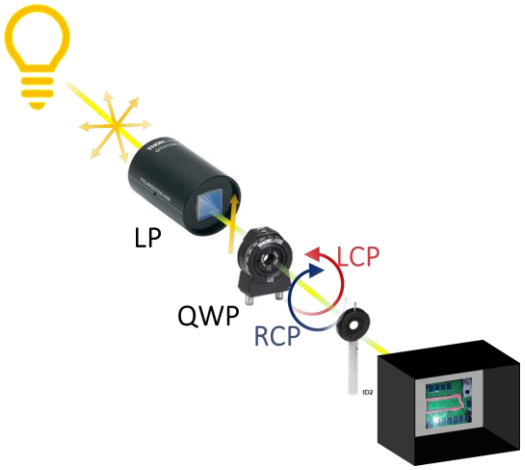

Figure S27. Schematic representation of the set-up utilized to measure the EQE dependence to circularly polarized light. In particular was used a 600-2700 nm superchromatric quarter waveplate (SAQWP05M-1700) from Thorlabs.

Table S6. Open-circuit voltage, short-circuit density current, Power Conversion Efficiency (PCE) and Fill Factor obtained from the best performing pixel in the blade coated organic solar cell of the enantiopure compound (*S,S*)-**1** blended with **ITIC-4F** varying the cell architecture, the thickness and the annealing process. Bulk heterojunctions were prepared by mixing equal proportions of the donor and acceptor at a concentration of 20 mg/mL, then stirred at 40°C for two hours. The resulting solution was blade-coated at 80°C as described above. For the bilayer structure, separate solutions of donor and acceptor were prepared at the same concentration (20 mg/mL) and sequentially blade-coated, with the acceptor layer applied first, followed by the donor layer. A thin layer (from 50 to 20 nm) was achieved by increasing the blade coater speed and reducing the solution volume from 50 to 20 µL of the bulk heterojunction mixture. In contrast, the thick layer (300 to 200 nm) was obtained by reducing the speed of the blade coater and by depositing twice the same layer.

Cell architecture	*V_{oc} (V)*	*I_{sc} (mA/cm^2)*	*PCE (%)*	*FF (%)*
BHJ	***0.44***	***-0.77***	***0.15***	***32***
BHJ Annealed	***0.8***	***-0.44***	***0.25***	***35***
Bilayer	***0.59***	***-0.95***	***0.7***	***15***
Bilayer annealed	***0.65***	***-0.3***	***0.6***	***30***
Thin layer	***0.13***	***-2.3***	***0.13***	***23***
Thin layer annealed	***0.03***	***-4.5***	***0.18***	***40***
Thick layer	***0.6***	***-0.36***	***0.7***	***34***
Thick layer annealed	***0.3***	***-1.08***	***0.4***	***15***

See plots overleaf

Device characteristics summarised in Table S6.

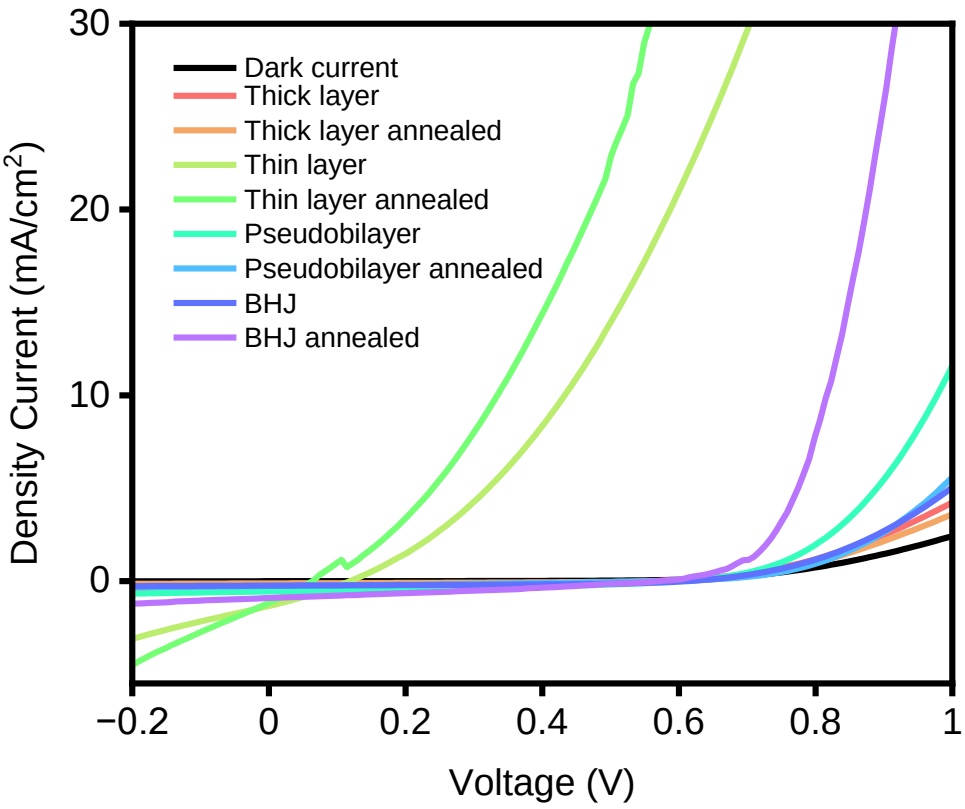

Table S7 Open-circuit voltage, short-circuit density current, Power Conversion Efficiency (PCE) and Fill Factor obtained from the best performing pixel in the blade coated BHJ organic solar cell of the enantiopure compound (*S,S*)-**1** blended with ITIC-4F and the two enantiomers (*S,S*)-**1** :(*R,R*)-**1** blended in equal proportion with **ITIC-4F.**

Formulation of the AL	*V_{oc} (V)*	*J_{sc} (mA/cm^2)*	*PCE (%)*	*FF (%)*
(S,S)-1:ITIC-4F	***0.44***	***-0.77***	***0.15***	***32***
(S,S)-1:(R,R)-1:ITIC-4F	***0.6***	***-0.62***	***0.18***	***49***

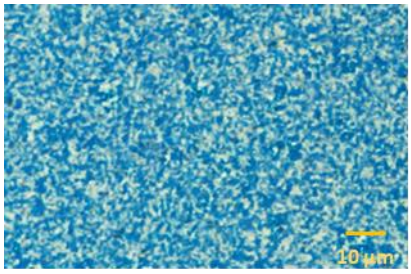

Optical micrograph of (*S,S*)-1:(*R,R*)-1:ITIC-4F

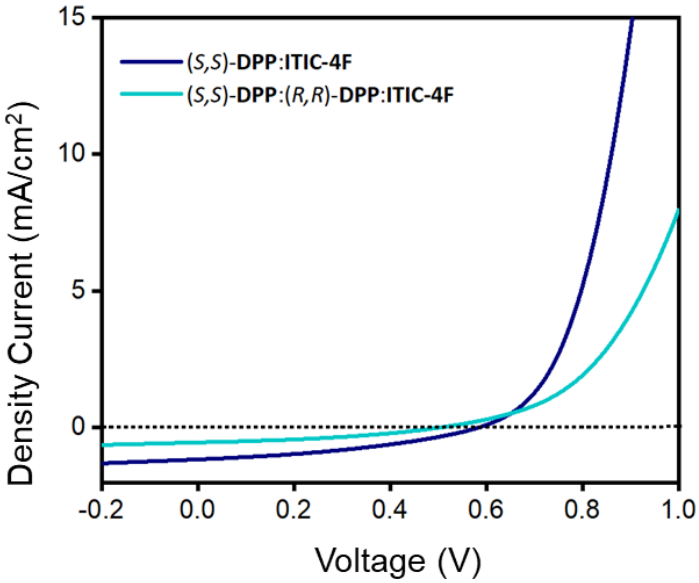

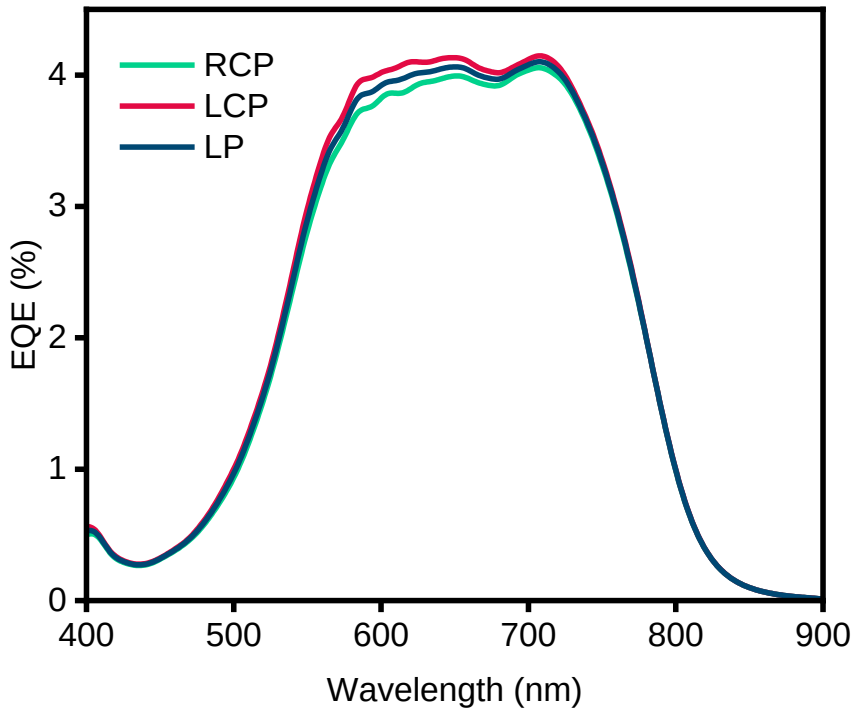

Figure S28. EQE measurements with linearly polarized (LP) light and right and left circularly polarized light (RCP and LCP respectively) for devices made from (*S,S*)-**1** and **ITIC-4F** (Device no. 2 in a solar cell, approximate thickness 140 nm). To avoid any degradation effects, experiments were systematically performed in the sequence starting with RCP followed by LCP and then LP light.

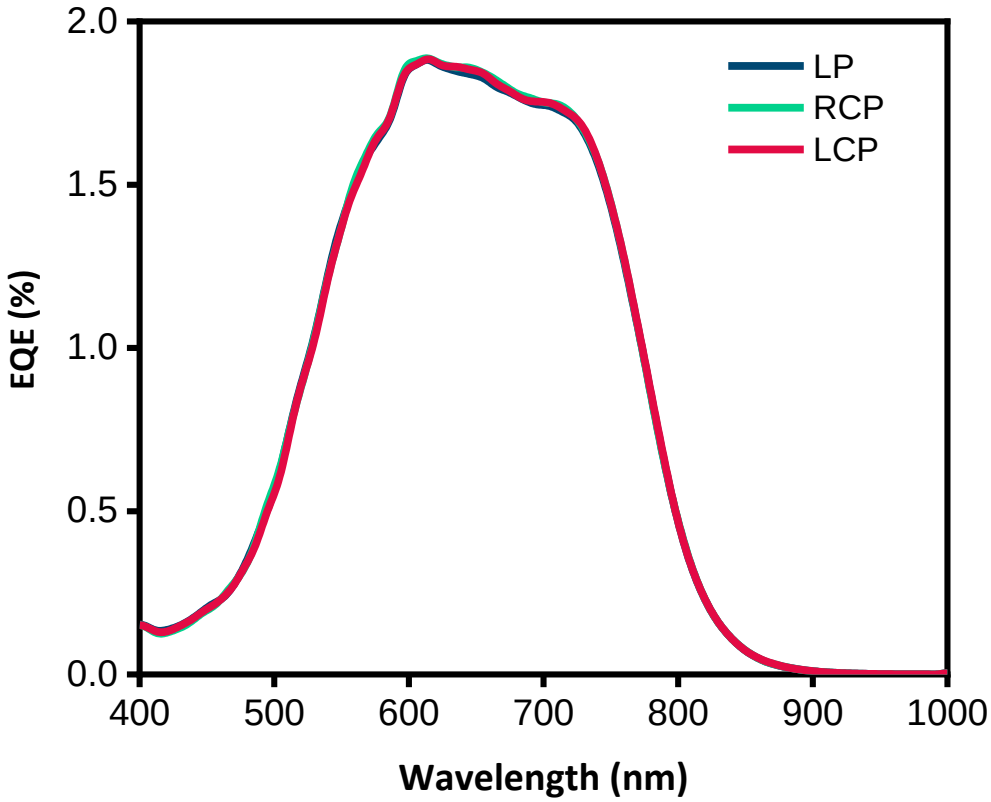

Figure S29. EQE measurements with linearly polarized (LP) light and left and right circularly polarized light (LCP and RCP respectively) for devices made from an equimolar mixture of the enantiomers (*S,S*)-**1** and (*R,R*)-**1** and **ITIC-4F** (ratio 1:1:2).

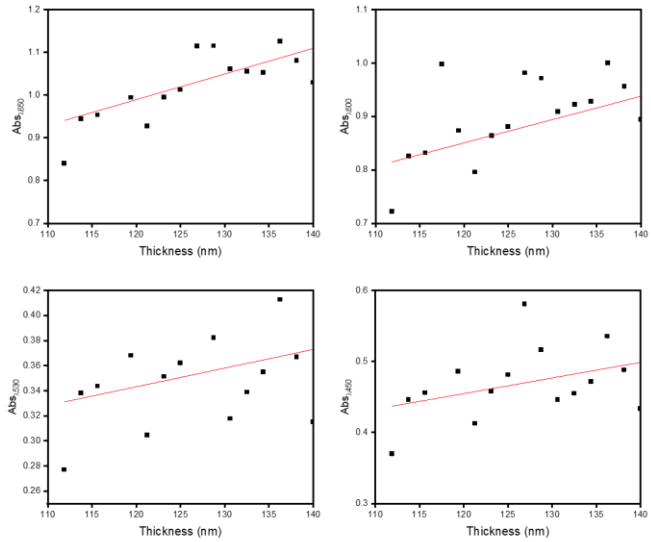

Equation	y = a + b*x
Plot	avg 530
Weight	No Weighting
Intercept	0.1647 ± 0.16663
Slope	0.00149 ± 0.00131
Residual Sum of Squares	0.02513
Pearson's r	0.29954
R-Square (COD)	0.08972
Adj. R-Square	0.0197

Equation	y = a + b*x
Plot	avg 650 nm
Weight	No Weighting
Intercept	0.2684 ± 0.22267
Slope	0.00601 ± 0.00176
Residual Sum of Squares	0.05207
Pearson's r	0.67324
R-Square (COD)	0.45325
Adj. R-Square	0.4142

Equation	y = a + b*x
Plot	avg 450
Weight	No Weighting
Intercept	0.19123 ± 0.18304
Slope	0.0022 ± 0.00144
Residual Sum of Squares	0.03033
Pearson's r	0.38888
R-Square (COD)	0.15123
Adj. R-Square	0.08594

Equation	y = a + b*x
Plot	avg 600 nm
Weight	Instrumental (=1/ei^2)
Intercept	0.32608 ± 0.09604
Slope	0.00437 ± 7.76027E-4
Residual Sum of Squares	422.19544
Pearson's r	0.83298
R-Square (COD)	0.69385
Adj. R-Square	0.67198

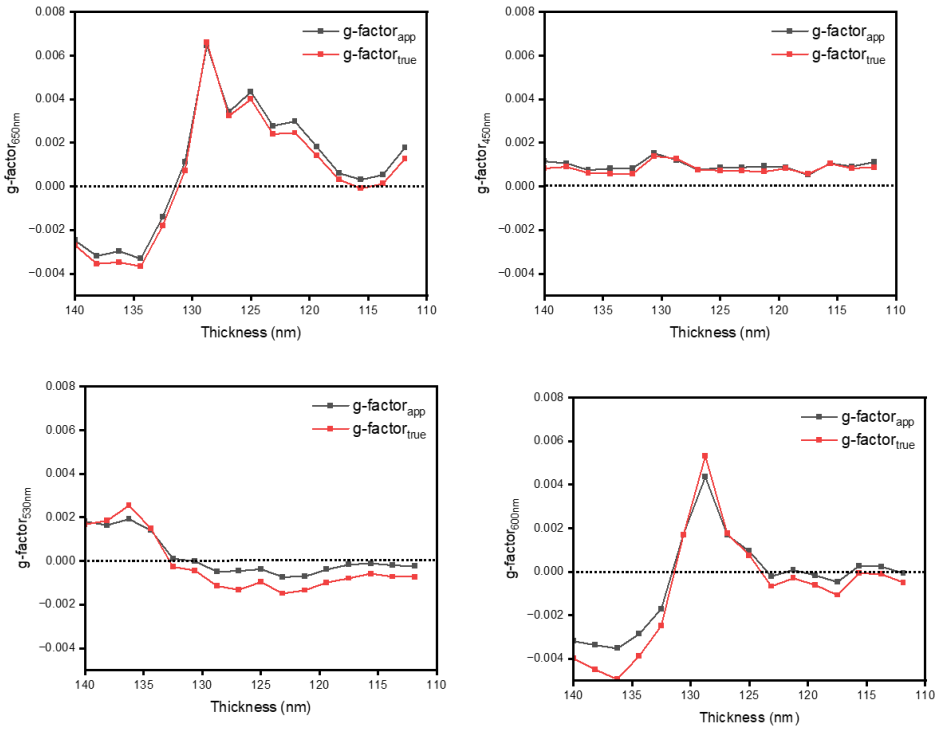

Figure S30. : At the top linear log fits obtained for four different wavelengths (650 nm, 600 nm, 530 nm and 450 nm), by fitting the absorption data from the 16x3 grid presented in Figure 9 against the device thickness, we observed a linear trend. and below using the intercept data, we corrected the absorption values for reflection and scattering losses by applying the equation outlined in M. Schulz, J. Zablocki, O. S. Abdullaeva, S. Brück, F. Balzer, A. Lützen, O. Arteaga and M. Schiek, Nat. Commun., 2018, 9, 2413.

$$-Abs^{meas} = -\log(1-R)^2 + \frac{\alpha}{\ln(10)} \cdot d \qquad (1)$$